

Synthesis of the groundwater investigations in the Lower Waihemo/Shag River Valley

F Mourot MA Coble M Moreau M Herpe

**GNS Science Consultancy Report 2022/91
November 2022**



DISCLAIMER

This report has been prepared by the Institute of Geological and Nuclear Sciences Limited (GNS Science) exclusively for and under contract to Otago Regional Council. Unless otherwise agreed in writing by GNS Science, GNS Science accepts no responsibility for any use of or reliance on any contents of this report by any person other than Otago Regional Council and shall not be liable to any person other than Otago Regional Council, on any ground, for any loss, damage or expense arising from such use or reliance.

Use of Data:

Date that GNS Science can use associated data: November 2022

BIBLIOGRAPHIC REFERENCE

Mourot F, Coble MA, Moreau M, Herpe M. 2022. Synthesis of the groundwater investigations in the Lower Waihemo/Shag River Valley. Wairakei (NZ): GNS Science. 80 p. Consultancy Report 2022/91.

CONTENTS

EXECUTIVE SUMMARY.....	VI
1.0 INTRODUCTION	1
2.0 BACKGROUND INFORMATION.....	2
2.1 Setting	2
2.1.1 Study Area and Waihemo/Shag River	2
2.1.2 Climate	2
2.1.3 Geology	5
2.1.4 Hydrogeology	5
2.1.5 Soils and Land Use	9
2.2 Otago Regional Council Monitoring Programme	9
2.2.1 Background	9
2.2.2 Otago Regional Council Initial Investigations.....	10
2.2.3 Otago Regional Council Monitoring Sites Installation and Data Collection	11
2.2.4 Otago Regional Council and Otago Regional Council-led Complementary Investigations.....	15
3.0 DATA INTERPRETATION METHODS	18
3.1 Groundwater Quantity.....	18
3.1.1 Aquifer Boundary.....	18
3.1.2 Aquifer and River Hydrographs	18
3.1.3 Piezometric Maps	18
3.1.4 Aquifer Hydraulic Properties.....	18
3.2 Groundwater Quality.....	19
3.2.1 Hydrochemistry Data	19
3.2.2 Nitrate Concentrations and Loads.....	20
3.2.3 Water Dating and Tracer Measurements	21
3.3 Conceptual Models	21
4.0 RESULTS OF THE STUDY AND DISCUSSION.....	22
4.1 Groundwater Quantity.....	22
4.1.1 Aquifer Boundary.....	22
4.1.2 Aquifer and River Hydrographs	26
4.1.3 Piezometric Maps	26
4.1.4 Aquifer Hydraulic Properties.....	29
4.2 Groundwater Quality	29
4.2.1 Hydrochemistry.....	29
4.2.2 Nitrate Concentrations and Loads.....	37
4.2.3 Tracer Measurements	39
4.3 Conceptual Models	44
4.3.1 Aquifer Structure and River Interaction	44
4.3.2 Water Inputs and Outputs to the Aquifer	45

5.0	CONCLUSION AND RECOMMENDATIONS	46
5.1	Conclusion.....	46
5.2	Recommendations.....	47
6.0	ACKNOWLEDGEMENTS	48
7.0	REFERENCES	48

FIGURES

Figure 2.1	Location of the study area, approximately corresponding to the Shag Alluvial Aquifer boundary, as delineated by the Regional Plan: Water (RPW) and located in the Lower Waihemo/Shag River Valley (North Otago).	3
Figure 2.2	Mean annual rainfall (left) and mean actual evapotranspiration (right) over the 1996–2006 period in the Waihemo/Shag River catchment (after Henderson 2019).	4
Figure 2.3	Geology of the Lower Waihemo/Shag River Valley (Martin et al. 2021) with the Otago Regional Council Regional Plan: Water (RPW) Shag Alluvial Aquifer boundary and programme monitoring sites	7
Figure 2.4	Land cover classes in the Waihemo/Shag River catchment (as mapped in 2018 by Manaaki Whenua Landcare Research (2022) and available in the Land Resource Information System (LRIS) Portal) with the Otago Regional Council Regional Plan: Water (RPW) Shag Alluvial Aquifer boundary and programme monitoring sites	8
Figure 2.5	Modelled cumulative residence time distributions and mean residence times of 2, 3, 20 and 22 years were calculated using 70% and 80% exponential piston-flow models (EPM), which yielded age distributions for groundwater and surface water sites measured in this study.	17
Figure 4.1	Current Shag Alluvial Aquifer boundary in relation to geological and water level information, northwest area (between Craig Road and Sutherland Road).	23
Figure 4.2	Current Shag Alluvial Aquifer boundary in relation to geological and water level information, central area (between Sutherland Road and east of Horse Range Road).	24
Figure 4.3	Current Shag Alluvial Aquifer boundary in relation to geological and water level information, southeast area (between east of Horse Range Road and the coast).	25
Figure 4.4	Mean daily groundwater levels (GWL; high-frequency monitoring: lines; manual measurements: marker symbols) and river stage (dashed coloured lines) in the Lower Waihemo/Shag River Valley (from August 2017 to August 2022).	27
Figure 4.5	Piezometric contours for the Shag Alluvial Aquifer on 22/05/2018 (relatively high Waihemo/Shag River stage and groundwater level conditions).	28
Figure 4.6	Major ion chemistry at the monitoring sites depicted as a Piper diagram (top) and a Stiff diagram (bottom).	32
Figure 4.7	Median nitrate concentrations between July 2017 and September 2018 for the Otago Regional Council monitoring sites.	33
Figure 4.8	Major ion concentrations at the monitoring sites from September 2017 to September 2018.	34
Figure 4.9	Nutrient concentrations at the monitoring sites from September 2017 to September 2018.....	35
Figure 4.10	Trace metal concentrations at the monitoring sites from September 2017 to September 2018.	36
Figure 4.11	Timeseries of rainfall, nitrate concentrations (high-frequency monitoring and grab samples), groundwater levels for the Shag Alluvial Aquifer and flows for the Waihemo/Shag River from August 2017 to September 2018.....	38

Figure 4.12	Nitrate loads estimated from daily flows and daily nitrate concentrations from high-frequency (HF) data and grab samples (GS) for the Waihemo/Shag River at Craig Road (EM495), Switchback Road (EM542) and Shakey Bridge (FD208) from September 2017 to August 2018.	39
Figure 4.13	Stable isotope compositions for Lower Waihemo/Shag River Valley groundwater (red) and surface water (blue) samples.	40
Figure 4.14	Hydrogen ($\delta^2\text{H}$) and oxygen ($\delta^{18}\text{O}$) isotope results from surface water and groundwater samples collected on 22/05/2018 in the Lower Waihemo/Shag River Valley.	41
Figure 4.15	Radon results from this study, including surface water sampled from the Waihemo/Shag River in February and March 2017, and from groundwater bores in February, March, and October 2017.	43
Figure 4.16	Conceptual model of the structure and river interaction for Shag Alluvial Aquifer, in the Lower Waihemo/Shag River Valley (adapted from Hauer et al. 2016).	44
Figure 4.17	Conceptual model of the water inputs and outputs for the Shag Alluvial Aquifer, in the Lower Waihemo/Shag River Valley (adapted from Hauer et al. 2016).	45

TABLES

Table 2.1	Groundwater-related investigations undertaken in the Lower Waihemo/Shag River Valley before 2017.	5
Table 2.2	Summary of the Quaternary gravel formations in the Lower Waihemo/Shag River Valley after Cameron et al. (2003).	6
Table 2.3	Summary of the Otago Regional Council monitoring programme: sites and parameters monitored.	13
Table 2.4	Summary of the technical specifications and monitoring sites for the high frequency nitrate sensors.	14
Table 2.5	Groundwater (GW) and surface water (SW) site information, the percent exponential-piston model (EPM) flow used to calculate ages, and the mean residence time and minimum residence time results including estimated uncertainty.	17
Table 3.1	Summary of the slug test analyses.	19
Table 4.1	Hydraulic conductivities and transmissivities estimated from the slug tests.	29
Table 4.2	Median values for hydrochemical parameters, from September 2017 to September 2018, at the groundwater sites.	31
Table 4.3	Stable isotope results for groundwater and surface water samples collected on 22/05/2018, in the Lower Waihemo/Shag River Valley.	40

APPENDICES

APPENDIX 1 RAINFALL DATA.....	53
APPENDIX 2 EARLIER GEOLOGICAL MAP AND ASSOCIATED GEOLOGICAL CROSS-SECTIONS	54
A2.1 Earlier Geological Map	54
A2.2 Earlier Geological Cross-Sections	55
APPENDIX 3 LITHOLOGICAL LOGS OF THE BORES DRILLED FOR THE PROGRAMME	56
APPENDIX 4 SOIL MAPS AND INFORMATION	57
A4.1 Soil Maps with Soil Drainage	57
A4.2 Soil Reports.....	59
A4.3 Nitrogen Leaching Susceptibility	61
APPENDIX 5 RADON AND AGE DATING LAB RESULTS.....	63
A5.1 Radon Results.....	63
A5.2 Age Dating Results.....	64
APPENDIX 6 HIGH-FREQUENCY NITRATE MONITORING SENSORS.....	65
A6.1 TriOS NICO Sensor.....	65
A6.2 HydroMetrics Nitrate GW50 Sensor.....	67
APPENDIX 7 SLUG TESTS	69
A7.1 Summary of the Slug Test Parameters	69
A7.2 Slug Test Analyses.....	70
APPENDIX 8 PIEZOMETRIC MAP FOR JANUARY 2018.....	73
APPENDIX 9 WAIHEMO/SHAG RIVER FLOW AND NITRATE LOADS	74
A9.1 Waihemo/Shag River Flow (High-Frequency Monitoring)	74
A9.2 Waihemo/Shag River Flow (Gauging Measurements)	75
A9.3 Waihemo/Shag River Nitrate Load Estimates	77
APPENDIX 10 ESTIMATION OF GROUNDWATER FLUXES TO THE WAIHEMO/SHAG RIVER.....	79

APPENDIX FIGURES

Figure A2.1	Detailed geology (particularly of Quaternary gravel deposits) of the Lower Waihemo/Shag River Valley (Cameron et al. 2003).	54
Figure A2.2	Geological cross-sections of the Lower Waihemo/Shag Aquifer Valley (Cameron et al. 2003). ..	55
Figure A4.1	Soil types and drainage capability in the Lower Waihemo/Shag River Valley (northwest part) (Manaaki Whenua Landcare Research 2022).	57
Figure A4.2	Soil types and drainage capability in the Lower Waihemo/Shag River Valley (eastern part) (Manaaki Whenua Landcare Research 2022).	58
Figure A4.3	Soil nitrogen leaching susceptibility in the Lower Waihemo/Shag River Valley (northwest part) (Manaaki Whenua Landcare Research 2022).	61

Figure A4.4	Soil nitrogen leaching susceptibility in the Lower Waihemo/Shag River Valley (eastern part) (Manaaki Whenua Landcare Research 2022).	62
Figure A6.1	General description of the TriOS NICO sensor (TriOS 2022).	65
Figure A6.2	Technical specifications of the TriOS NICO sensor (TriOS 2022).	66
Figure A6.3	General description of the HydroMetrics Nitrate GW50 sensor (HydroMetrics 2022).	67
Figure A6.4	Technical specifications of the HydroMetrics Nitrate GW50 sensor (HydroMetrics 2022).	68
Figure A7.1	AQTESOLV Pro curve fitting analysis for bore J43/0122.	70
Figure A7.2	AQTESOLV Pro curve fitting analysis for bore J43/0123.	71
Figure A7.3	AQTESOLV Pro curve fitting analysis for bore J43/0124.	72
Figure A8.1	Piezometric contours for the Shag Alluvial Aquifer based on groundwater level measurements on 16/01/2018 (relatively low Waihemo/Shag River stage and groundwater level conditions). ..	73
Figure A10.1	Range of calculated discharge rates for reaches 2, 3 and 5 (see locations in Figure 4.15) of the Waihemo/Shag River using different radon groundwater input concentrations.	80

APPENDIX TABLES

Table A1.1	Rainfall statistics for EM359/Stoneburn monitoring station from January 2000 to July 2022 (based on Otago Regional Council data).	53
Table A3.1	Lithological description of the new bores of the monitoring programme as logged by the driller and the geologist after Mouroit (2018).	56
Table A4.1	Description of the soils present in the Lower Waihemo/Shag River Valley, based on Smap after Manaaki Whenua Landcare Research (2022).	59
Table A4.2	Glossary of soil description vocabulary after Manaaki Whenua Landcare Research (2022).	60
Table A5.1	Radon sampling site information and results from February, March and October 2017.	63
Table A5.2	Tritium, CFCs, and Halon-1301 results.	64
Table A7.1	Summary of the slug test parameters at each bore, adapted from Mouroit (2018).	69
Table A9.1	Mean monthly and mean annual flows (in m ³ /s) for the Waihemo/Shag River high-frequency flow monitoring sites EM495/Craig Road, EM542/Switchback Road and FD208/Shakey Bridge (from September 2017 to May 2020).	74
Table A9.2	Results of monthly gauging measurements (in m ³ /s) for the Waihemo/Shag River (February 2017 to May 2020 period).	75
Table A9.3	Annual mean daily nitrate loads estimated from high-frequency (HF) and grab-sample (GS) monitoring data for the Waihemo/Shag River at three locations: EM495/Craig Road, EM542/Switchback Road and FD208/Shakey Bridge (from September 2017 to August 2018).	77

EXECUTIVE SUMMARY

The Waihemo/Shag River (WS River) catchment (North Otago) has limited water resources, with very low river flows in dry periods and no water available for primary allocation. In the Lower WS River Valley (southeast of Glenpark), the WS River interacts with a shallow unconfined aquifer, the Shag Alluvial Aquifer (SAA), hosted in Quaternary gravel deposits. This groundwater resource is of prime importance locally as it supplies Palmerston with drinking water and can yield water during dry periods. Due to its interaction with the WS River, the SAA is allocated as surface water in the Otago Regional Plan: Water (Otago Regional Council 2004). This plan also classifies the SAA as 'nitrogen sensitive'.

In 2017, Otago Regional Council (ORC) initiated a series of investigations to better characterise the SAA, and its interaction with the WS River, and estimate nitrogen fluxes between land, groundwater and surface water. These ORC-led (and mostly operated) investigations included: a drilling campaign (eight bores), hydraulic testing, water level and hydrochemistry monitoring (eight river sites and eight bores), water dating, tracer measurements (radon, stable isotopes) and high-frequency nitrate sensing (three river sites and one bore). Most of the investigations were undertaken between February 2017 and August 2018, with some sites still being monitored in November 2022. In May 2022, GNS Science was commissioned to analyse the collected data, summarise the new knowledge gained and make recommendations for future monitoring or further work.

Results point to heterogeneity of the SAA's dynamics and hydraulic properties. SAA's areas located along the current WS riverbed or in river paleochannels are hosted in young/clean alluvial gravels and showed good hydraulic properties and strong interaction with the WS River (i.e. recharge and discharge according to the location and/or season). Groundwater in these areas was weakly mineralised and young (mean residence time (MRT) ≤ 2 years). SAA's areas located further away from the riverbed and closer to the valley margins are hosted in older weathered gravels that contain a variable fraction of clay and silt. They had poor aquifer properties, were more mineralised and contained older groundwater (MRT up to 20 years). Connections with the WS River were limited in these areas and mainly consisted of discharges into the WS River, while rainfall was the main source of recharge.

High-frequency nitrate monitoring highlighted the effect of high rainfall events on river and groundwater nitrate concentrations. For example, induced nitrate pulses in groundwater could lead to high nitrate concentrations discharged to the WS River, increasing river nitrate concentrations downgradient from these discharges. Calculations of nitrate loads in the WS River indicated increasing loads from Craig Road downstream to Shakey Bridge (at the end Chisholm Road), with values of ~ 77 kg/d and ~ 109 kg/d, respectively, for September 2017 to August 2018. This load increase reflects land use activities producing nitrogenous nutrients (e.g. agricultural activities, treated wastewater discharges) in the Lower WS River Valley.

Recommendations are to continue monitoring surface water and groundwater quality and quantity in an integrated way that allows for better management of the SAA and the WS River due to their strong interaction. However, the number of monitoring bores could be reduced. The high-frequency nitrate data provides context for the nitrate concentration variability and can be used to optimise future targeted sampling. However, we recommend validating the datasets using operational information not provided for this study. Geophysical information would also help refine the characterisation of the SAA's thickness, extent, and aquifer properties. We recommend undertaking a review of existing surveys as a first step before deploying any new investigations. Finally, groundwater flow and contaminant transport models could be developed if a detailed understanding of nitrate fluxes related to land use activity and management is required.

1.0 INTRODUCTION

The Lower Waihemo/Shag River Valley (Lower WS River Valley; North Otago) has been the subject of several groundwater studies over the last few decades (e.g. Cameron et al. 2003; Irricon Consultants 1995; Turnbull and Fraser 2005). These studies investigated the characteristics of groundwater resources of the lower valley (i.e. aquifer systems, recharge sources and storage volumes) and outlined complex interaction between groundwater and surface water.

In 2017, Otago Regional Council (ORC) initiated a monitoring programme to better characterise the Shag Alluvial Aquifer (from here on referred to as 'SAA'), its connection to surface water, and the nitrate fluxes between land, groundwater and surface water. The aim was to provide additional scientific information to refine the current regulation, e.g. quantity and quality allocation limits, and land use restrictions (Mourot 2017, 2018). This ORC-led (and mainly operated) monitoring programme included:

- a) Two radon sampling campaigns undertaken by GNS Science (GNS) to inform the selection of monitoring sites (February and March 2017).
- b) Drilling of nine boreholes and the installation of six piezometers (July to August 2017).
- c) Installation of instrumentation to continuously monitor groundwater and surface water levels (seven new sites in addition to one existing site) and nitrate concentrations (three sites installed in July 2017 for surface water; one site installed in December 2017 for groundwater).
- d) Monthly collection of groundwater and surface water samples for chemistry, monthly manual measurements of groundwater levels, and monthly stream flow gauging measurements (August 2017 to September 2018).
- e) Hydraulic testing of bores (June 2018).
- f) Collection of water samples for tritium age dating and stable isotope analyses (two sampling campaigns: December 2017 and May 2018).

Groundwater levels are still monitored continuously in four of these bores.

Due to capacity constraints within ORC, only some of the data listed hereabove were analysed and reported on until now (e.g. Mourot (2018)).

In May 2022, GNS was commissioned by ORC (under an Envirolink funding grant) to: (a) analyse and report on the various datasets collected; (b) develop a conceptual model for the SAA; (c) provide recommendations for future monitoring in the catchment; and, as relevant, suggest additional investigations to complement the local knowledge.

This current work will inform the new Land and Water Plan to ensure the sustainable management and protection of the freshwater resources and their values in the Lower WS River Valley (e.g. drinking water supply, mahinga kai gathering, support to stream ecological health).

2.0 BACKGROUND INFORMATION

2.1 Setting

2.1.1 Study Area and Waihemo/Shag River

The study area is located north of Palmerston township (North Otago) in the Lower WS River Valley and roughly corresponds to the area mapped in the Regional Plan: Water (RPW; Otago Regional Council 2004) as the SAA (Figure 2.1).

The Waihemo/Shag River (from here on referred to as ‘WS River’) is a small waterway flowing from the slopes of the Kakanui Peak (in the northwest) towards the Pacific Ocean just south of Shag Point/Matakaea (Figure 2.1). For most of its course, it flows through confined meandering channels, with a bed made of gravels, boulders and bedrock (Olsen and Ozanne 2014). Investigations of WS River channel morphology and sedimentation point to a very low natural sediment yield, with significant rates of degradation until 2009 that contributed to bank erosion, bed rock exposure and channel incision along the length of the river (Otago Regional Council 2009). In 2014, an updated survey by Williams (2014) indicated a change from an overall degradation to an overall aggradation/stability state. Yet, some sections were still degrading (e.g. between Craig Road and Munro Road).

The WS River drains a catchment of ~550 km² and has a highly variable flow regime, with flows ranging between less than 0.03 m³/s (dry periods/low flow events) to more than 400 m³/s (flood events). The median flow was estimated at 0.71 m³/s at Craig Road (September 1993 to May 2014; Olsen and Ozanne 2014). The water quality of the WS River is generally good, however, increasing trends in nitrogen were observed, pointing to nitrogen leaching from groundwater (Olsen and Ozanne 2014; Otago Regional Council 2022).

2.1.2 Climate

The mean annual rainfall observed over the 1996–2006 period in the WS River catchment varied between ~570 mm/yr (e.g. Green Valley) and ~1155 mm/yr (e.g. Kakanui Mountains; Figure 2.2; Henderson 2019). ORC operates a rain gauge at Stoneburn (rainfall station EM359; located in the eastern part of the catchment; Figure 2.2). Based on the recorded data, the mean annual rainfall was 637 mm/yr between January 2000 and July 2022 (Appendix 1), with the highest annual rainfall in 2018 (962 mm/yr) and the lowest annual rainfall in 2020 (375 mm/yr). Over the January 2000 to July 2022 period (at Stoneburn rainfall station; Appendix 1), on average, the wettest month was January (71 mm/mth) and the driest month was September (37 mm/mth), followed by March and June (40 and 41 mm/mth, respectively).

Mean annual actual evapotranspiration (AET) ranged between 490 mm/yr (e.g. Kakanui Mountains, Stoneburn) and 630 mm/yr (e.g. Pigroot Hill) over the 1996–2006 period (Figure 2.2; Henderson 2019). The mean AET for the WS River catchment was ~1155 mm/yr between 1996 and 2006 (Henderson 2019).

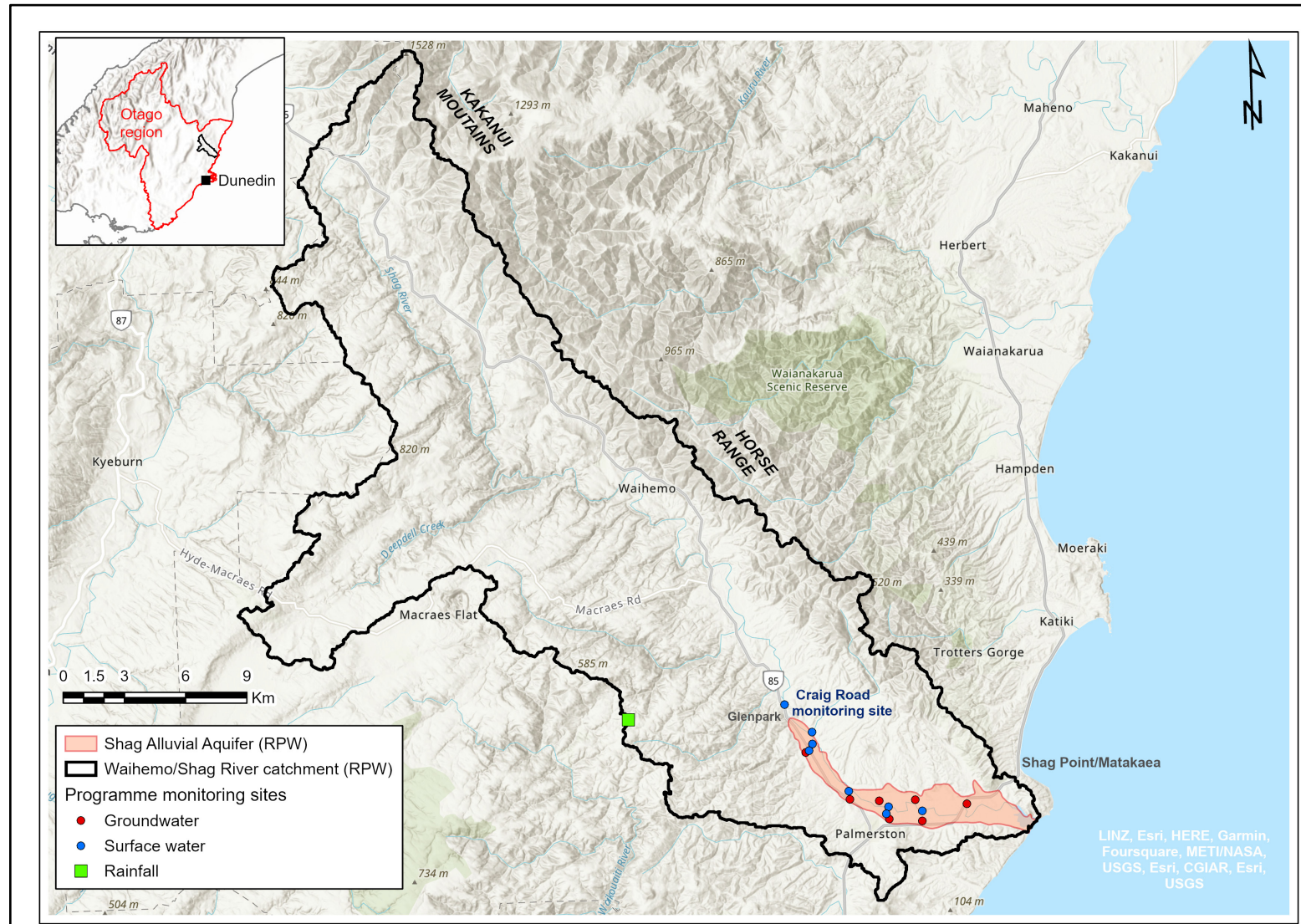


Figure 2.1 Location of the study area, approximately corresponding to the Shag Alluvial Aquifer boundary, as delineated by the Regional Plan: Water (RPW) and located in the Lower Waihemo/Shag River Valley (North Otago). Inset shows the location of the Waihemo/Shag River catchment relative to the Otago regional boundary.

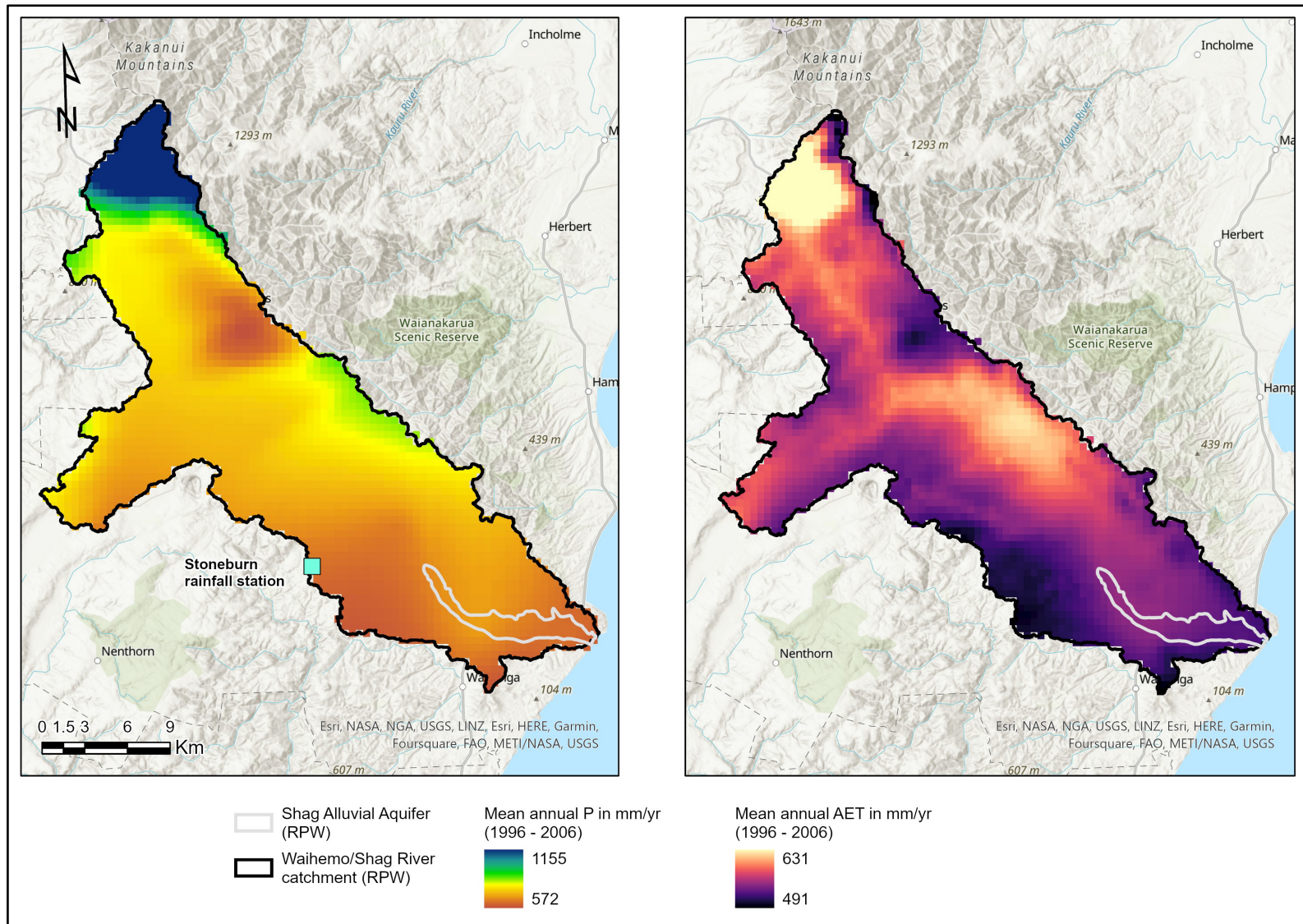


Figure 2.2 Mean annual rainfall (left) and mean actual evapotranspiration (right) over the 1996–2006 period in the Waihemo/Shag River catchment (after Henderson 2019).

2.1.3 Geology

The geology of the WS River Valley (Figure 2.3; Cameron et al. 2003; Forsyth et al. 2001; Martin et al. 2021; McMillan 1999); Appendix 2 and 3) consists of late Paleozoic and Mesozoic basement rocks (Otago Schist, Blue Mountain Limestone), overlain by Tertiary sedimentary rocks (e.g. Taratu Formation, Abbotsford Formation), capped by thin Quaternary alluvial deposits (e.g. Late Pleistocene river deposits). Small areas of Cenozoic volcanics rocks from the Dunedin Volcanic Group are also present and form local peaks within the sediments (e.g. Mount Puketapu and Janets Peak).

The Lower WS River Valley is affected by the Waihemo Fault System, which is a complex fault system comprising at least seven northwest-trending and steeply northeast-dipping reverse faults (Cameron et al. 2003; McMillan 1999). These faults have offset the basement and sedimentary rocks but have not affected recent surficial deposits (geological cross-sections in Appendix 2).

2.1.4 Hydrogeology

2.1.4.1 Background

Prior to the launch of the ORC monitoring programme, a series of groundwater investigations were undertaken in the Lower WS River between 1984 and 2005 to supply water to Palmerston township and support further economic development in the WS River Valley (Table 2.1).

Table 2.1 Groundwater-related investigations undertaken in the Lower Waihemo/Shag River Valley before 2017.

Year	Purpose of the Investigation	Reference
1984	Investigate the potential use of Blue Mountains water supply.	ER Garden and Partners Ltd* (1984)
1995	Locate monitoring bores for water quality and water levels.	Irricon Consultants (1995)
2002	Review how to better use the Blue Mountains water supply.	D. Hamilton & Associates* (2002)
2002	Monitor North and Coastal Otago river catchments.	Otago Regional Council* (2000)
2003	Assess potential water resources in the Shag River catchment.	Stewart* (2003)
2003	Assess potential alternative sources of water for the Lower WS River Valley, with a focus on groundwater.	Cameron et al. (2003)
2005	Apply some of the recommendations of Cameron et al. (2003) and in particular undertake a drilling investigation programme.	Turnbull and Fraser (2005)

Note: * references to these reports were found in other publications, but the reports could not be recovered and therefore were not used in the hydrogeological summary provided in this section.

2.1.4.2 Hydrogeological Summary

Four potential groundwater-bearing formations, associated with the geological formations described by McMillan (1999) (Appendix 2), were identified by Cameron et al. (2003):

- The Blue Mountains Formation¹, which is an extensively recrystallised marble formation including some interbedded mudstone. Spring water from this formation is piped and provides a rural water supply for the WS River Valley's community.
- The Volcanics¹, which are associated with some springs emerging on the flanks of Mount Puketapu and are used by local farmers for stock water supply.
- The Taratu Formation¹, which consists of quartz gravels and sands possibly hosting a confined aquifer overlain by the low permeability Abbotsford Mudstone Formation. One bore near Sutherland Road (I43/0022) might have tapped this formation. It is reported as artesian with 'very hard' water (Irricon Consultants 1995).
- The Quaternary Gravels (Table 2.2), which are alluvial deposits made of gravels, sands and silts from the Smilie, Morven, Pagon Road and Modern Gravel formations. These gravels rest on an eroded mudstone surface (the Abbotsford Formation).

2.1.4.3 The Shag Alluvial Aquifer

The SAA is the most accessible and main water source in the Lower WS River Valley. This aquifer is unconfined and hosted in the Quaternary Gravels, comprising the Morven, Pagon Road and Modern Gravel formations (Table 2.2; mapped in RPW). Differences in the lithology of these formations explain the heterogeneous water-bearing properties of the SAA. The potential to receive recharge from the WS River depends on the specific location (e.g. relative aquifer elevation to the river, presence of outcropping/or very shallow mudstone acting as hydraulic barrier).

Table 2.2 Summary of the Quaternary gravel formations in the Lower Waihemo/Shag River Valley after Cameron et al. (2003).

Quaternary Gravel Formations (From the Oldest to the Youngest)	Lithology	Aquifer Potential
Smilie Formation	Moderately to highly weathered deposits.	Poor water-bearing due to high clay content and elevation above the WS River level.
Morven Formation	Gravels that consist of slightly weathered clasts in a slightly weathered sand matrix.	Water-bearing but permeability reduced by infiltrated clay in the matrix.
Pagon Road Formation	Gravels that grade laterally (towards the hillsides) into fined-grained sands and silts.	Water-bearing potential reduces toward the hillsides.
Modern Gravels	Fresh (unweathered) well-rounded pebbly to cobbly gravels, in a relatively open sandy matrix.	High potential but risk of river depletion.

The SAA is inferred to receive recharge from rainfall and from the WS River. The streams located on the foothills are mainly incised into low permeability formations (e.g. Abbotsford Mudstone) and therefore unlikely to recharge the SAA. Interaction with the WS River has mainly been investigated by differential gauging measurements and is summarised in Cameron et al. (2003).

¹ Further investigations would be needed to confirm the aquifer potential of this formation (Cameron et al. 2003).

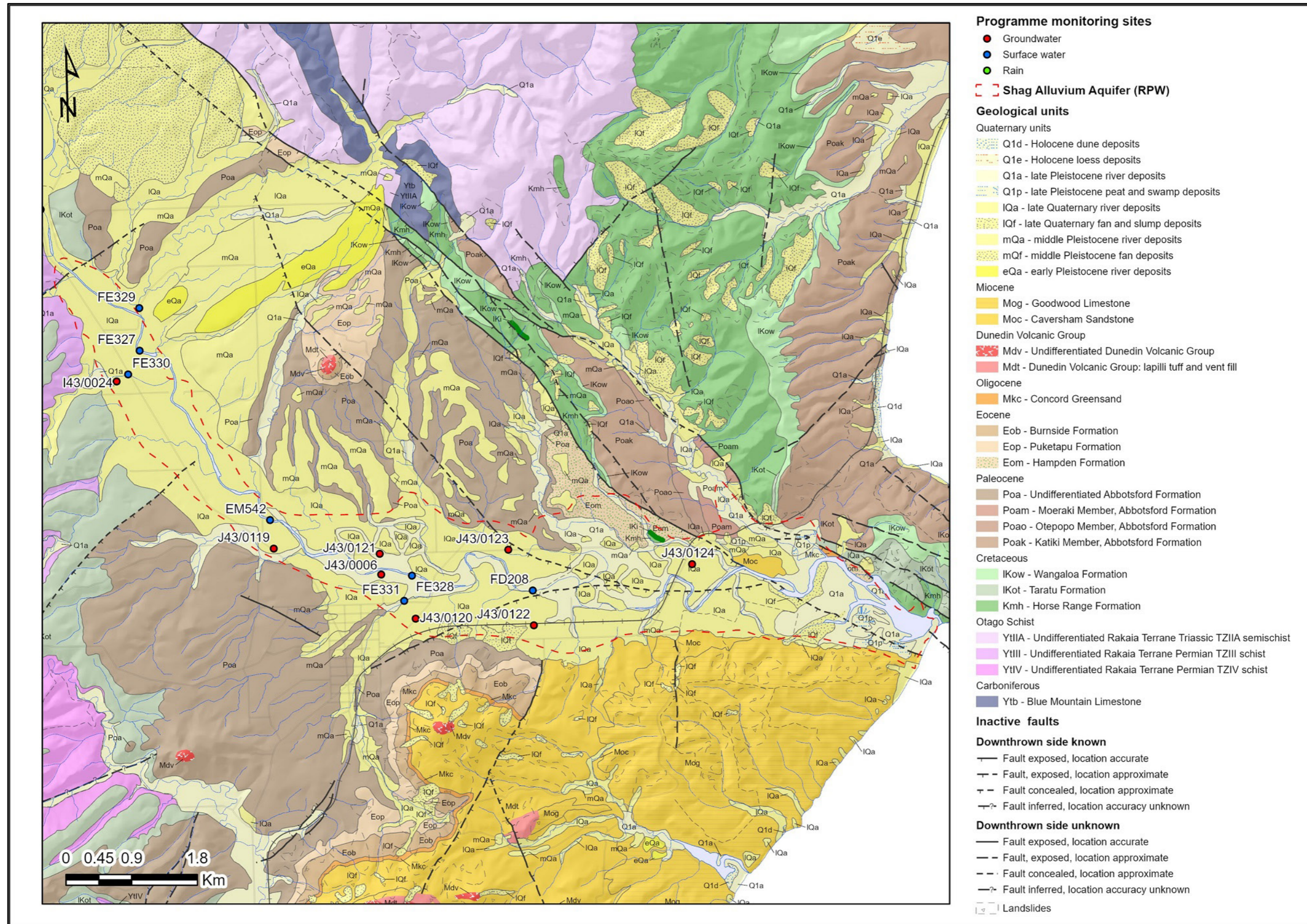


Figure 2.3 Geology of the Lower Waihemo/Shag River Valley (Martin et al. 2021) with the Otago Regional Council Regional Plan: Water (RPW) Shag Alluvial Aquifer boundary and programme monitoring sites (see Section 2.2 for more details on monitoring sites).

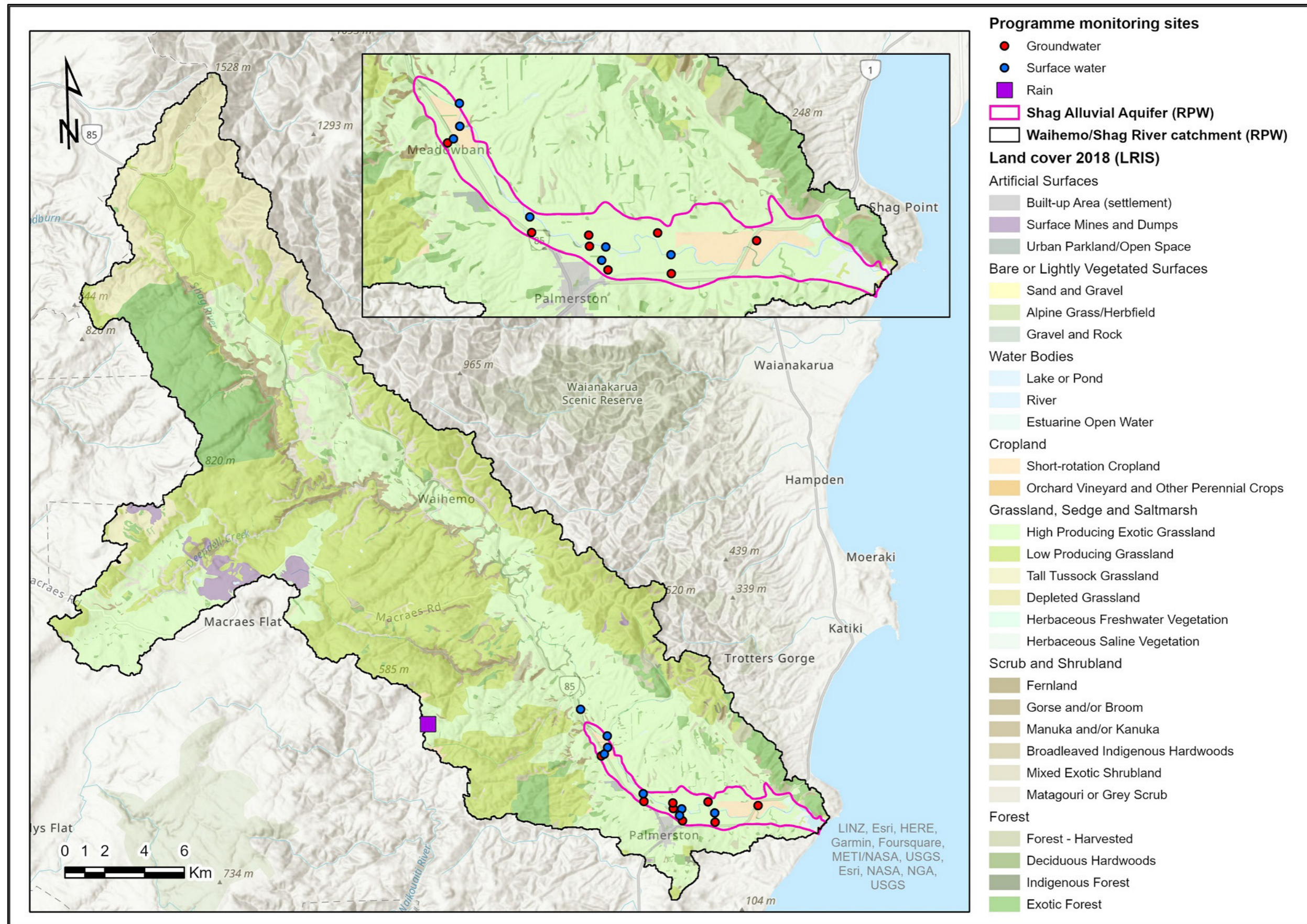


Figure 2.4 Land cover classes in the Waihemo/Shag River catchment (as mapped in 2018 by Manaaki Whenua Landcare Research (2022) and available in the Land Resource Information System (LRIS) Portal) with the Otago Regional Council Regional Plan: Water (RPW) Shag Alluvial Aquifer boundary and programme monitoring sites (see Section 2.2 for more details on monitoring sites).

2.1.5 Soils and Land Use

2.1.5.1 Soils

Soils in the Lower WS River Valley (Appendix 4; Manaaki Whenua Landcare Research 2022) originate from alluvium or loess and include the following types:

- Silty soils (e.g. Claremont, Eyre, Timaru, Waimakariri, Barrhill, Taitapu, Wakanui).
- Sandy soils (e.g. Greenpark, Rangitata).
- Loamy soils (e.g. Rakaia).

Soil depth varies from very shallow (10–20 cm) to deep (>1 m). Soils located on the WS River margins are usually classified as ‘well drained’, while soils present on the valley margins or close to the estuary are mostly ‘poorly drained’. The nitrogen leaching susceptibility of these soils ranges from ‘very high’ (e.g. for most of the soils bordering the WS River) to ‘low’ for soils located near the estuary (Appendix 4; Manaaki Whenua Landcare Research 2022).

2.1.5.2 Land Use

The WS River catchment is dominated by agricultural and forestry land use (Figure 2.4). In 2018, the main land use classes were ‘low producing’ and ‘high producing exotic’ grasslands, covering ~42% and 33% of the catchment, respectively (LRIS Portal 2020). Other represented classes were ‘exotic forest’, ‘tall tussock grassland’ (9% of the catchment each), ‘matagouri or grey scrub’ and ‘gorse and/or broom’ (3% of the catchment each).

Other land uses are ‘surface mine or dump’ and ‘short-rotation crops’ (1% of the catchment each in 2018). Macraes Gold Mine (near Macraes Flat, Figure 2.4) is operated by Oceana Gold in the catchment of Deepdell Creek. Discharge of mine tailings into this tributary of the WS River has historically affected the riverbed morphology (Black et al. 2004).

The main land uses mapped within the SAA boundary are ‘high producing exotic grassland’ and ‘short-rotation crops’ (Figure 2.4).

Irrigation is practiced in the Lower WS River Valley (e.g. pivot, K-lines; Ministry for the Environment Data Service 2017). However, agricultural development has been constrained by the lack of water availability in the catchment (i.e. primary allocation is currently over-allocated; Olsen and Ozanne 2014).

2.2 Otago Regional Council Monitoring Programme

2.2.1 Background

The 2016–2017 ORC Annual Plan included implementing a freshwater monitoring programme to improve the freshwater quality in the Lower WS River Valley (Mourot 2018). The SAA is currently classified as a ‘nitrogen sensitive zone’ in the RPW, with a maximum nitrogen load threshold of 20 kg/ha/yr (Otago Regional Council 2004). The RPW also includes a provision to include aquifer nitrogen concentration limits to complement freshwater quality protection policies (table in Schedule 15.3).

The objectives of the ORC monitoring programme were to:

- Better characterise the geometry of the aquifer (lateral extent and thickness) by drilling eight new bores.

- Derive hydraulic properties of the aquifer by using slug tests.
- Better characterise the groundwater flows and interaction between groundwater and surface water by (i) monitoring groundwater and surface water levels and river flows, (ii) undertaking radon investigations, and (iii) monitoring the hydrochemistry.
- Identify recharge sources and assess groundwater ages by sampling for stable and age dating isotopes.
- Assess the quality of the SAA and WS River and the impact of land use by monitoring groundwater and surface water chemistry, with a focus on nitrogen (e.g. high-frequency nitrate monitoring).

2.2.2 Otago Regional Council Initial Investigations

2.2.2.1 Bore Investigation

ORC undertook an initial investigation in 2016 to identify potential bores that could be used for monitoring purposes in the Lower WS River Valley. Apart from well I43/0024 (near Mc Elwee Road), it was not possible to use existing bores. The main reason was that several bores recorded in the ORC database could not be found in the field. Most of the bores mentioned in previous studies (e.g. Cameron et al. 2003) have probably been backfilled since. ORC decided to drill and install new bores to implement the monitoring programme.

2.2.2.2 Radon Investigation

To help with the selection of drilling sites, ORC commissioned GNS to undertake a radon (^{222}Rn) survey to characterise the interaction between the WS River and the SAA (Martindale and Lovett 2017; Mourot 2018).

^{222}Rn is a soluble gas and a short-lived isotope (half-life ~3.8 days) which is an intermediate daughter from the decay of ^{238}U , occurring at very low levels in most rocks and soils. Radon is typically abundant in groundwater, whereas surface water concentrations are negligible due to degassing. Identification of elevated radon concentrations in rivers therefore indicates groundwater discharge to the river. However, groundwater fluxes based on radon concentrations alone can yield over-estimated flux rates due to the additional radon source contribution from parafluvial and hyporheic flow² (Cartwright and Hofmann 2016). Simplified estimations of the hyporheic zone area, and thus the radon contribution from hyporheic flow, can be made (Cartwright and Hofmann 2016; Tonina and Buffington 2011), but the contribution from parafluvial flow is uncertain. Therefore, the contribution of parafluvial flow to a river system using radon concentrations was also investigated in this study.

Samples were collected along a 16 km reach of the WS River, where groundwater-surface water interaction was inferred. Fieldwork was undertaken in February 2017, under low flow conditions (~0.32 m³/s at EM495/Craig Road). Surface water samples were collected from 27 sites along the WS River at ~500 m intervals, and two groundwater samples were collected from shallow bores. Stream flow measurements were undertaken by ORC at seven concurrent sites (Figure 4.15 (top), Appendix 9). At each location, field parameters including electrical conductivity (EC), temperature, and dissolved oxygen (DO) were collected when possible (Appendix 5).

² The parafluvial zone is located in the area that is flooded during high flows and dries during low flows. The hyporheic zone is the region of sediment beneath and alongside a stream bed, where shallow groundwater and surface water are mixing.

The results of the February 2017 sampling campaign were summarised by Martindale and Lovett (2017), and showed that groundwater discharge could be identified in several areas along the WS River study area. The weak correlation between radon and flow gauge data suggests a highly interconnected and active parafluvial system in the WS River system, which interacts with the groundwater flows. The water from bore J43/0006 located near the riverbank yielded a radon concentration of 17.0 Bq/L, which suggests that it is highly connected to the river system. This contrasts with bore I43/0024 with a radon concentration of 179.5 Bq/L.

The February 2017 radon data provided more detailed information about groundwater discharge patterns than the flow gauge data alone. However, it also highlighted highly heterogeneous discharge along the river (see Section 4.2.3.2). Specifically, radon was relatively low near Craig Road and increased over the first 1.5 km of the river (north of bore I43/0024), suggesting groundwater discharge was more important over this area (Figure 4.15). Similarly, north of bore J43/0119, some segments of the river had elevated radon (2.05 to 3.34 Bq/L; Figure 4.15).

Based on these results, Martindale and Lovett (2017) recommended a high-resolution radon sampling study to refine the rate at which radon degasses from the river. This data was collected with the support of ORC staff to investigate where radon measurements indicated groundwater discharge compared to signals from degassing. Therefore, a further 30 radon samples from the WS River were collected from 20 to 21 March 2017, at a finer spatial interval (200 m) and under slightly higher flow conditions (~0.56 m³/s at EM495/Craig Road). At this time, four samples were also collected from within the riverbed gravels to investigate potential parafluvial flow. One additional groundwater sample was collected from bore BH2WDC (near Horse Range Road bridge) on 23 March 2017. Finally, in October 2017, six bore samples were collected for radon, including re-sampling at site I43/0024 (Appendix 5). Results of the March and October 2017 radon investigations have not been previously published and are presented in this report (Section 4.2.3.2).

2.2.3 Otago Regional Council Monitoring Sites Installation and Data Collection

The drilling investigations took place in July and August 2017 and led to (i) the completion of eight machine boreholes (rotary and sonic drilling in 140 mm and 75 mm, respectively; lithological logs in Appendix 3) and (ii) the installation of six (100 mm or 50 mm ID PVC) piezometers (Mourot 2018).

Pressure transducers were installed in five piezometers (J43/0119, J43/0121, J43/122 and J43/124) and at two river sites (EM542/Switchback Road and FD208/Shakey Bridge) to monitor groundwater levels and river stage, respectively, with a 15 min time step. High-frequency nitrate sensors were also installed at three surface water sites (EM495/Craig Road, EM542/Switchback Road and FD208/Shakey Bridge) in July 2017 and in bore J43/0121 in December 2017 (details in Section 2.2.3.2).

In addition to these new monitoring sites, existing State of the Environment (SOE) monitoring sites were also used, including:

- EM495, monitoring the WS River stage, flow and water quality (surface water suite) at Craig Road.
- J43/0006, monitoring the water quality of the SAA at Palmerston water supply.

Lastly, rainfall data was obtained by using Stoneburn rain gauge station (EM359).

2.2.3.1 Monitoring Sites used in the Programme

The established monitoring programme included eight bores, eight surface water sites and one rainfall site (details of the monitoring sites and monitoring parameters in Table 2.3; location of the sites in Figure 2.3 and Figure 2.4).

2.2.3.2 High-Frequency Nitrate Monitoring

High-frequency (continuous) monitoring has gained interest in New Zealand over the last five years, with a majority of deployments in riverine environments. In situ sensors allow the characterisation of rapid water quality changes that are not captured by discrete (spot) sampling and could affect human and aquatic health (Hudson and Baddock 2019).

Accordingly, four high-frequency nitrate monitoring sites were installed near other programme monitoring sites recorders (Table 2.4; Figure 2.3). The aim was to improve the current characterisation of nitrate concentrations in the river and in the groundwater, but also to help constrain groundwater and surface water interaction:

- Three TriOS NICO sensors (hyperspectral instruments) were installed by ORC in July 2017 in the WS River. The TriOS NICO sensor uses four detection channels that enable optical determination of nitrate by absorption and also compensates for turbidity. Conductivity and temperature were also monitored (TriOS 2022; Appendix 6).
- One HydroMetrics GW50 groundwater nitrate sensor was installed by Lincoln Agritech in December 2017 in a borehole tapping the SAA: bore J43/0121³. This sensor uses optical technology and also compensates for turbidity (HydroMetrics 2022; Appendix 6).

ORC staff also collected manual grab samples to verify and calibrate the high-frequency monitoring data (regime indicated in Table 2.4).

³ The preferred site was J43/0119, but it could not be used due to the insufficient water height in the piezometer at the time of the installation.

Table 2.3 Summary of the Otago Regional Council monitoring programme: sites and parameters monitored.

Location ID ¹	Other Name or ID	Type ²	NZTM Easting	NZTM Northing	Quality Monitoring ³	Quantity Monitoring	Start Date ⁴	End Date ⁴
I43/0024	NA	GW	1418246	4964766	GW suite + silica	HF GW level	29/08/2017	On-going
J43/0119	Shag at Bore 3 or BH3	GW	1420396	4962478	GW suite + silica	HF GW level	18/08/2017	On-going
J43/0120	Shag at Bore 4 or BH4	GW	1422339	4961519	GW suite + silica	Manual GW level	18/10/2017	20/09/2018
J43/0121	Shag at Bore 5 or BH5	GW	1421850	4962405	GW suite + silica + HF nitrate	HF GW level	18/08/2017	On-going
J43/0122	Shag at Bore 6 or BH6	GW	1423961	4961427	GW suite + silica	HF GW level	29/08/2017	On-going
J43/0123	Shag at Bore 7 or BH7	GW	1423610	4962461	GW suite + silica	Manual GW level	15/08/2017	20/09/2018
J43/0124	Shag at Bore 8 or BH8	GW	1426129	4962266	GW suite + silica + HF conductivity	HF GW level	29/08/2017	On-going
J43/0006	Palmerston water supply	GW	1421870	4962122	GW SOE suite	Manual GW level	1995	On-going
EM495	Shag at Craig Road	SW	1417203	4967124	GW suite + silica + HF nitrate	HF stage/flow	1995	On-going
FE327	Shag at Jones Road Ford	SW	1418559	4965189	GW suite + silica	Flow, monthly gauging	27/02/2017	26/05/2020
EM542	Shag at Switchback Road	SW	1420348	4962869	GW suite + silica + HF nitrate	HF stage/flow, monthly gauging	12/09/2017	11/07/2018
FE328	Shag at Mill Road	SW	1422290	4962110	GW suite + silica	Flow, monthly gauging	12/09/2017	7/08/2018
FD208	Shag at Shakey Bridge	SW	1423945	4961907	GW suite + silica + HF nitrate	HF stage/flow, monthly gauging	18/07/2017	28/05/2020
FE329	Blue Mountain Creek at confluence	SW	1418556	4965770	GW suite + silica	-	-	-
FE330	McElwee Creek at Palmerston-Dunback Road	SW	1418403	4964865	GW suite + silica	-	-	-
FE331	Township Creek at confluence	SW	1422184	4961763	GW suite + silica	Tentative gauging ⁵	-	-
EM359	Shag at Stoneburn rainfall site	Rain	1409542	4966370	NA	HF rainfall monitoring	1985	On-going

¹ Location of the sites is provided in Figure 2.3 and Figure 2.4. Lithological logs for the drilled bores are provided in Appendix 3.

² GW: groundwater; SW: surface water.

³ The water monitoring data used in this study is from July 2017 to September 2018. For HF nitrate monitoring, dates are provided in Table 2.4.

⁴ Start and end dates are for water quantity monitoring.

⁵ The monitoring site was not suitable for gauging measurement.

HF: high-frequency (= continuous).

Table 2.4 Summary of the technical specifications and monitoring sites for the high frequency nitrate sensors.

Sensor	Measurement Range (mg/L NO ₃ -N)	Measurement Accuracy (mg/L NO ₃ -N)	Site ID	Other Site ID or Name	Type ¹	Start Date	End Date ²	Time Step used for High-Frequency Sensors	Frequency Grab Samples ³
TriOS NICO	0.05–6	± 5% + 0.1	EM495	Shag River at Craig Road	SW	18/07/2017	On-going	15 min	Weekly
			EM542	Shag River at Switchback Road	SW		11/07/2018		
			FD208	Shag River at Shakey Bridge	SW		28/05/2020		
HydroMetrics GW50	0–60	± 5% + 0.1	J43/0121	Shag at Bore 5 or BH5	GW	20/12/2017	17/10/2018	24 h	Monthly

¹ SW: surface water; GW: groundwater.

² In this report, high-frequency data has been analysed until 31/08/2018 (c. end of the study monitoring programme).

³ After calibration period. Calibration period required more frequent grab sampling.

2.2.4 Otago Regional Council and Otago Regional Council-led Complementary Investigations

2.2.4.1 Slug Tests

Slug tests are used to estimate aquifer materials' hydraulic properties in the tested bore's immediate vicinity. A change in hydraulic conditions is initiated by dropping/removing a solid object (a mechanical slug) or adding water to the water column. The water-level fluctuations in the bore are recorded to capture the induced change in the hydraulic head, until a static water-level is reached. Slug tests were undertaken in June 2018 at bores J43/0119, J43/0120, J43/0121, J43/0122, J43/0123 and J43/0124 (Mourot 2018; Appendix 7; bore locations shown in Figure 2.3).

2.2.4.2 Stable Isotopes

The stable isotope composition of meteoric water depends on the history of the water masses with regard to temperature-dependent kinetic processes, such as evaporation of water from the sea and re-precipitation. For example, rivers from colder, higher-altitude catchments usually have a depleted (more negative) isotope composition than local low-altitude rain near the coast. Thus, the isotopic composition of groundwater can be used to distinguish whether recharge is derived from the river or from local rainfall. Similarly, the stable isotope composition of surface waters can be used to investigate contributions from local versus distal sources – particularly if the sources have distinct isotopic ratios.

The stable isotope ratios $^{18}\text{O}/^{16}\text{O}$ and $^2\text{H}/^1\text{H}$ are expressed using δ (delta) notation and represent the difference in parts per thousand between isotope ratios in water relative to those in Vienna Standard Mean Ocean Water (V-SMOW): $\delta^{18}\text{O} (\text{‰}) = [(^{18}\text{O}/^{16}\text{O})_{\text{sample}} / (^{18}\text{O}/^{16}\text{O})_{\text{VSMOW}} - 1]$. $\delta^2\text{H}$ is expressed in a similar way. Stable isotope analyses for this study were carried out in the Stable Isotope Laboratory at GNS Science (Lower Hutt). Water samples were analysed following methods described by Lis et al. (2008) using an Isoprime mass spectrometer; for $\delta^{18}\text{O}$ by water equilibration at 25°C using an Aquaprep device, for $\delta^2\text{H}$ by reduction at 1100°C using a Eurovector Chrome HD elemental analyser.

All results are reported with respect to V-SMOW2, normalised to internal standards: SM1 with reported values of -29.12‰ for $\delta^{18}\text{O}$, -227.4‰ for $\delta^2\text{H}$, and INS11 with reported values of -0.36‰ for $\delta^{18}\text{O}$, -3.8‰ for $\delta^2\text{H}$. The analytical precision for this instrument is $\pm 0.2\text{‰}$ for $\delta^{18}\text{O}$ and $\pm 2.0\text{‰}$ for $\delta^2\text{H}$.

2.2.4.3 Water Dating and Tracer Measurements

Three shallow groundwater samples and one river water sample were collected in December 2017 (summer, low flow conditions) and May 2018 (winter, high-flow conditions) to improve the understanding of water dynamics (e.g. groundwater residence times and groundwater-surface water interaction) in the Lower WS River Valley. Tritium, chlorofluorocarbons (CFCs), sulphur hexafluoride (SF_6) and halon were measured from groundwater sites, and tritium was also measured from one surface water site. The methods and results were originally presented by van der Raaij (2019) and are summarised below.

Tritium (^3H) is a component of the water molecule and forms an ideal tracer for groundwater studies. Model ages, including mean residence time and minimum residence time, using tritium is based on radioactive decay of tritium after rainwater penetrates the ground during recharge. The half-life of tritium is 12.32 years. Tritium is produced naturally by cosmic radiation in the

upper atmosphere but was also released into the atmosphere by nuclear weapons testing (Stewart and Morgenstern 2001). A single tritium analysis may give ambiguous residence times because of this irregularly shaped peak in abundance over the last 70 years (e.g. International Atomic Energy Agency 2006). Often this will be resolved by measuring the change in tritium concentration in groundwater over a time interval of a few years or by comparison to CFCs and SF₆ data from the same samples.

Halon-1301 and CFCs are entirely synthetic gaseous compounds. Significant production of CFCs began in the 1930s and halon-1301 in the 1950s. SF₆ is predominantly anthropogenic, with industrial production starting in the 1950s. However, a small amount of SF₆ is also produced in certain volcanic minerals and fluids. Groundwater dating using CFCs, SF₆ and halon-1301 is possible due to the steady increase in atmospheric concentrations of these gases since production began. These gases are dissolved in recharge waters and are isolated from the atmosphere when this recharge enters the groundwater zone. Thus, the gases hold a record in the groundwater of past atmospheric concentrations. CFCs have been measured continuously in the atmosphere at various sites worldwide since the late 1970s. However, CFC concentrations have begun to decline since they were phased out following the Montreal Protocol in 1987, and therefore CFCs have lost some effectiveness for age-dating over this period (International Atomic Energy Agency 2006).

The results and interpretations (van der Raaij 2019) are summarised below (Table 2.5; Figure 2.5). At sites J43/0119 and J43/0121, the groundwater was relatively young, with mean residence times (MRTs) of 2 to 3 years and with no statistically significant difference in age during the winter (May) versus summer (December). The oldest groundwater was found at site J43/0122, with MRTs of 20 and 22 years in the summer and winter, respectively. This older age is consistent with the bore being screened at a greater depth within a confined aquifer.

Groundwater ages – MRTs and minimum residence times – were calculated assuming 70% exponential-piston mixed flow. Surface water sample EM495 was calculated using a higher proportion of exponential-piston flow mixing (80%; Table 2.5) to better approximate the wide range of travel times for water at the sampling location. It should be noted that the calculated ages are relatively insensitive to the model parameters; changing the proportion of exponential-piston mixed flow altered the calculated MRT by less than ± 1 year.

Model results yielded MRT of c. 2 to 3 years for sites within the unconfined aquifer (J43/0119 and J43/0121) and, including uncertainty overlapped with the MRTs for the surface water samples at site EM495. The river water ages being similar to ages of the alluvial aquifer sites highlights the likelihood of interaction between groundwater and surface water in the Lower WS River Valley.

Although there was no resolvable difference in MRT during the winter versus summer, Halon, CFC-12 and CFC-13 concentrations were slightly elevated in the winter for sites J43/0121 and J43/0122, which are located north and northeast of Palmerston (Appendix 5).

Table 2.5 Groundwater (GW) and surface water (SW) site information, the percent exponential-piston model (EPM) flow used to calculate ages, and the mean residence time and minimum residence time results including estimated uncertainty.

Sample ID	Sample Type	Bore Depth (Screened Depth)	Aquifer Lithology	Aquifer Confinement	Sample Date	EPM (%)	Mean Residence Time (Years)	Minimum Residence Time (Years)
J43/0119-Dec	GW	4.3 (2.5–4.0)	Alluvium	Unconfined	14/12/2017	70	3 ± 1	0.9 ± 0.3
J43/0119-May					22/05/2018		2 ± 1	0.6 ± 0.3
J43/0121-Dec		5 (1.5–4.5)	Alluvium	Unconfined	14/12/2017		2 ± 1	0.6 ± 0.3
J43/0121-May					22/05/2018		2 ± 1	0.6 ± 0.3
J43/0122-Dec		10 (6.5–9.5)	Alluvium	Confined	14/12/2017		20 ± 1	6.0 ± 0.3
J43/0122-May					22/05/2018		22 ± 1	6.6 ± 0.3
EM495-Dec	SW	-	-	-	14/12/2017	80	3 ± 1	0.6 ± 0.3
EM495-May					22/05/2018		2 ± 1	0.4 ± 0.3

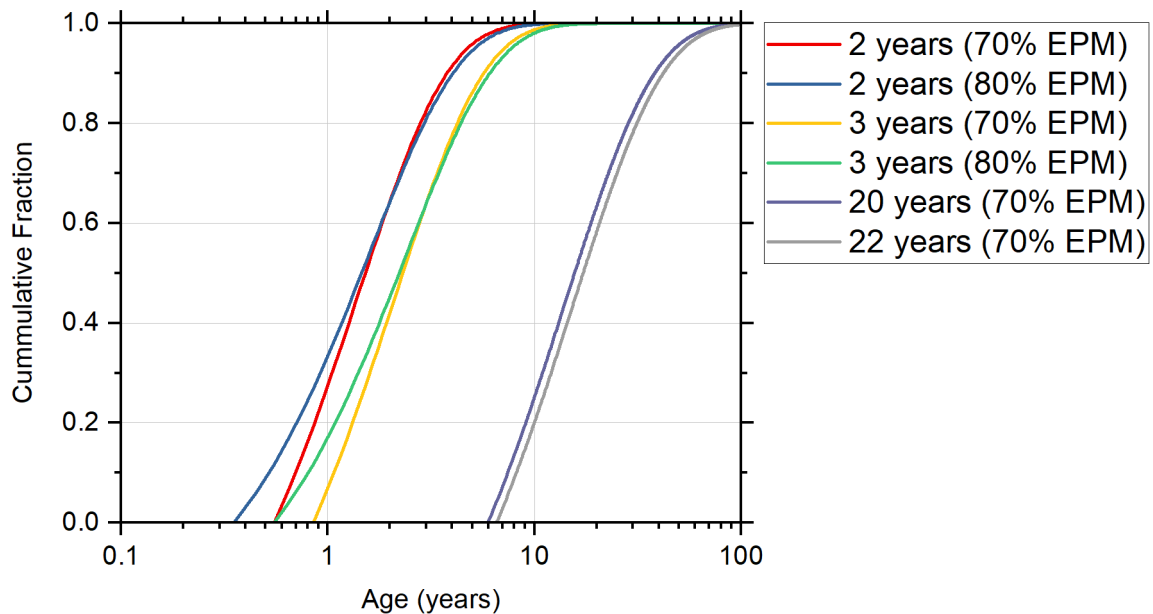


Figure 2.5 Modelled cumulative residence time distributions and mean residence times of 2, 3, 20 and 22 years were calculated using 70% and 80% exponential piston-flow models (EPM), which yielded age distributions for groundwater and surface water sites measured in this study.

3.0 DATA INTERPRETATION METHODS

3.1 Groundwater Quantity

3.1.1 Aquifer Boundary

The lateral extent of the aquifer was questioned due to the existence of several dry bores within the current SAA boundary.

To refine the current delineation of the SAA (see RPW), we used:

- The data collected as part of the ORC monitoring programme (e.g. lithological logs of the drilled bores, groundwater levels and river stage levels).
- Data from other studies, e.g. geological map of Martin et al. (2021), and LiDAR data acquired in May 2017 by Aerial Surveys (2017).

To compare the elevation of the WS River stage with the groundwater elevation, all the water level data available was used:

- For the SAA: the groundwater level data collected as part of the monitoring programme and records from the ORC well database (i.e. often the depth to groundwater recorded after drilling of the bore).
- For the WS River: the river stage data collected as part of the monitoring programme and the river stage inferred from the May 2017 LiDAR survey. This was done by extracting the elevation at the places where radon samples were collected in the river in February 2017.

3.1.2 Aquifer and River Hydrographs

Mean daily values of groundwater levels (five sites) for the SAA and mean daily values of WS River stage (three sites) were used to prepare aquifer and WS River hydrographs. The groundwater level data collected manually (two sites) was also added to complement this dataset. All levels (river stage and groundwater levels) were converted to the same datum i.e. Above Mean Sea Level in metres (AMSL m) by using surveyed reference points (e.g. top of casing for the bores; Mourot 2018). Mean daily rainfall at the closest rainfall site (EM359/Stoneburn) was also plotted for reference.

3.1.3 Piezometric Maps

Timeseries of groundwater levels were analysed to determine periods where the groundwater levels were at the lowest and the highest between July 2017 and August 2018. Two dates close to these periods (i.e. 16/01/2018 and 22/05/2022) for which groundwater level were manually measured were then selected to have additional groundwater level data. Groundwater levels were converted to the same datum (AMSL m). Piezometric contours were created using the Kriging method in ArcGIS Pro to interpolate contours from data points.

3.1.4 Aquifer Hydraulic Properties

Hydraulic properties were derived from slug tests undertaken in June 2018 by the ORC (Section 2.2.4.1) for three bores. Due to technical issues in the field (e.g. not enough water displacement generated in the bores), the data collected for bores J43/0119, J43/0120 and J43/0121 did not allow for a reliable estimation of the hydraulic conductivity (Appendix 7). As a result, those tests were not included in the analysis of this report. Five other slug tests undertaken at bores J43/0122, J43/0123 and J43/0124 were analysed using AQTESOLV Pro

software (Table 3.1). The early response part of the tests was used for hydraulic conductivity estimation. According to Sun and Koch (2014), this did not lead to over-estimations considering the bore settings. Transmissivity was estimated by multiplying the conductivity by the aquifer thickness estimated at the bores. For unconfined conditions, the aquifer thickness was calculated as the difference between the static water level measured before the slug tests and the bore depth (corresponding to the hydrogeological basement). For the confined bore, the aquifer thickness was estimated as the difference between the bottom of the confining layer and the bore depth (corresponding to the hydrogeological basement).

Table 3.1 Summary of the slug test analyses.

Bore ID	Confinement Status	Slug Test Type used for Analysis*	Solution used
J43/0122	Confined	Slug falling head	Hvorslev (1951) early response
		Slug rising head	
J43/0123	Unconfined	Water falling head	Bouwer and Rice (1976) early response
		Slug rising head	
J43/0124	Unconfined	Water falling head	

* The best quality tests were used for analysis. Some tests (e.g. slug falling head for J43/123) were not used because they resulted in 'noisy' responses.

3.2 Groundwater Quality

3.2.1 Hydrochemistry Data

The hydrochemistry monitoring data consists of water analyses collected at one rainfall site, eight groundwater bores and eight surface water sites located within the Lower WS River Valley (Table 2.3). Groundwater bore screen depths range from 1.5 m to 9.5 m below ground level (Appendix 7). The bulk of the data consists of water sampled between July 2017 and September 2018. Bore I43/0024 has been monitored between 1995 and 2000 and J43/0006 since 1995 as a SOE monitoring bore. The surface water site EM495/WS River at Craig Road has been monitored since 1989, with less frequent monitoring from c. 2000 onwards. The sampling frequency varies from monthly at groundwater sites, and most surface water sites, to weekly measurements at surface water sites EM495, EM542 and FD208 reduced to monthly observations from February 2018.

The hydrochemistry dataset provided by ORC consists of up to 84 parameters, including field parameters, laboratory analyses, microbiological indicators and ecosystems monitoring (e.g. taxa richness or Macroinvertebrate Community Index). In this report, a subset of the dataset was extracted which included the following parameters measured at the time of sampling: pH, temperature, EC, DO and groundwater level; and the following laboratory parameters: calcium (Ca), magnesium (Mg), potassium (K), sodium (Na), bicarbonate (HCO₃), chloride (Cl), sulphate (SO₄), boron (B), bromide (Br), fluoride (F), total silica (SiO₂), total oxidised nitrogen (NNN), nitrate-nitrogen (NO₃-N), nitrite-nitrogen (NO₂-N), ammonia (NH₃-N), dissolved iron (Fe), dissolved manganese (Mn), dissolved arsenic (As), dissolved chromium (Cr) and dissolved reactive phosphorus (DRP). All samples were analysed at Hill Laboratory.

Four unusually high or low EC measurements were identified and inferred to be associated to a unit conversion error. They were subsequently modified after examination of the time series at each site. One pH measurement was recorded below 2 at Bore J43/0121 and was removed for time series examination.

3.2.2 Nitrate Concentrations and Loads

3.2.2.1 High-Frequency Nitrate Data Cleaning and Processing

ORC provided high-frequency nitrate data as hourly and daily average data (csv files) for surface water and groundwater, respectively. Hudson and Baddock (2019) concluded that for most purposes, hourly average or even daily average data appeared adequate in their review of high-frequency water quality data using case studies in Otago (Kakanui River) and Southland (Aparima River).

High-frequency nitrate data was cleaned to remove:

- Data collected during the calibration period (e.g. December 2017 to February 2018 data for groundwater).
- Erroneous data (e.g. negative data in the WS River after high-flow events), as inferred to be due to fouling or post-cleaning issues.

In addition, a 'tentative' bias correction was undertaken for all sensors (TriOS NICO and HydroMetrics GW50), as a systematic error was observed in comparison to the grab samples for each sensor. The observed biases were inferred to be due to optical interferences with natural waters (Hudson and Baddock 2019). The nitrate concentrations derived from high-frequency sensing were higher than the grab samples, with differences of ~0.065 mg/L, ~0.08 mg/L, and ~0.22 mg/L for WS River at EM542/Switchback Road, FD208/Shakey Bridge and EM495/Craig Road, respectively. For groundwater (SAA at J43/0121), nitrate concentrations derived from high-frequency sensing were ~0.65 mg/L higher than grab samples over the 5/03/2018–5/06/2018 period, and, after further maintenance (21/06/2018–31/08/2018 period), only ~0.05 mg/L higher. A 'tentative' bias correction was applied to the raw data with the offset values mentioned above. However, this bias correction might require further analysis (see Pellerin et al. 2013 and Section 5.2).

The 'cleaned and processed' high-frequency data was then plotted in relation to:

- WS River stream flow, rainfall (EM359/Stoneburn station) and grab samples data for the WS River sites (i.e. EM495/Craig Road, EM542/Switchback Road and FD208/Shakey Bridge), using hourly time steps.
- Groundwater elevation (SAA at J43/012), rainfall (EM359/Stoneburn station) and grab sample data for the groundwater site (SAA at J43/0121), using daily average data.

3.2.2.2 Calculations of Nitrate Loads

Nitrate loads correspond to the calculation of the flux of nitrate transported in a river. In addition to contaminant concentrations, contaminant loads are important metrics of the National Policy Statement for Freshwater Management freshwater quality accounting system (Ministry for the Environment 2020). In particular, contaminant load calculations are required to manage land-based activities. The contaminant loads delivered by a river catchment correspond to the product of the river flow and the contaminant concentration.

Hudson and Baddock (2019) report that the uncertainty in the load estimation decreases as the frequency of concentration measurement increases. These authors showed that daily measurements are adequate for load estimation based on the results of the Kakanui River and Aparima River case studies (Otago and Southland, respectively). Therefore, we estimated daily mean nitrate loads at three WS River sites (i.e. EM495/Craig Road, EM542/Switchback

Road and FD208/Shakey Bridge) for each month between September 2017 and August 2018, by using the following data for each site:

- a) Daily mean flow data for each month.
- b) Daily mean nitrate concentrations for each month:
 - Calculated from high-frequency nitrate monitoring.
 - Inferred from the grab samples collected over these months.

Differences between months (or seasons) and between sites (upstream to downstream) were also investigated.

3.2.3 Water Dating and Tracer Measurements

As mentioned earlier (Section 2.2), the tritium model ages, and the first radon sampling campaign (February 2017), were analysed prior to this study. The focus of the current work was therefore to: (i) report on and interpret tracer result data not covered by any previous study (e.g., stable isotope data, second radon sampling campaign in March 2017); and (ii) synthesise the different data collected and their insights in terms of SAA dynamics' characterisation (e.g. potential groundwater discharge to the WS River).

3.2.3.1 Stable Isotope Data

Stable isotope compositions measured in the Lower WS River Valley (surface water and groundwater samples) were compared to the local meteoritic water line to investigate isotopic signatures.

3.2.3.2 Radon Data

Results from the second radon sampling campaign (March 2017) and collected groundwater samples were mapped and interpreted in relation to previous understanding (Martindale et al. 2017; Martindale and Lovett 2017). A synthesis of the knowledge resulting from the different radon investigations was then undertaken.

3.3 Conceptual Models

Two types of conceptual models for the SAA were developed:

- SAA structure and its interaction with the WS River.
- Water inputs and outputs to and from the SAA.

The models were based on (i) aquifer characterisation acquired through Lower WS River Valley investigations, (ii) literature on the interaction of shallow aquifers and rivers in alluvial valleys, and (iii) inferences based on local observations and hydrogeological expertise.

4.0 RESULTS OF THE STUDY AND DISCUSSION

4.1 Groundwater Quantity

4.1.1 Aquifer Boundary

The current SAA boundary is delineated in the RPW (Otago Regional Council 2004) and includes Late Pleistocene river deposits (Q1a; beige colour in Figure 4.1, Figure 4.2 and Figure 2.3) and older late Quaternary river deposits (IQa; light yellow in Figure 4.1, Figure 4.2 and Figure 2.3) located adjacent to the WS River. However, several drilling campaigns (e.g. mentioned by Mourot (2018) and Turnbull and Fraser (2005)) encountered dry bores within this boundary. Lithological logs report the occurrence of shallow mudstone in most bores.

In the northwest area of the Lower WS River Valley (Figure 4.1; between Craig Road and Sutherland Road), the elevation of the mudstone (e.g. on Jones Road) was higher than the water elevation in the river (e.g. near Jones Road ford) and in the aquifer (closest bore north of Mc Elwee Road). An interpretation is proposed later (Section 4.3.1) that suggests redefining the SAA boundary based on the findings herein.

In the central area (Figure 4.2; between Sutherland Road and east of Horse Range Road), the bores located on the SAA southern margins showed higher groundwater levels than the river levels. Bores located on the left bank of the WS river generally had lower groundwater levels than river levels. A few dry bores could suggest the need (i) to narrow the northern SAA boundary to exclude Tertiary sediments (brown colour in Figure 4.2), e.g. draw the boundary closer to Fleming Road; and (ii) to pinch the boundary east of Horse Range Road to exclude the dry bores where the mudstone is very shallow.

In the southeast area (Figure 4.3; between east of Horse Range Road and the coast), the water levels were relatively similar between groundwater and the river, with a flattening of the topography and an inferred reduction of the water table slope. River water levels were also influenced by the tides. A few dry bores have been drilled near the northern SAA boundary (mainly in Tertiary sediments (brown colour in Figure 4.3)). We suggest excluding these Tertiary sediments from the aquifer boundary polygon and bringing the northern SAA boundary closer to Fleming Road and the recent alluvial sediments.

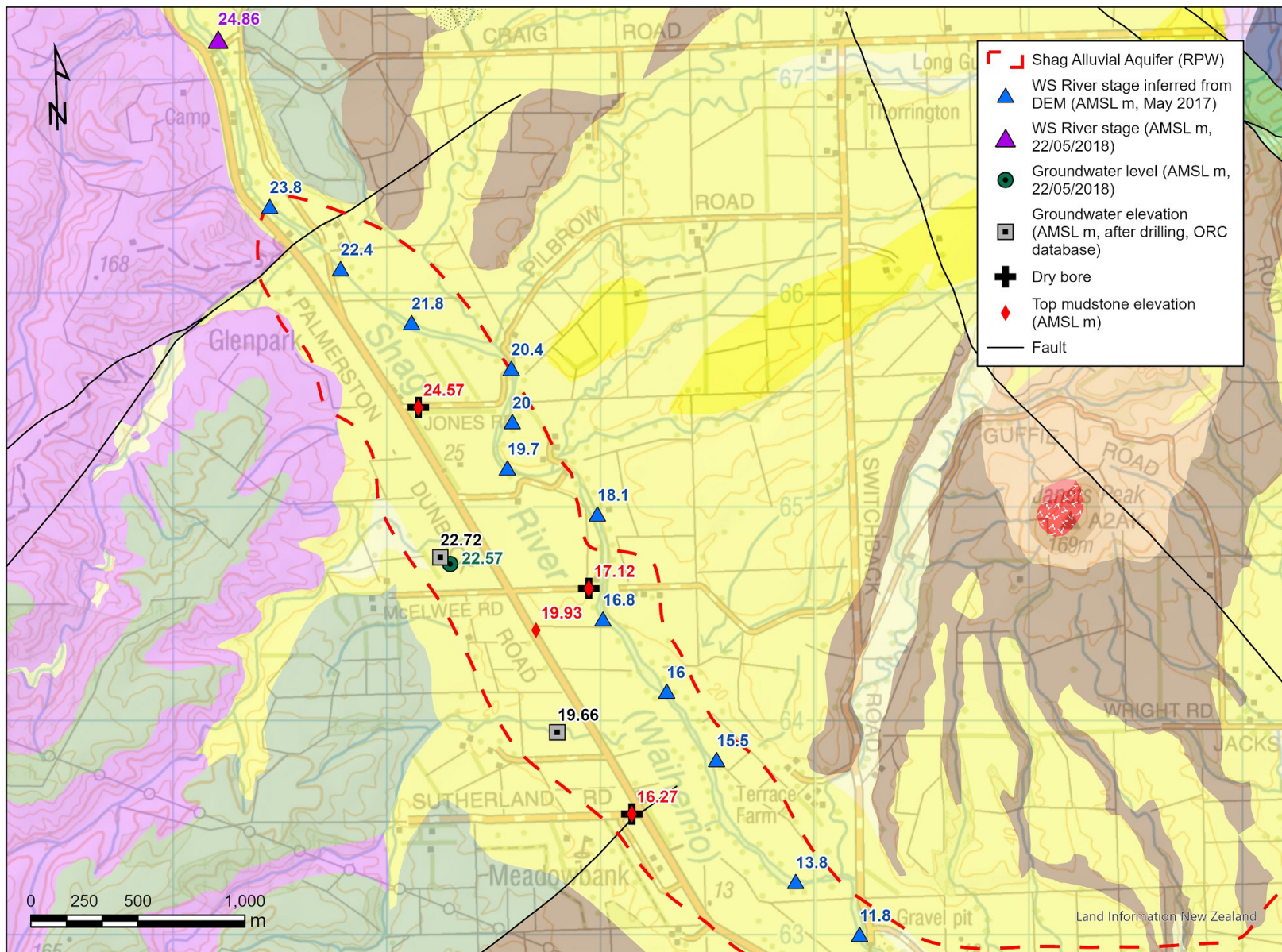


Figure 4.1 Current Shag Alluvial Aquifer boundary in relation to geological and water level information, northwest area (between Craig Road and Sutherland Road).

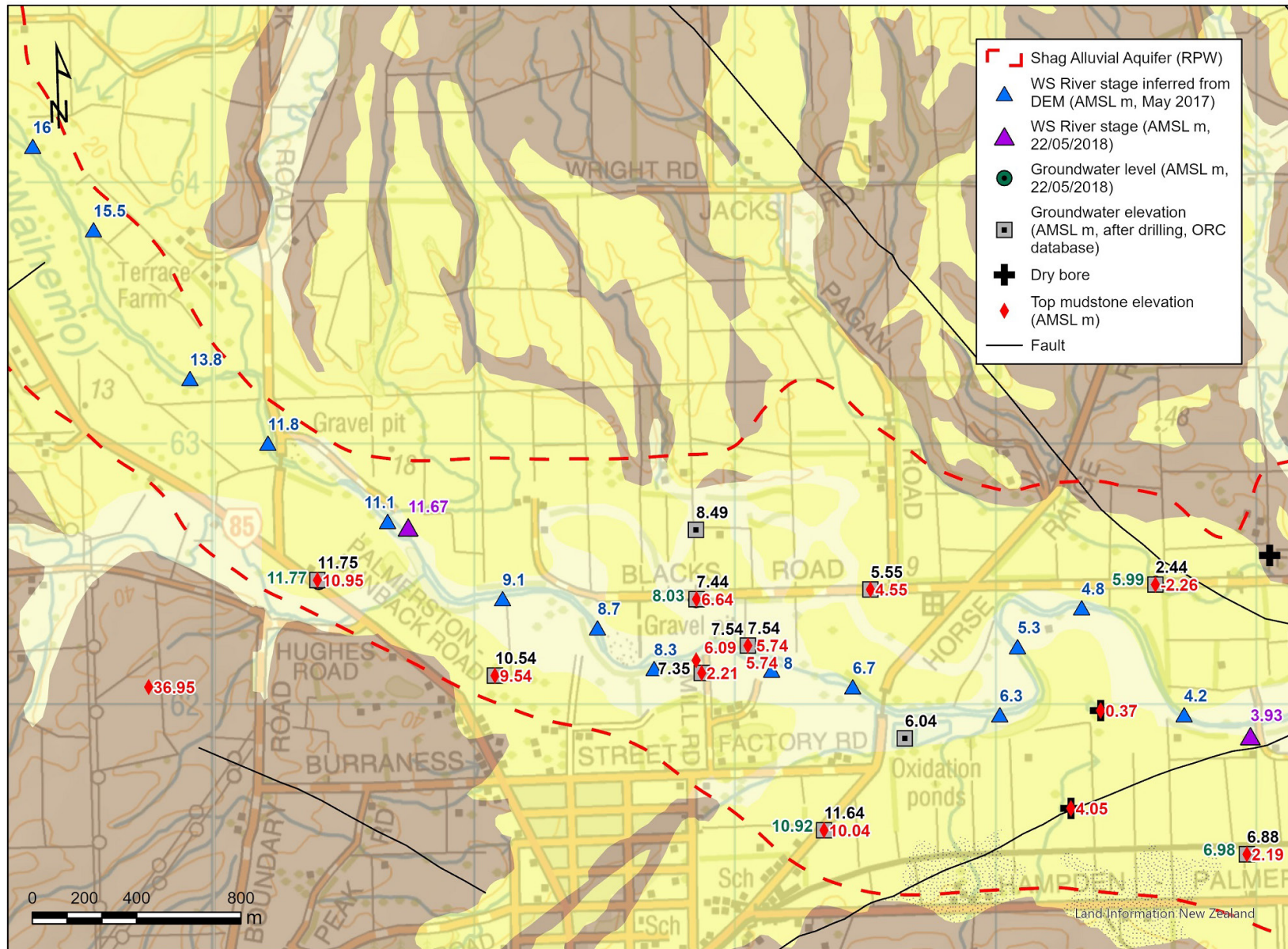


Figure 4.2 Current Shag Alluvial Aquifer boundary in relation to geological and water level information, central area (between Sutherland Road and east of Horse Range Road).

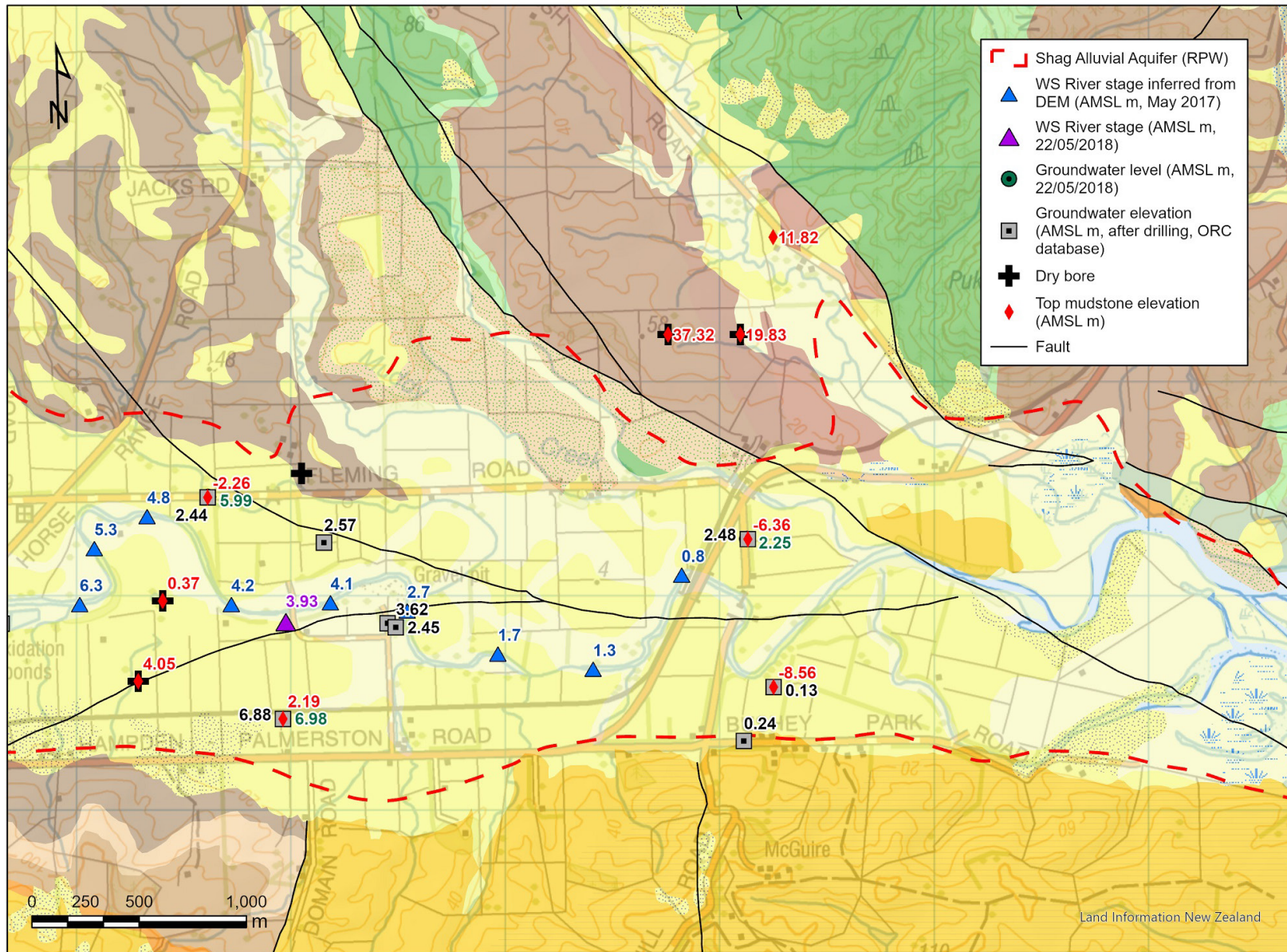


Figure 4.3 Current Shag Alluvial Aquifer boundary in relation to geological and water level information, southeast area (between east of Horse Range Road and the coast).

4.1.2 Aquifer and River Hydrographs

Over the period from 1/07/2017 to 31/07/2022, the seasonal differences in WS River stage elevations were between ~1.7 m at EM542/Switchback Road and ~3.6 m at EM495/Craig Road and FD208/Shakey Bridge (Figure 4.4). During the same period, continuously monitored groundwater levels in the SAA had seasonal variations between ~1.6 m (at J43/0119) and ~2.1 m (at J43/0121).

Most of the monitoring sites (with the exception of J43/0122) responded quite rapidly to rainfall event pulses (e.g. 2/02/2018, 21/11/2018 and 3/01/2021; Figure 4.4). Conversely, the extended relatively dry period observed from c. 15/02/2020 to c. 15/12/2020 was also noticeable on all sites' hydrographs with a flattening of the water levels and a declining trend for J43/0122. This last bore is confined and showed 'buffered' signals.

The SAA hydrograph at J41/0119 was similar (signals and water elevation) to the WS River hydrograph at EM542/Switchback Road, suggesting a degree of interaction with the WS River (Figure 4.4). The bore J41/0121 hydrograph was also very similar to the WS River hydrograph at EM542/Switchback. However, it had sharper rises in groundwater water levels than J43/0119, suggesting more direct interaction with the WS River.

Manual measurements of water levels in J43/0120 lacked the fine-scale resolution and yielded relatively consistent groundwater levels through time. This groundwater level dataset points to the limitations of discrete monitoring, as pulses might have been missed. This consistent groundwater level though time could also suggest that bore J43/0120 is not well connected to the rest of the SAA. Results for bore J43/0123 were more varied and indicated a signal similar to the bore J43/0124 hydrograph (Figure 4.4).

4.1.3 Piezometric Maps

Generally, flows in the SAA followed the valley topography (Figure 4.5; Appendix 8). In the upper part of the SAA, flows were directed from the northwest to the southeast. Near Switchback Road, the flows turned towards the east and northeast, suggesting recharge from the Palmerston township area/Mount Puketapu slopes. Yet, this might have been an artefact caused by bore J43/0120 data. This bore might be perched or disconnected from the SAA. The groundwater gradient was steeper in the narrower upper part of the SAA (until approximately Switchback Road) then flattened with the widening of the valley near the coast. There was little difference observed between the piezometric maps established for a relatively dry period (16/01/2018; Appendix 7) and for a wet period (22/05/2018; Figure 4.5), except for generally higher levels for the latter. However, the representativeness of the prepared piezometric maps must be considered with caution due to (i) the small number of groundwater level measurements (seven), (ii) their distribution in the Lower WS River Valley (e.g. no bores in the most upgradient and downgradient mapped areas of SAA) and (iii) the fact that they do not reflect the presence of dry bores. Accordingly, no interpretation of the piezometric contour shape was provided in term of groundwater and surface water interaction as the level of detail of the piezometric maps was considered insufficient to correctly represent the complexity of this interaction in the Lower WS River Valley.

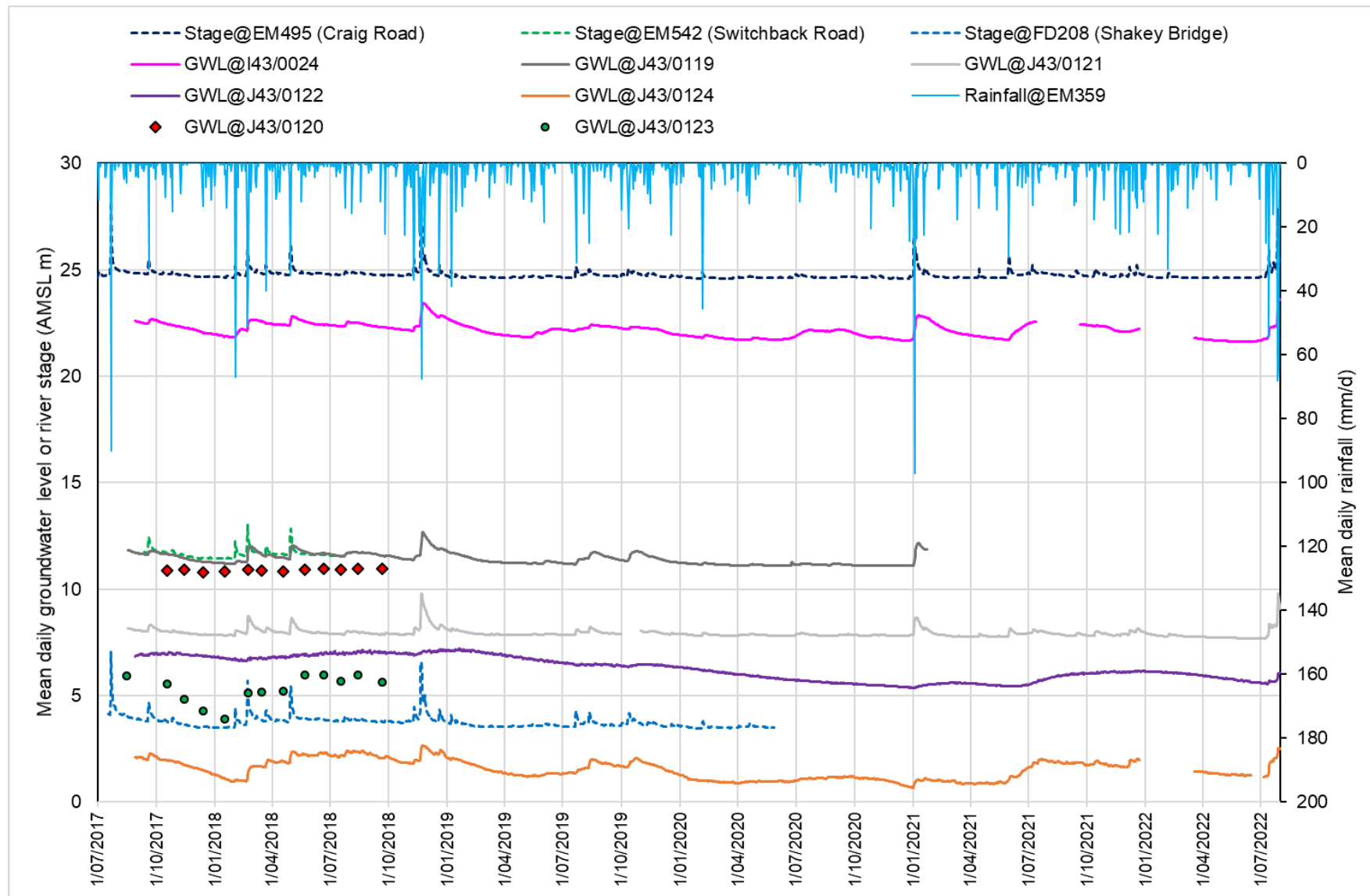


Figure 4.4 Mean daily groundwater levels (GWL; high-frequency monitoring: lines; manual measurements: marker symbols) and river stage (dashed coloured lines) in the Lower Waihemo/Shag River Valley (from August 2017 to August 2022). Rainfall for the same period is shown in blue at the top of the graph. Site locations are provided in Figure 2.2 and Figure 2.3.

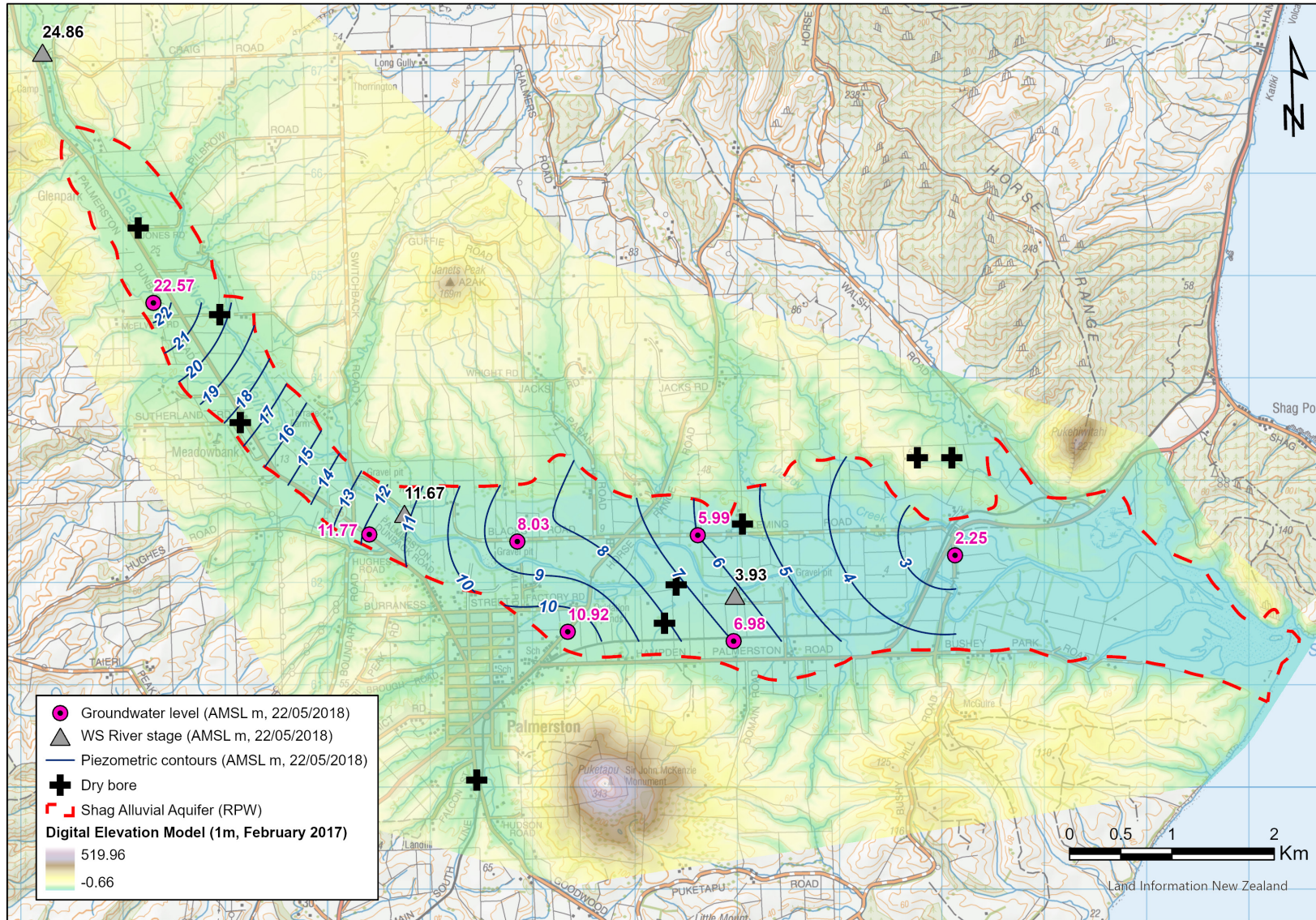


Figure 4.5 Piezometric contours for the Shag Alluvial Aquifer on 22/05/2018 (relatively high Waihero/Shag River stage and groundwater level conditions). River stage data (and inferred connection between surface water and groundwater) were not used to draw these contours, and corrections to consider dry bores have not been applied.

4.1.4 Aquifer Hydraulic Properties

The hydraulic conductivities estimated from the slug test analyses (i.e. for the aquifer material in the immediate vicinity of the tested bores) ranged from 10 to 15.8 m/day at bores J43/0122, J43/0123 and J43/0124 (Table 4.1). These values are slightly below the literature values for clayey gravels (e.g. 86 m/d; Freeze and Cherry 1979), but still in the same order of magnitude. This might be due to the larger portion of clay and silt at these sites (lithological logs in Appendix 3).

Transmissivity values ranged between 60 and 110 m²/d, with the lowest value for J43/0122 and the highest value for J43/0124 (Table 4.1). These estimates are consistent with the lower range of transmissivities for gravel aquifers in New Zealand (19 to 43,200 m²/d) reported by Meilhac et al. (2010). Relatively similar values (<500 m²/d) were given for the Kakanui-Kauru Alluvium Aquifer by Heller (2001), with a comparatively similar aquifer context.

Table 4.1 Hydraulic conductivities and transmissivities estimated from the slug tests.

Bore ID	Slug Test Type	Solution used	Estimated Hydraulic Conductivity K (m/d)	Estimated Aquifer Thickness (m)	Transmissivity (m ² /d)
J43/0122	Slug falling head	Hvorslev (1951) early response	14.2	5.9	83.8
	Slug rising head		15.8		93.2
	Water falling head		10.0		59.0
J43/0123	Slug rising head	Bouwer and Rice (1976) early response	11.3	6.3	71.2
	Water falling head		11.2		70.6
J43/0124	Water falling head	Bouwer and Rice (1976) early response	14.7	7.3	107.3

4.2 Groundwater Quality

4.2.1 Hydrochemistry

Groundwater exhibited a greater range in total dissolved content than surface water⁴, with median EC ranging from 232 µS/cm (J43/0121) to 922 µS/cm (J43/0124) from September 2017 to September 2018 (Figure 4.6). The second highest EC, 799 µS/cm, was measured at bore I43/0024, which is the most upgradient groundwater site in the study area. Most groundwaters were characterised as Na-Cl type, contrasting with dilute Ca-Mg-HCO₃ type surface waters. Bore J43/0121 was an exception, showing a chemistry similar to surface waters (Figure 4.6). This well's low total dissolved solids content was consistent with its location within younger Quaternary sediments, suggesting a strong hydraulic connection with the WS River (Figure 2.3). Overall, EC decreased along the flow paths (i.e. towards the coast) with a larger contribution of river water recharging the SAA.

In contrast to the other bores' chemistry, bore J43/0124 had a strong reducing condition signature demonstrated by low DO concentrations (median of 0.26 mg/L) and detectable concentrations of trace metals that are only mobile under reducing conditions (e.g. As, Cr, Fe and Mn; Table 4.2). It is worthwhile to note that at this bore, As and Mn concentrations (0.036 mg/L and 0.79 mg/L, respectively) were well above the Maximum Admissible Values as

⁴ Surface water median EC ranged mainly between 186 µS/cm (EM495) and 246 µS/cm (FE329) from September 2017 to September 2018. However, two elevated median EC were measured for surface water: 371 µS/cm (FE330) and 639 µS/cm (FE331). Impact from land use is inferred for these sites.

defined in the New Zealand Drinking Water Standard (NZDWS), which are 0.01 mg/L and 0.4 mg/L, respectively (Ministry of Health 2018). Although bore J43/0123 also exhibited low DO concentration (0.39 mg/L), its chemical signature was more similar to the other bores, with significantly lower Fe (0.44 mg/L compared to 19 mg/L at J43/0124) and Mn concentrations (0.72 mg/L) also exceeding the NZDWS. The NZDWS also include Guideline Values (GVs) which are set for aesthetic purposes. Of relevance to this study are Fe and Mn GV (0.04 and 0.2 mg/L, respectively), above which staining of laundry occurs, and the NH₃-N GV (1.2 mg/L), which corresponds to an odour threshold. These GV were exceeded at bores I43/0024, J43/0120, J43/0123 and J43/0124 (Table 4.2).

Nitrogen can occur in groundwater in either NO₃-N or NH₃-N form, depending on oxygen levels within the aquifer. NO₂-N concentrations were minimal at all sites. The transition between forms is a natural, microbiologically induced process. Moderate to low NO₃-N concentrations (medians of 0.02 mg/L to 4.95 mg/L, Table 4.2; Figure 4.7) were observed, which is consistent with oxygenated water. Where DO concentrations were low, only bore J43/0124 recorded elevated NH₃-N concentration (median of 2.4 mg/L). Generally, NO₃-N groundwater concentrations increased significantly (from 1.00 mg/L to 4.95 mg/L) along the flow path.

For surface water, median NO₃-N concentrations (Figure 4.7) ranged between 0.03 mg/L and 0.22 mg/L for the WS River at EM495/Craig Road and FE328/Mill Road, respectively. FE327/Jones Road also presented higher median NO₃-N concentrations (0.17 mg/L). Groundwater discharge might have occurred upstream of Jones Road and Mill Road. An elevated median NO₃-N concentration for surface water (0.99 mg/L) was observed for FE329/Blue Mountain Creek. This might reflect the impact of local land use on this creek.

DRP concentrations were low (0.004 mg/L to 0.007 mg/L) except at bores J43/0122 and I43/0024 (0.022 mg/L and 0.023 mg/L, respectively). Both bores are far apart, suggesting a local source near each bore.

Examination of the time series data over the September 2017 to September 2018 period yielded the following information (Figure 4.8, Figure 4.9 and Figure 4.10):

- Low water levels were observed during February 2018 at all bores. Furthermore, strong seasonal variations in groundwater temperatures were measured, with the lowest in November. Bore J43/0120's amplitude was the highest, with the highest temperature measured for groundwater (up to 17°C).
- A DO reduction was observed in May 2018 at all bores apart from the reducing ones (i.e. bores J43/0123 and J43/0124).
- Strong seasonal variations in major ion concentrations were measured for bores I43/0024, J43/0119, J43/0120 and J43/0124. For instance, the highest major ion concentrations were observed in December for bore I43/0024 and in June for bore J43/0119. Low amplitude seasonal variations were observed for major ions at J43/0121 and J43/0122. Ca, Cl, Na and SO₄ were the most changing parameters.
- FE331/Township Creek site's temporal pattern deviated from the other river and stream sites, with an opposite response (low major ion concentrations when the other sites had high major ion concentrations). This site is likely to have been impacted by urban discharges from Palmerston township.
- Nitrogen species temporal patterns varied between groundwater sites: relatively stable at I43/0024; to a peak in January to February at J43/0119; highly variable at J43/0120; to a low in March, followed by a slight rise in April 2018 (J43/0120, J43/0121); a NO₃-N increase at bore J43/0122 and a NH₃-N decrease at bore J43/0124 between July 2017

and September 2018. In contrast, three sharp increases in NO₃-N (September 2017, February 2018, March 2018) were observed at multiple surface water sites, with the noticeable exception of FE330 and FE331.

- DRP was relatively stable at most monitoring sites, except for a strong peak (January to April 2018) at the FE331 surface water site.
- At bore J43/0124, As and Mn concentrations exhibited a slight increase over the period, whereas Fe concentrations peaked in December 2017 to gradually decrease returning to September 2017 concentrations. The other low DO concentration site exhibited a rise in Mn concentrations over the same period (J43/0123).

Table 4.2 Median values for hydrochemical parameters, from September 2017 to September 2018, at the groundwater sites. NA indicates where measurements were not available. Grey and yellow background cells highlight values above the New Zealand Drinking-Water Standard Guideline Values and Maximum Admissible Values, respectively (Ministry of Health 2018). Units are mg/L except for EC (μ S/cm), groundwater levels (GWL; AMSL m), temperature ($^{\circ}$ C) and pH (pH units).

	Parameters	I43/0024	J43/0006	J43/0119	J43/0120	J43/0121	J43/0122	J43/0123	J43/0124
Field parameters	DO	NA	NA	7.8	3.8	6.6	4.5	0.39	0.26
	EC	799	221	463	NA	232	382	358	922
	GWL	NA	NA	12	11	8.0	6.9	5.6	2.1
	pH	7.0	7.15	6.6	NA	6.5	6.1	6.5	7.0
	Temperature	NA	NA	11	13	12	12	12	12
Major ions	Ca	28	22	26	17	24	19	24	41
	K	111	1.4	63	116	16	57	48	101
	Mg	154	5.65	65	49	75	43	78	310
	Na	4.9	15	5.0	1.9	1.3	1.4	2.9	14
	HCO ₃	16	65.5	13	9.7	5.8	6.6	7.4	30
	Cl	122	14	45	100	15	45	35	90
	SO ₄	25	18.9	14	28	11	40	19	30
	SiO ₂	67	10.2	48	52	19	34	28	2.5
Nutrients	DRP	0.0040	0.0056	0.0070	0.0075	0.0061	0.022	0.023	0.0040
	NH ₃ -N	0.068	0.005	0.0050	0.018	0.0050	0.0050	0.067	2.4
	NNN	0.82		2.7	4.0	1.1	5.0	0.017	0.0023
	NO ₂ -N	0.0045	0.001	<0.001	0.015	<0.001	<0.001	<0.001	<0.001
	NO ₃ -N	1.00	0.785	2.7	4.0	1.1	5.0	0.016	0.0016
Trace metals	As	0.0010	0.001*	<0.001	<0.001	<0.001	<0.001	<0.001	0.037
	B	0.47	NA	0.035	0.036	0.024	0.038	0.038	0.19
	Br	0.46	NA	0.18	0.12	0.070	0.33	0.18	0.55
	Cr	<0.0005	0.0005*	<0.0005	<0.0005	<0.0005	<0.0005	<0.0005	0.0006
	F	0.88	0.12	0.12	0.37	0.100	0.29	0.17	0.62
	Fe	0.62	0.02	0.020	0.020	0.020	0.020	0.44	19
	Mn	0.051	0.0005	0.0006	0.059	<0.0005	0.0092	0.72	0.79

* These values are likely to be '<0.001' (for As) or '<0.0005' (for Cr) i.e. below the detection limits.

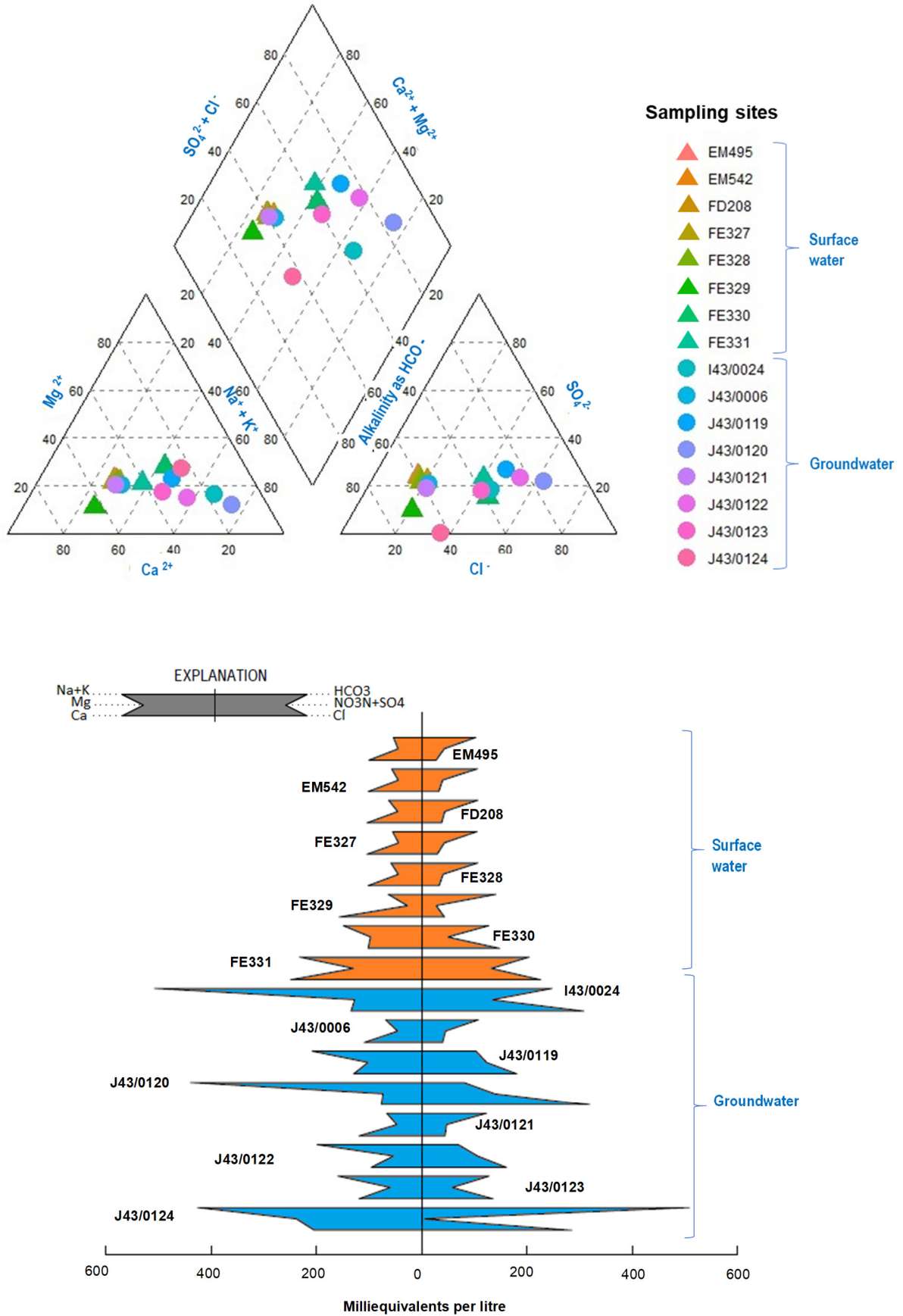


Figure 4.6 Major ion chemistry at the monitoring sites depicted as a Piper diagram (top) and a Stiff diagram (bottom).

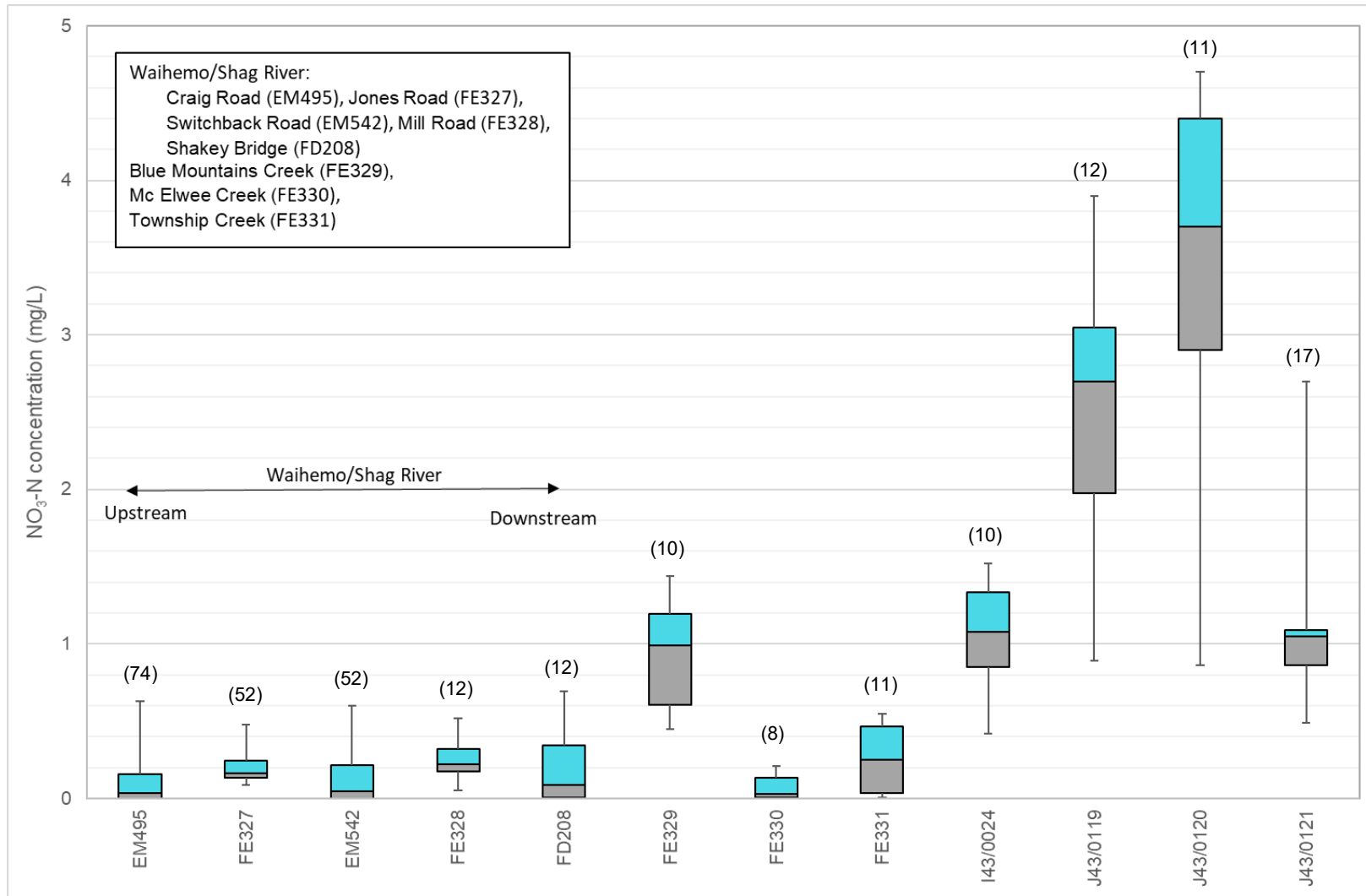


Figure 4.7 Median nitrate concentrations between July 2017 and September 2018 for the Otago Regional Council monitoring sites. Number of samples in brackets. Note: Bores J43/0123 and J43/0124 are not included as these bores have negligible nitrate concentrations. Nitrogen seems to be absent in J43/0123 and is present as NH₃ at J43/0124.

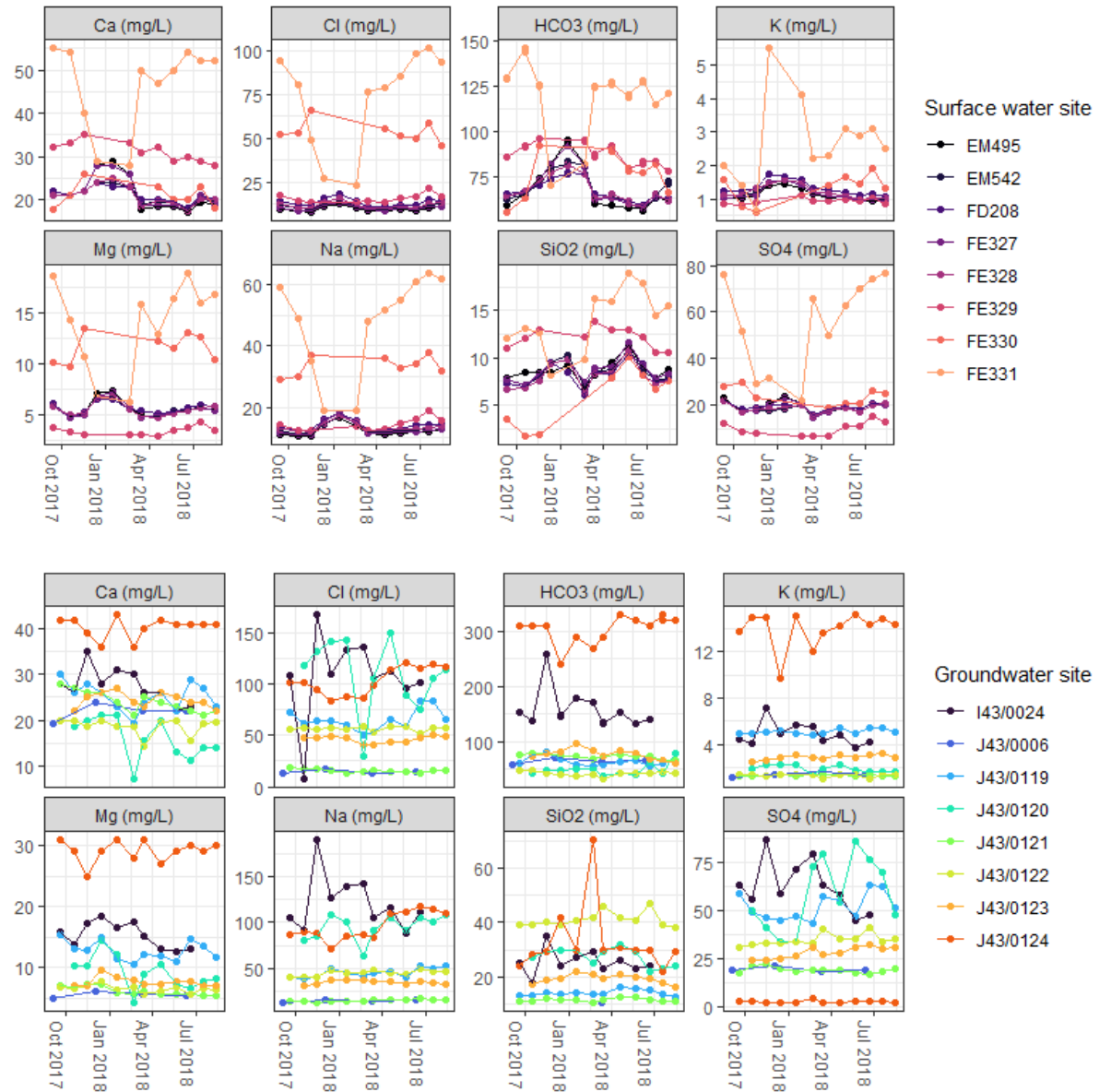


Figure 4.8 Major ion concentrations at the monitoring sites from September 2017 to September 2018.

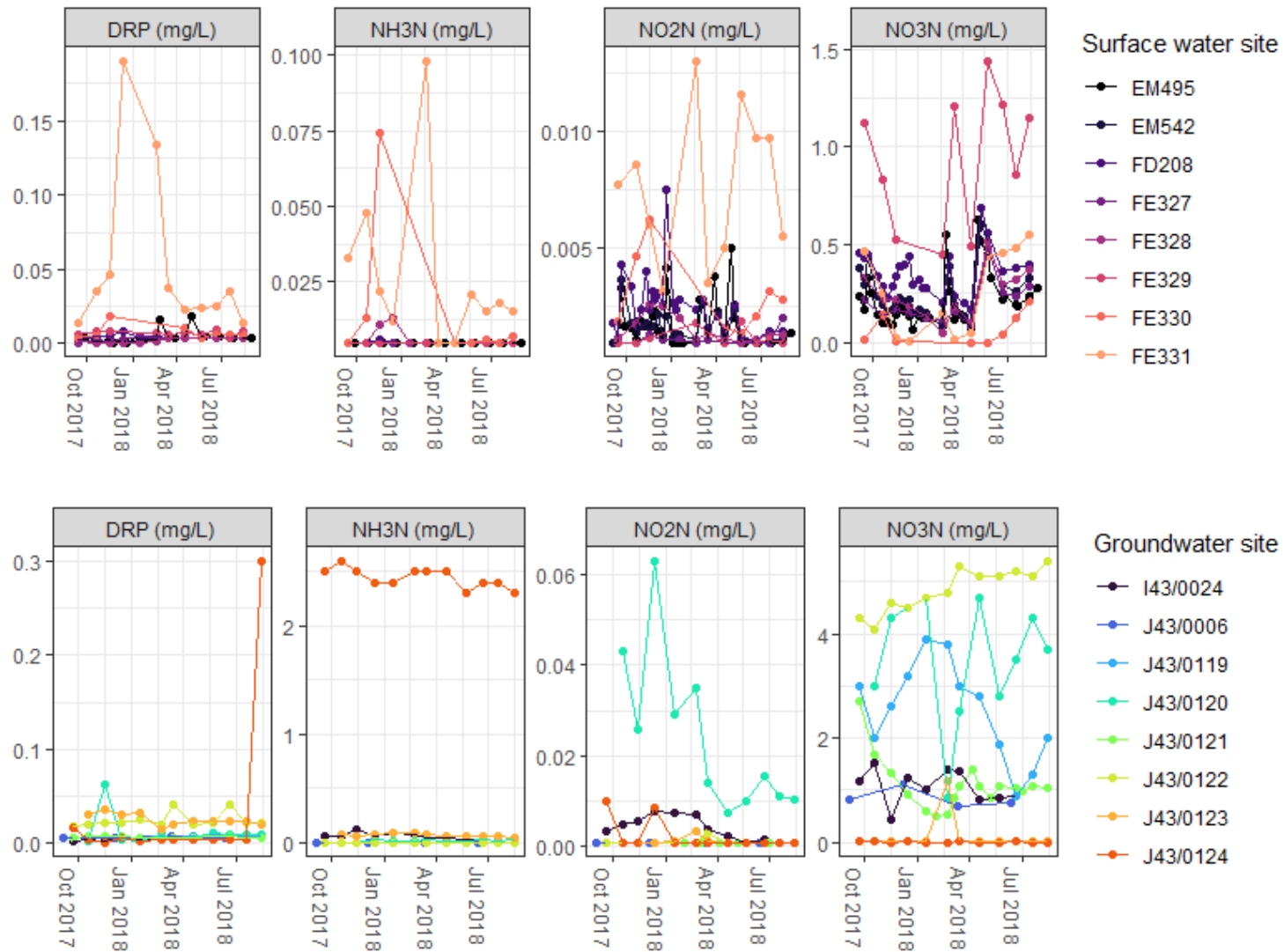


Figure 4.9 Nutrient concentrations at the monitoring sites from September 2017 to September 2018.

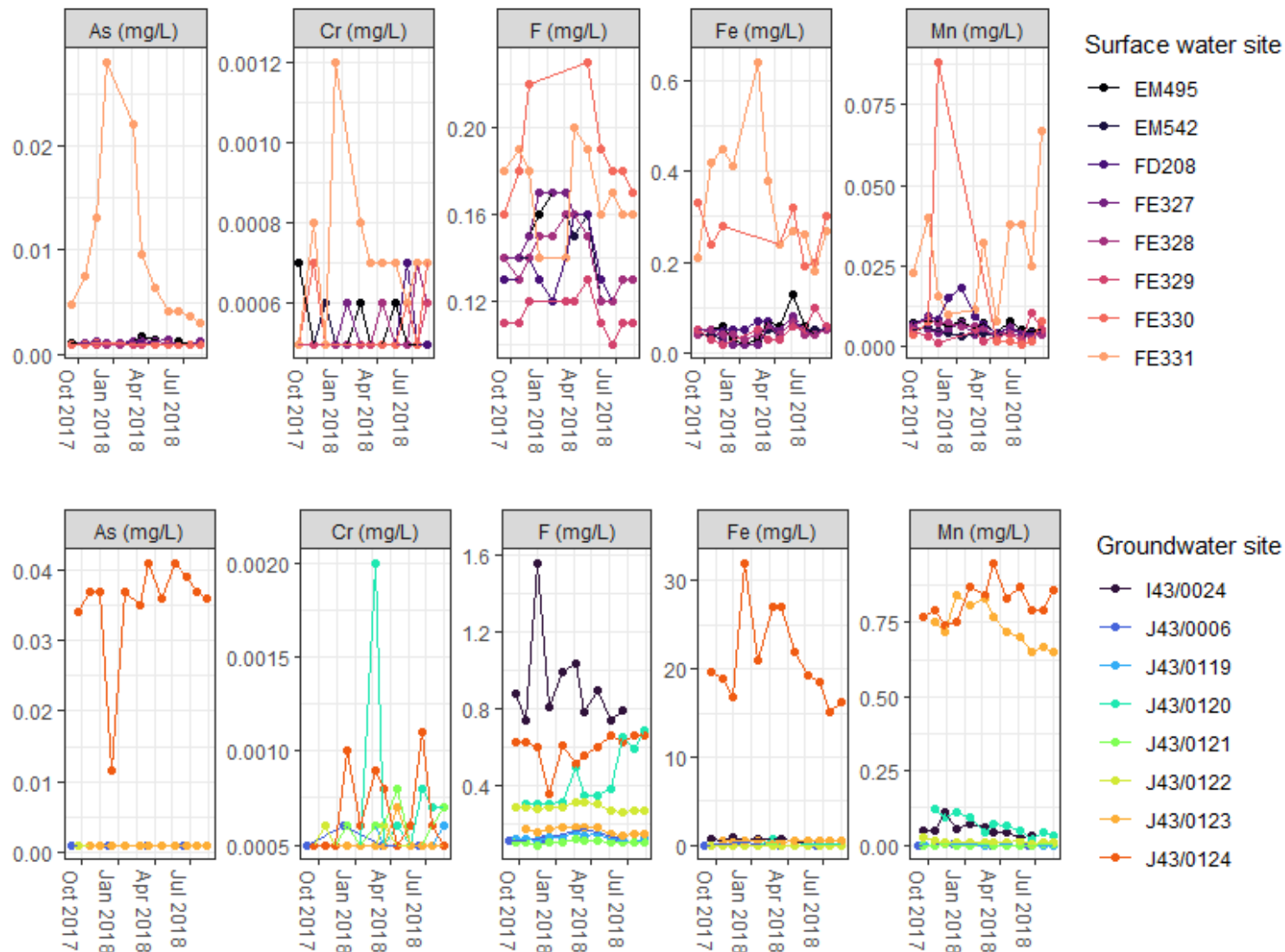


Figure 4.10 Trace metal concentrations at the monitoring sites from September 2017 to September 2018.

4.2.2 Nitrate Concentrations and Loads

4.2.2.1 Nitrate Concentrations

The nitrate concentrations recorded in the SAA (at J43/0121) and in the WS River at three locations (EM495/Craig Road, EM542/Switchback Road and FD208/Shakey Bridge) point to similar fluctuations: higher nitrate concentrations were observed shortly after high rainfall events (e.g. 2/02/2018, 21/02/2018 and 29/04/2018). These were accompanied by higher streamflow and groundwater levels (Figure 4.11). Conversely, lower nitrate concentrations were observed during dry periods (e.g. November 2017 to January 2018) for these sites. The results from the WS River grab samples show that high concentrations associated with high flows are not well represented in this dataset (i.e. nitrate concentrations were not well captured during high flow and flood events).

The WS River graphs (Figure 4.11) indicate increasing nitrate concentrations from upstream (EM495/Craig Road) to downstream (FD208/Shakey Bridge), which points to the effects of land use and nitrate-enriched groundwater discharges to the WS River (e.g. upstream FD208/Shakey Bridge). The pulses in groundwater levels were accompanied by pulses in groundwater nitrate concentrations, likely associated with recharge events mobilising nitrate accumulated in the soils (Figure 4.11). As discussed earlier (Section 4.1.2), bore J43/0121 is highly connected and receiving recharge from the WS River. Its low nitrate concentrations and response to rainfall/high river flow events are not representative of less connected parts of the aquifer (e.g. bore J43/0119). These aquifer areas, for which rainfall is the main source of recharge, had higher nitrate concentrations associated with land use (e.g. agriculture). Discharge from groundwater with higher nitrate concentrations to the WS River is inferred to have occurred in the lower reaches (e.g. near Shakey Bridge).

4.2.2.2 Nitrate Load Estimates

Nitrate load estimates (Figure 4.12; Appendix 9) showed strong monthly variations in the WS River for all sites, with the smallest loads in December 2017 and January 2018 (e.g. ~2 to 4 kg/d in January 2018) and the largest loads in February and May 2018 (e.g. ~200 to 460 kg/d in February 2018). These variations are correlated to the WS River flow (Appendix 9): the lowest flows were observed in December 2017 and January 2018 (e.g. 0.1 m³/s at FD208/Shakey Bridge in January 2018) and the highest flows in February and May 2018 (e.g. 9.6 m³/s at FD208/Shakey Bridge).

The loads estimated from high-frequency nitrate monitoring are consistently higher than the ones derived from grab sample nitrate concentrations. This can be explained by:

- a) The fact that most of the time grab samples did not capture high flow events with higher nitrate concentrations, where nitrates were leached to the river.
- b) The high frequency nitrate datasets used for the load estimations have not been corrected. However, it is likely that the sensors overestimated the actual nitrate concentrations and that these datasets present a bias (Section 3.2.2.1).

The actual nitrate loads in the WS River probably ranged between the loads estimated from high-frequency nitrate monitoring and those calculated from grab-sample concentrations. The average of these two estimates, expressed as mean daily loads from September 2017 to August 2018 yields ~77 kg/d at EM495/Craig Road, ~82 kg/d at EM542/Switchback Road and ~109 kg/d at FD208/Shakey Bridge. This is consistent with the cumulative effect of land use in the WS River from the upstream site (EM495/Craig Road) to the downstream site (FD208/Shakey Bridge).

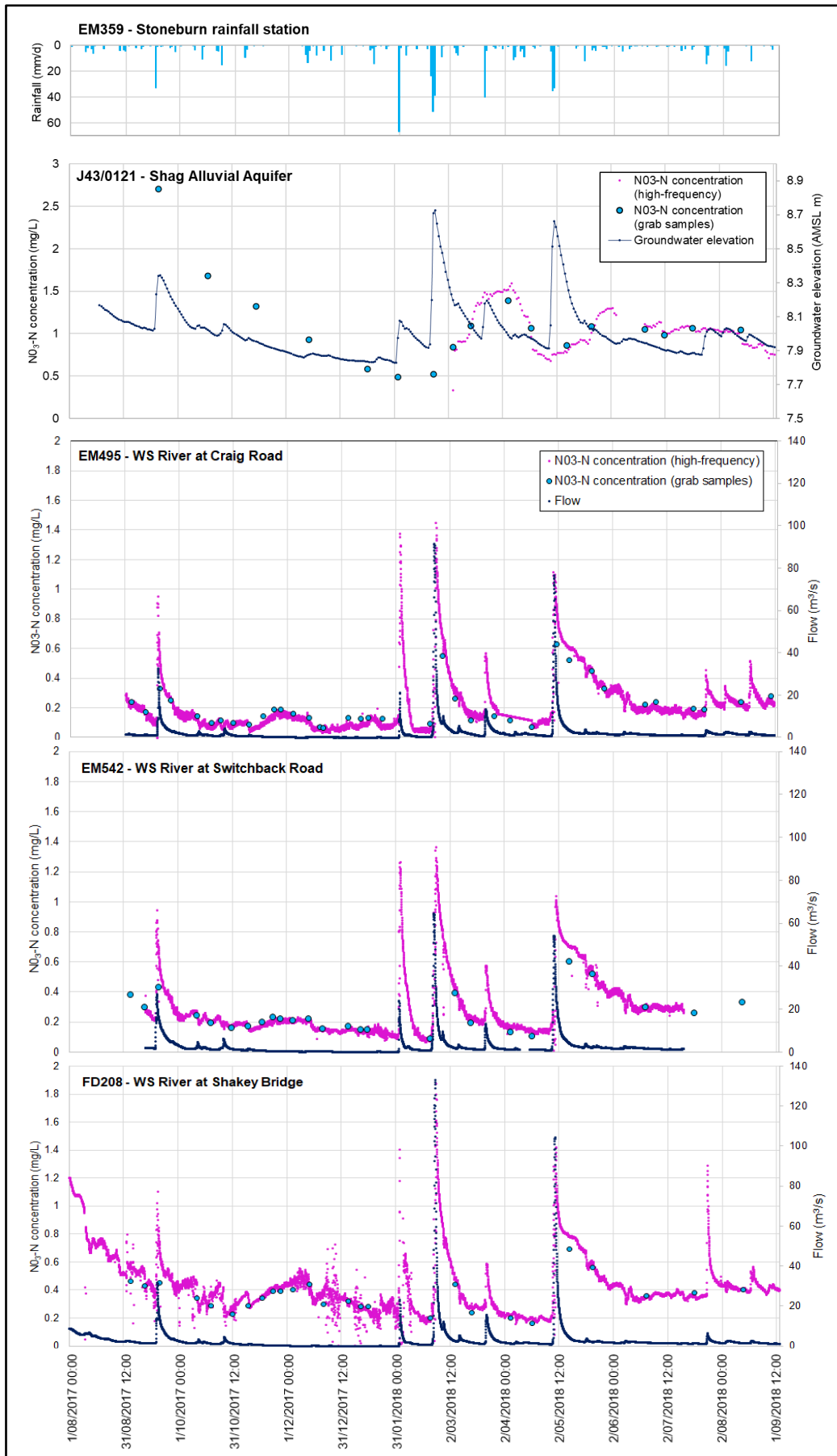


Figure 4.11 Timeseries of rainfall, nitrate concentrations (high-frequency monitoring and grab samples), groundwater levels for the Shag Alluvial Aquifer and flows for the Waihemo/Shag River from August 2017 to September 2018.

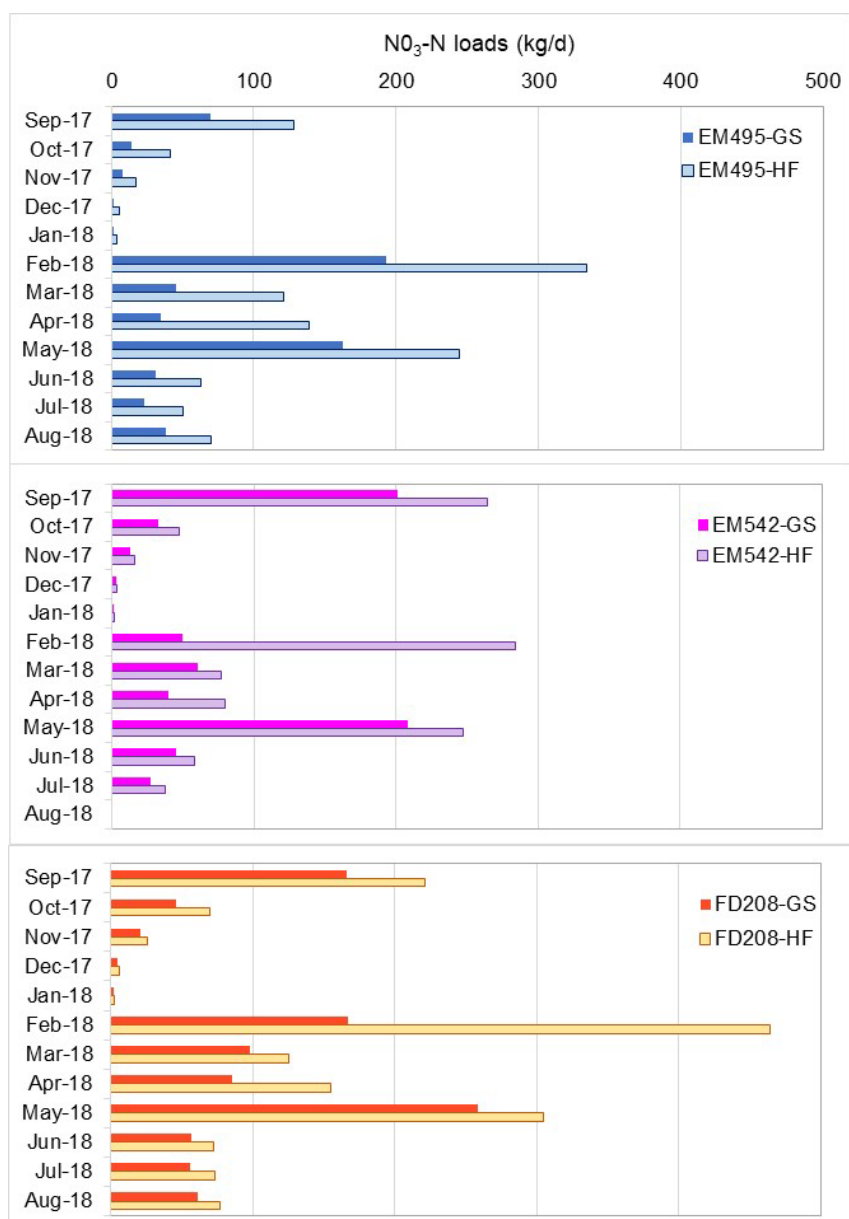


Figure 4.12 Nitrate loads estimated from daily flows and daily nitrate concentrations from high-frequency (HF) data and grab samples (GS) for the Waihemo/Shag River at Craig Road (EM495), Switchback Road (EM542) and Shakey Bridge (FD208) from September 2017 to August 2018.

4.2.3 Tracer Measurements

4.2.3.1 Stable Isotopes Data

Stable isotope compositions measured as part of this study were close to the local meteoritic water line (Figure 4.13), indicating that precipitation had occurred mostly under saturated conditions without post-condensation evaporation. In the Lower WS River Valley, groundwater $\delta^{18}\text{O}$ ranged from -8.2‰ to -6.5‰ and $\delta^2\text{H}$ ranged between -60.6‰ and -47.2‰ . Surface waters generally overlapped but extended to more depleted compositions; $\delta^{18}\text{O}$ ranged from -8.7‰ and -7.4‰ and $\delta^2\text{H}$ from -63.6‰ and -51.5‰ (Table 3.1). These results are consistent with surface waters being derived from a more regional, higher-elevation source.

Stable isotope values measured in groundwater and surface water (Figure 4.13; Table 4.3) overlapped the compositions measured from surface water in the South Island, New Zealand (data compiled by Lachniet et al. (2021)). However, the data from this study and the surface

water line from Lachniet et al. (2021) are slightly lower than a New Zealand meteoric water line proposed by a previous study (Frew et al. 2011), pointing to the effect of evaporation.

Groundwater stable isotope $\delta^{18}\text{O}$ and $\delta^2\text{H}$ values were generally more positive near the coast, west of Palmerston, compared to inland sites (Figure 4.14). This is typical of a coastal rain-out effect (Dansgaard 1964) where inland precipitation is generally more negative than coastal precipitation due to the loss of heavier isotopes. Additionally, with the exception of bore J43/0121, which also yielded more negative values, the surface water samples had more negative values than the groundwater samples. Water chemistry from bore J43/0121 is similar to surface water samples, suggesting that the groundwater at the shallow bore (5 m depth with screen interval from 1.5 to 4.5 m) was derived from local surface water input.

Table 4.3 Stable isotope results for groundwater and surface water samples collected on 22/05/2018, in the Lower Waihemo/Shag River Valley.

Site ID	Sample Type ¹	Sample Processing	$\delta^2\text{H}$ (‰)	$\delta^2\text{H}$ (±)	$\delta^{18}\text{O}$ (‰)	$\delta^{18}\text{O}$ (±)
FE329	SW	Surface water filtered	-53.8	1.0	-7.6	0.2
FE330		Surface water filtered	-51.5	1.0	-7.4	0.2
EM495		Surface water unfiltered	-63.6	2.0	-8.7	0.2
J43/0119	GW	Groundwater unfiltered	-50.9	2.0	-7.3	0.2
J43/0121			-60.6	2.0	-8.2	0.2
J43/0122			-49.2	2.0	-7.0	0.2
J43/0123			-46.5	2.0	-6.5	0.2
J43/0124			-47.2	2.0	-6.7	0.2
I43/0024			-50.3	2.0	-7.0	0.2

¹ SW: surface water; GW: groundwater.

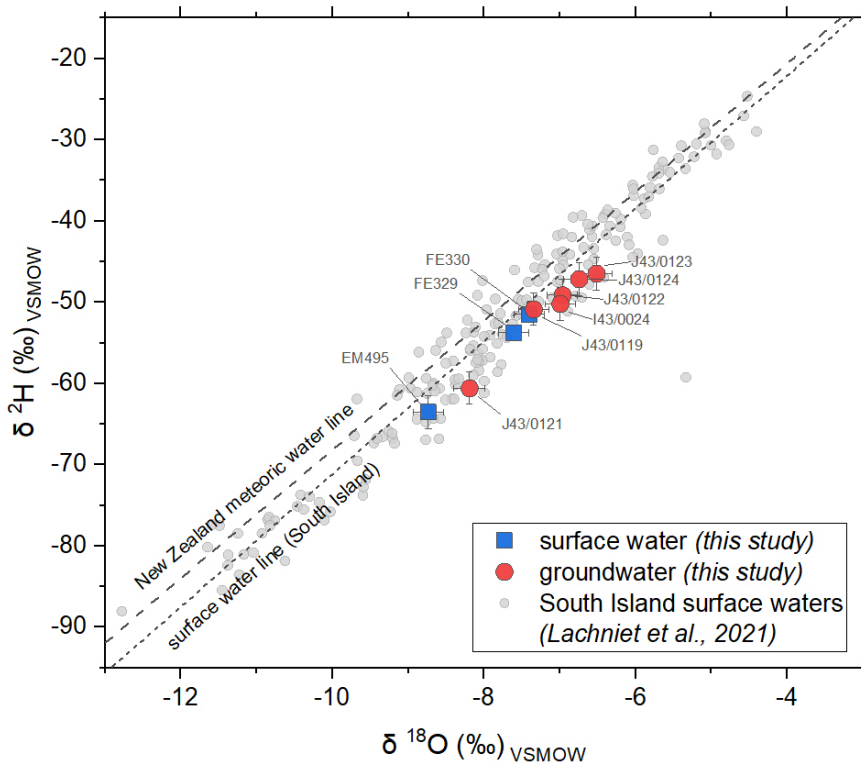


Figure 4.13 Stable isotope compositions for Lower Waihemo/Stag River Valley groundwater (red) and surface water (blue) samples. The New Zealand meteoric water line ($\delta^2\text{H} = 7.92 * \delta^{18}\text{O} + 11.07$; Frew et al. 2011) and the surface water line for the South Island, New Zealand ($\delta^2\text{H} = 8.17 * \delta^{18}\text{O} + 10.57$; Lachniet et al. 2021) are shown for reference.

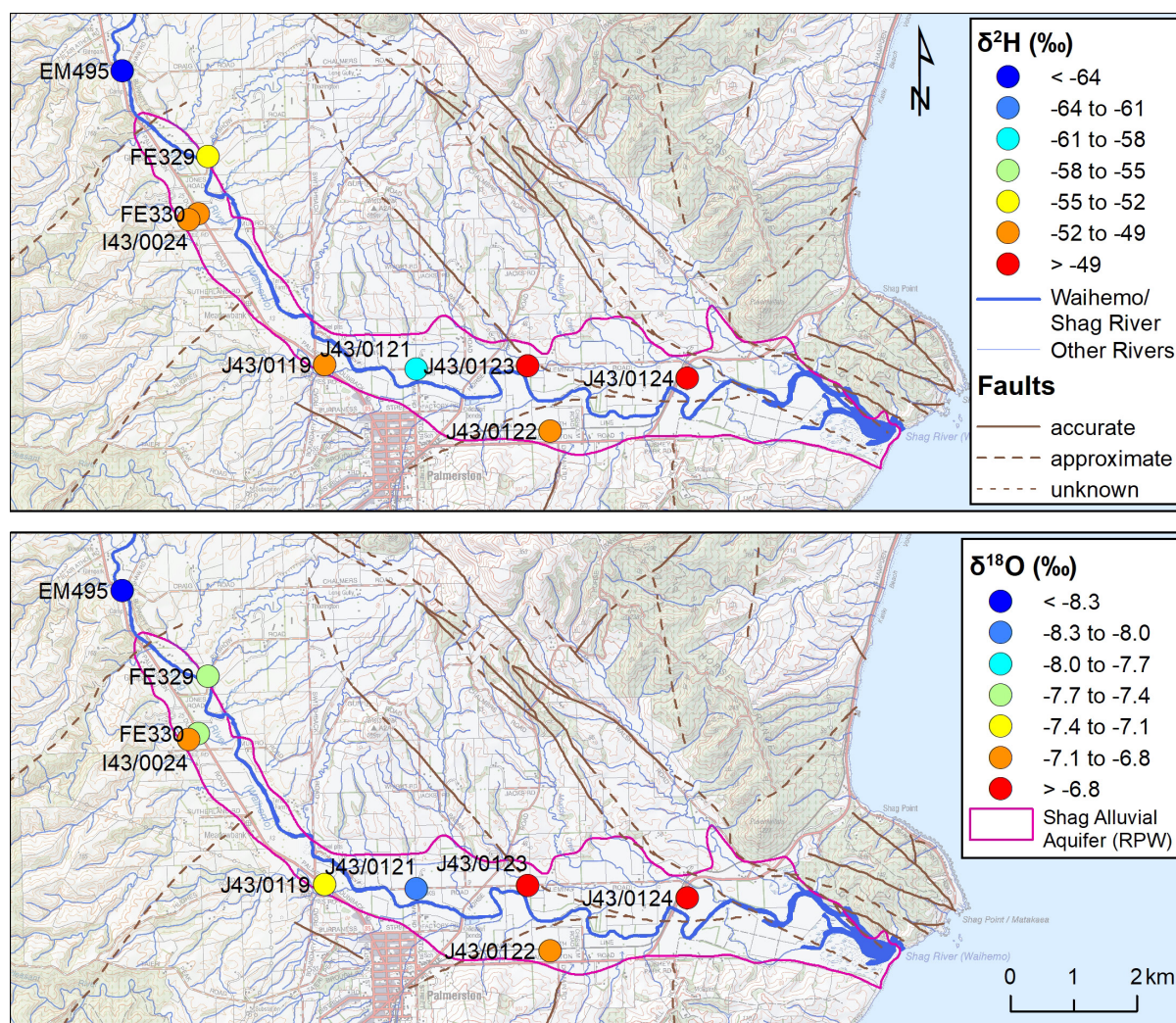


Figure 4.14 Hydrogen ($\delta^2\text{H}$) and oxygen ($\delta^{18}\text{O}$) isotope results from surface water and groundwater samples collected on 22/05/2018 in the Lower Waihemo/Shag River Valley.

4.2.3.2 Radon Data

Results from the February 2017 radon and flow gauge surveys identified areas where groundwater was being discharged into the WS River (Figure 4.15; Martindale and Lovett 2017). New radon measurements collected in March and October 2017 showed variable concentrations across the WS River study area (Figure 4.15).

With the exception of site I43/0024, groundwater radon concentrations ranged from 14.4 to 19.9 Bq/L. Site I43/0024 had significantly higher concentrations: 179.5 ± 9.7 Bq/L in February 2017 and 43.8 ± 2.5 Bq/L in October 2017 (Figure 4.15). The large differences in radon concentrations have not been observed in other regional studies, such as in the Hutt River or Waiohira Stream surveys (Martindale and van der Raaij 2018).

Surface water results from the second survey in March 2017 showed similar discharge patterns to the survey undertaken at the end of February 2017. The radon concentrations were slightly lower, which is expected due to the WS River flow being higher in the second survey. However, with the higher resolution sampling, the data highlights that sections of the WS River had radon concentrations that were not in agreement with flow gauge data – suggesting a contradictory interpretation of groundwater discharge patterns. For example, results from the first 800 m of the study showed low and slightly decreasing radon in February and consistently low radon in March, suggesting little or no groundwater discharge through that area until Jones Road,

where radon concentrations (and groundwater discharge) increased (Figure 4.15). Flow gauge data did not increase over this interval, but the radon data suggests some groundwater discharge. The discrepancy between the flow gauge data and the radon data is interpreted to be due to either parafluvial flow or low-discharge groundwater seepage or a combination of the two processes.

The higher-resolution radon sampling supports the interpretation of parafluvial flow. For example, north of bore J42/0119, radon increased east of Switchback Road and remained relatively constant over a distance of ~600 m. Where concentrations remained relatively constant, parafluvial flow is likely occurring.

Radon concentrations measured from the river gravels were the same, within analytical error, as nearby river samples for sites 03-gw2 and 03-gw3, suggesting parafluvial flow. The largest difference between gravel and adjacent river sites was 2.6 L^{-1} at sites 03-gw4 and 03-r4, respectively, confirming increased groundwater discharge into the river in this area, but not ~200 m north at 03gw3 (Figure 4.15). This observation further highlights the spatially heterogeneous interaction between surface and groundwater in the WS River.

Finally, the radon data was applied to a mass-balance calculation in an attempt to quantify groundwater flux in the gaining river reaches, and in an area where the radon and flow gauge results were inconsistent with one another (details in Appendix 10; Martindale et al. 2017). Results suggested that there were at least two different groundwater sources interacting with the river, and that the contribution of radon from parafluvial flow did not appear to be statistically significant. The reach where radon and flow gauging yielded conflicting results as to whether the reach was gaining or losing (Reach 2), was investigated. Concurrent streamflow gauging suggested a losing reach. However, radon concentrations within this reach were relatively high, from 2.0 to 2.9 Bq/L, which indicated groundwater discharge. This discrepancy may be explained by the existence of small, localised, groundwater seeps discharging at the northwest end of this reach. This is also consistent with the increased radon in riverbed-gravel samples (e.g. 03-gw3 and 03-gw4) and with parafluvial flow contributing to increased concentrations of radon further downstream in the reach. This area also has a mapped fault, which may be an additional source for localised groundwater discharge.

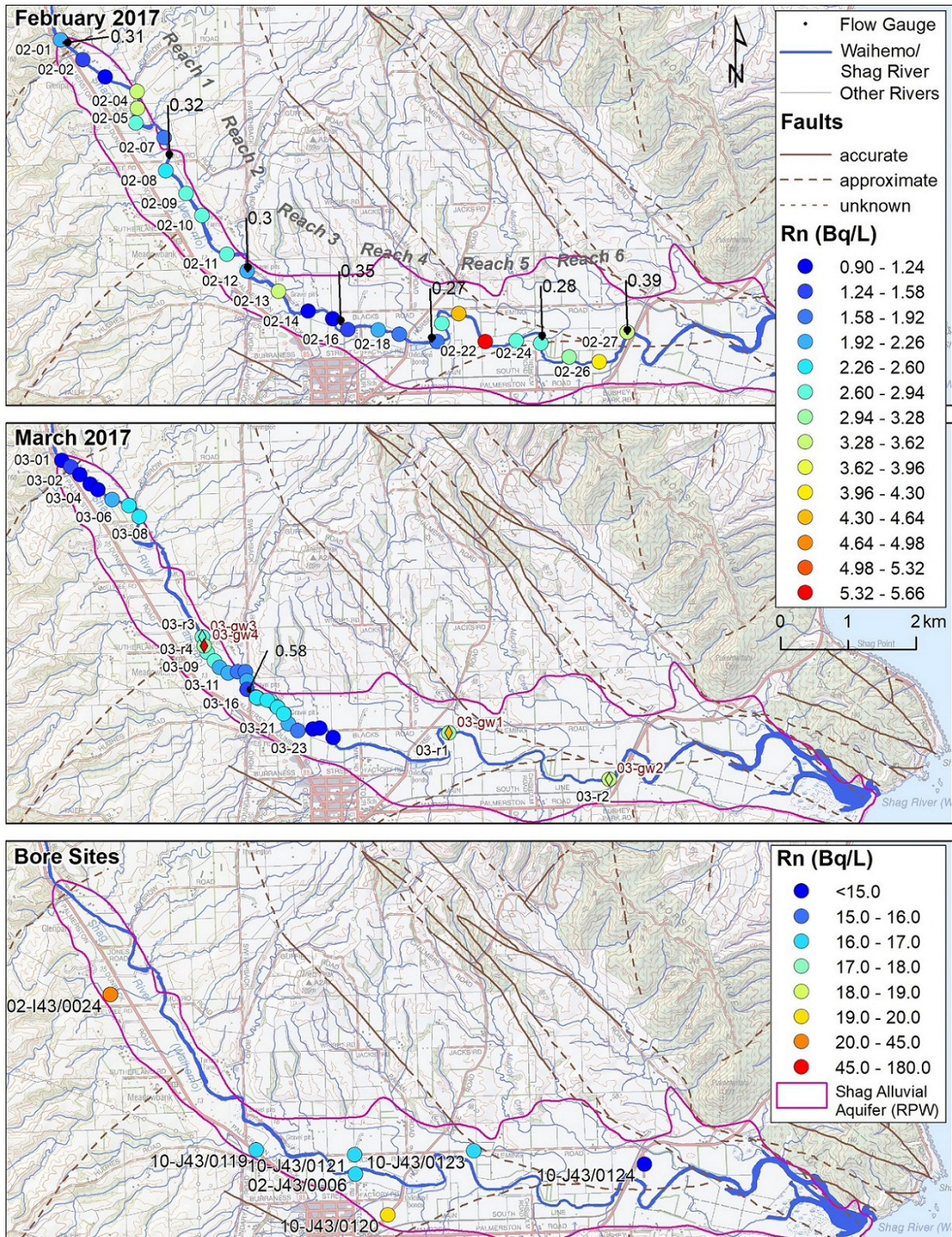


Figure 4.15 Radon results from this study, including surface water sampled from the Waihemo/Shag River in February and March 2017, and from groundwater bores in February, March, and October 2017. Flow gauge results are shown as m³/s, with reach sections labeled between gauging sites for February 2017. Reach sections 1, 3, 5 and 6 were gaining and reach sections 2 and 4 losing groundwater, respectively, during the February 2017 radon sampling campaign. Four shallow groundwater sites collected within the riverbed gravels in March 2017 are shown as diamonds (same colour range as the key), and site locations are labelled in Bordeaux colour. Note, that not all sample sites are labelled for February and March due to space limitations.

4.3 Conceptual Models

4.3.1 Aquifer Structure and River Interaction

The SAA is hosted in thin layers of Quaternary alluvial sediments, overlaying Tertiary mudstone, which is regarded as the hydrogeological basement (Figure 4.16). On the valley ranges, sediments directly overlay basement rock (mainly schist). The Quaternary sediments are very heterogeneous in the Lower WS River Valley (Section 2.1.4.3), and groundwater flow paths are controlled by sediment distribution and occurrence, with:

- Recent gravels located along the river or in river paleochannels, which are characterised by clean gravels and high hydraulic conductivity (aquifer).
- Older gravels, which are more weathered, contain a fraction of clay and silt and have low hydraulic conductivity (aquitard).
- Clay layers that can act as localised confining layers (aquiclude).

The heterogeneity explains the presence of dry bores close to productive bores. The most productive bores (e.g. Palmerston water supply bore near Mill Road) are directly tapping the river parafluvial flow. Within the system, water flows from groundwater to the river, and vice versa, depending on local groundwater and river-relative levels and sediments. For instance, in the upper part of the valley, the groundwater level is usually higher than the river level, which leads to the groundwater discharging to the river, also confirmed by radon results. Conversely, in the central part of the valley, the river recharges the SAA, as shown by the monitoring data from bore J43/0121 near Blacks Road.

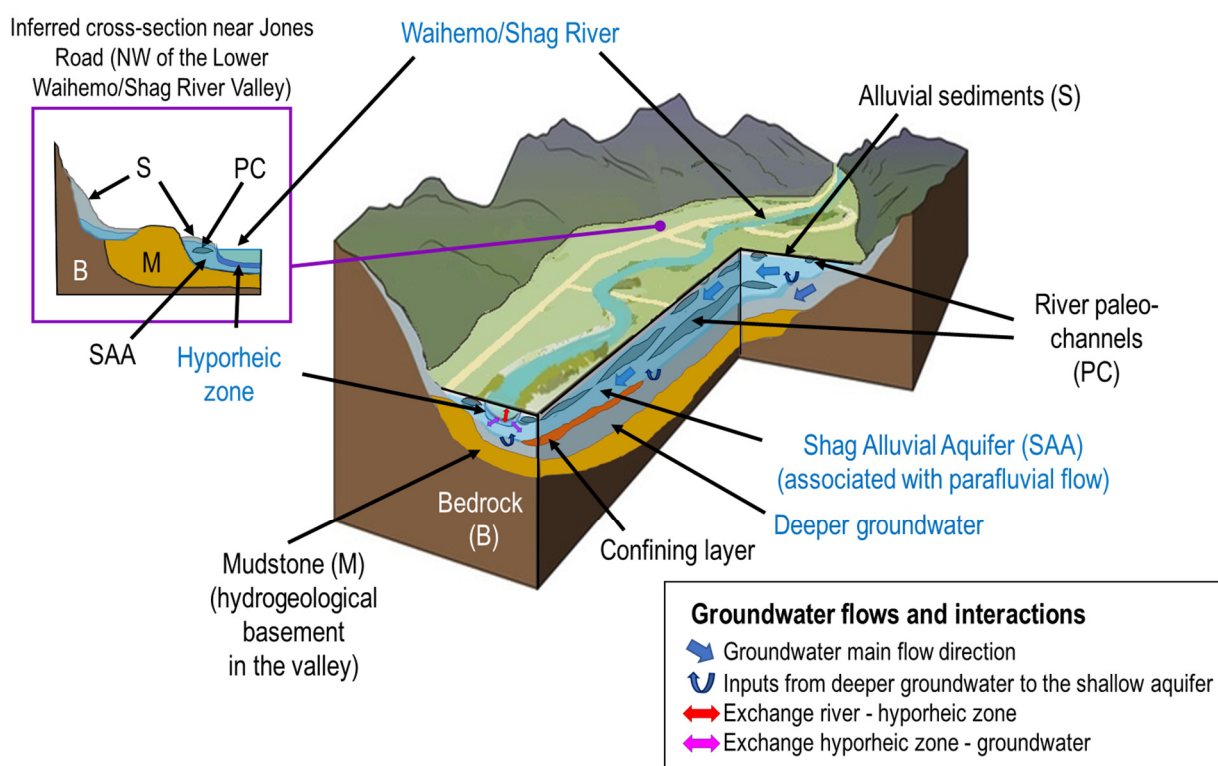


Figure 4.16 Conceptual model of the structure and river interaction for Shag Alluvial Aquifer, in the Lower Waihemo/Shag River Valley (adapted from Hauer et al. 2016). Note: In this schematic, features (e.g. topography, roads, river morphology, location of river paleochannels, confining layers, geological formation geometry) are represented in a simplified way that aims to illustrate the main local groundwater flows and interactions.

In the upper part of the valley (near Jones Road), local observations (i.e. mudstone present in the riverbed, drilling of dry bores with very shallow mudstone and presence of a productive well near the valley margin; I43/00024, near Mc Elwee Road) indicate a shallow mudstone hydrogeological basement. This could disconnect a part of the aquifer from the WS River and its parafluvial flow, as inferred in the cross-section in Figure 4.16.

4.3.2 Water Inputs and Outputs to the Aquifer

The main water inputs to the SAA come from rainfall and flow loss from the WS River and tributaries (Figure 4.17). The aquifer areas located along the valley margin receive almost exclusively rainfall recharge (e.g. I43/00024 but also probably J43/0120). Conversely, the areas located along the river that are highly connected to the river (parafluvial flow) have a large component of recharge from the WS River (e.g. J43/0121).

The main outputs from the SAA are water abstraction and discharge to the WS River (more important in the lower valley, e.g. near Shakey Bridge). This discharge is also more significant during dry periods and supports some base flow. However, reaches of the WS River can dry out during dry summers, which is likely caused by the aquifer's and river's disconnection due to shallow mudstone (see cross-section in Figure 4.16).

The SAA is located in a coastal plain, and its groundwater flows towards the coast and is inferred to discharge to the ocean. In addition, some groundwater can be lost by evapotranspiration. This is especially the case where groundwater is so shallow that tree roots can access and draw groundwater.

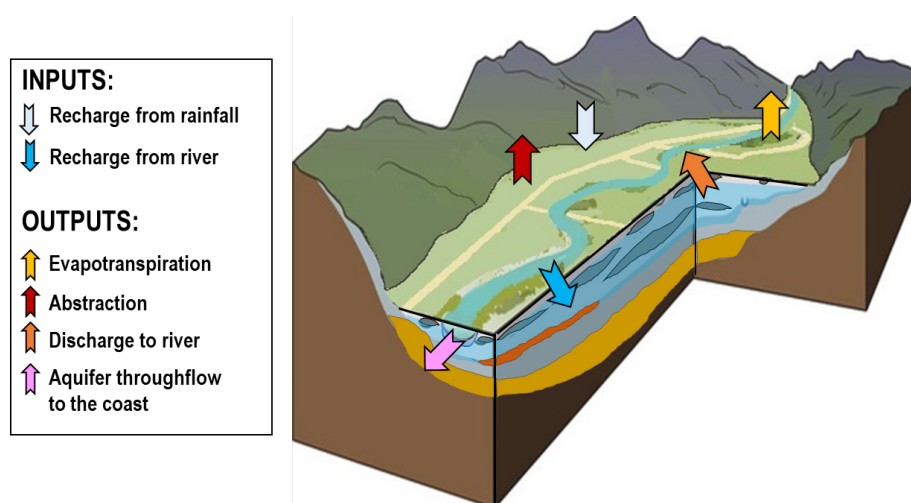


Figure 4.17 Conceptual model of the water inputs and outputs for the Shag Alluvial Aquifer, in the Lower Waihemo/Shag River Valley (adapted from Hauer et al. 2016). Note: In this schematic, features (e.g. topography, roads, river morphology, location of river paleochannels, confining layers, geological formation geometry) are represented in a simplified way that aims to illustrate water inputs and outputs to the Shag Alluvial Aquifer.

5.0 CONCLUSION AND RECOMMENDATIONS

5.1 Conclusion

A series of investigations, including a monitoring programme, was launched in the Lower WS River Valley by the ORC in 2017 to better characterise the local shallow aquifer (i.e. the SAA, as mapped by the Otago RPW). The current study aimed to analyse and interpret the data from that monitoring programme, covering five years of monitoring data plus data from complementary investigations (e.g. radon sampling survey in the WS River, age dating and stable isotope sampling in the WS River and SAA).

Both water level (aquifer and river hydrographs) and quality data pointed to the heterogeneity of the SAA, with:

- Highly connected parts of the aquifer to the WS River associated with more recent/cleaner alluvial sediments and young groundwater (MRT ≤ 2 years).
- Less well-connected parts to the WS River, associated with older/more weathered/clayey alluvial sediments and more mineralised and older groundwater (MRT up to 20 years).

Radon investigations also pointed to the spatially heterogeneous interaction between surface water and groundwater and suggested the presence of parafluvial flow and localised groundwater discharge.

High-frequency nitrate monitoring data indicated the influence of seasonal rainfall. For instance, high rainfall events caused nitrate pulses in groundwater, which led to increased river nitrate concentrations where groundwater was discharged to the river (e.g. upstream Shakey Bridge). Nitrate load calculations for the WS River showed the effect of land use in the Lower WS River Valley⁵, e.g. mean nitrate loads increased from upstream to downstream (~77 kg/d at EM495/Craig Road, ~82 kg/d at EM542/Switchback Road and ~109 kg/d at FD208/Shakey Bridge between September 2017 to August 2018).

These results, as well as the conceptual models (aquifer structure, interaction with the WS River and SAA water inputs and outputs), inform ORC on:

- Future monitoring in the Lower WS River Valley (e.g. sampling regime based on the high-frequency nitrate monitoring results, site selection according to hydrochemistry or recharge characteristics).
- Delineation of a more precise boundary for the SAA.
- Refinement of the current nitrogen regulations (e.g. nitrogen sensitive zone maps (RPW)) or introduction of other policies (e.g. groundwater quality allocation limits) in the new Land and Water Plan.
- Future development of groundwater flow and contaminant transport models.

⁵ Effects are mainly inferred to come from farming. However, some effect could also come from wastewater discharges. The nitrogen isotope analyses suggested below could help inform on the nitrogen origin.

5.2 Recommendations

In terms of monitoring, we recommend continued monitoring of surface water and groundwater quality and quantity in an integrated way that allows better management of the SAA and the WS River. This requires analysing the WS River water with similar groundwater chemical parameters for better comparison and alignment of sampling dates. The number of monitoring bores could be reduced. Potential monitoring sites of interest to maintain include:

- For surface water quantity: EM495/Craig Road, which is a strategic site (upstream in the Lower WS River Valley) with long-term records. Adding a second site downstream would be ideal for informing water exchanges in the Lower WS River Valley (e.g. FD208/Shakey Bridge).
- For surface water quality: the same sites as those used in this study (i.e. EM495/Craig Road and FD208/Shakey Bridge) would be interesting to capture the potential impacts of the land use in the Lower WS River Valley.
- For SAA groundwater levels and quality: bore J43/0119 might be the best candidate as it is inferred to receive recharge from both rainfall (over land) and the WS River. Therefore, it captures the influence of agricultural land use in the northwest part of the Lower WS River Valley and of the WS River. For operational aspects, it could be helpful to select J43/0119 as a groundwater quality monitoring bore and use J43/0124 to monitor groundwater levels. J43/0124 is located more downgradient but also captures the influence of both rainfall and surface water recharge.

The high-frequency nitrate monitoring datasets would need further processing and analysis to validate the measured concentrations (e.g. for bias correction; Pellerin et al. 2013). This would require other resources not available to us during this study (e.g. details about the calibration process, field operation logs). Formalised procedures for sensor deployment, operation, data cleaning and processing would be very valuable too, as it is our understanding that these sensors have been installed in other catchments. The roll-out of these sensors through different nitrogen-sensitive catchments would be very useful to inform future monitoring (sites and sampling regimes; Hudson and Baddock 2019).

In terms of complementary investigations, a review of any potential relevant geophysical investigations undertaken in the study area would be beneficial (e.g. passive seismic investigations undertaken for Hyde Resources; Hyde Resources Ltd. 2019) as a start. Subsurface geophysical data could help to:

- More precisely delineate the SAA (lateral extent, thickness).
- Provide new information on river paleochannels, productive and less productive aquifer zones.
- Estimate the height of the top of the mudstone hydrogeological basement that could inform interaction with the WS River and aquifer delineation for the areas where dry bores were drilled.

Nitrogen isotope samples could also be collected to confirm the source of nitrates (e.g. fertilisers, manure, septic tanks) and determine if nitrogen mineralisation or denitrification is taking place.

Finally, developing groundwater flow and contaminant transport models would help to investigate land use management scenarios and their impact on the SAA and WS River quantity and quality, as required.

6.0 ACKNOWLEDGEMENTS

The authors of this report would like to acknowledge Ben Mackey and Amir Levy (Otago Regional Council) for commissioning this work and the Envirolink Scheme for providing funding.

Special thanks to the following Otago Regional Council staff who provided significant support and involvement in this project: Malcom Allan, Nigel Stevenson, Paul Hannah, and Deborah Mills.

The support of the landowners, who gave permission to drill and access monitoring bores on their properties, has been essential to this monitoring programme. Many thanks to David Fleming, Ronald Sheat, Trevor Studholme and Jim Thomson. We are also grateful to the Waitaki District Council for permitting the drilling and the installation of monitoring bores on road reserves, which was also crucial to establishing the monitoring programme.

Thanks to Abigail Lovett and Heather Martindale (former GNS staff) for their contribution to undertaking the radon investigations and to Blair Miller (Lincoln Agritech) and Jens Rekker (former Lincoln Agritech staff) for installing and maintaining the groundwater high-frequency nitrate monitoring sensor.

Lastly, our acknowledgements go to Karyne Rogers and Conny Tschritter for reviewing this report and to Gina Pelham for formatting.

7.0 REFERENCES

- Aerial Surveys, editor. 2017. Gridded digital elevation model for the Lower Shag/Waihemo River. Auckland (NZ): Aerial Surveys.
- Black A, Craw D, Youngson JH, Karubaba J. 2004. Natural recovery rates of a river system impacted by mine tailing discharge: Shag River, East Otago, New Zealand. *Journal of Geochemical Exploration*. 84(1):21–34. doi:10.1016/j.gexplo.2004.02.002.
- Bouwer H, Rice RC. 1976. A slug test for determining hydraulic conductivity of unconfined aquifers with completely or partially penetrating wells. *Water Resources Research*. 12(3):423–428. doi:10.1029/WR012i003p00423.
- Cameron S, Forsyth PJ, Turnbull IM, Tait TM. 2003. Groundwater of the lower Shag Valley, North Otago. Wairakei (NZ): Institute of Geological & Nuclear Sciences. 36 p. Client report. Prepared for Waitaki District Council.
- Cartwright I, Hofmann H. 2016. Using radon to understand parafluvial flows and the changing locations of groundwater inflows in the Avon River, southeast Australia. *Hydrology and Earth System Sciences*. 20(9):3581–3600. doi:10.5194/hess-20-3581-2016.
- Dansgaard W. 1964. Stable isotopes in precipitation. *Tellus*. 16(4):436–468. doi:10.1111/j.2153-3490.1964.tb00181.x.
- D. Hamilton & Associates. 2002. Blue Mountain water supply. A review of potential better utilisation. Dunedin (NZ): D. Hamilton & Associates.
- ER Garden and Partners Ltd. 1984. Report on the utilisation of the Blue Mountains water supply. Dunedin (NZ): ER Garden and Partners Ltd. Prepared for Waihemo County Council.
- Forsyth PJ, Glassey PJ, Barrell DJA. 2001. Waitaki [map]. Lower Hutt (NZ): Institute of Geological & Nuclear Sciences. 1 map + 64 p., scale 1:250,000. (Institute of Geological & Nuclear Sciences 1:250,000 geological map; 19).
- Freeze RA, Cherry JA. 1979. Groundwater. Englewood Cliffs (NJ): Prentice-Hall. 604 p.
- Frew R, Van Hale R, Moore T, Darling M. 2011. A stable isotope rainfall map for the protection of New Zealand's biological and environmental resources. Dunedin (NZ): [Oritain]. 34 p. Prepared for Biosecurity New Zealand.
- Hauer FR, Locke H, Dreitz VJ, Hebblewhite M, Lowe WH, Muhlfeld CC, Nelson CR, Proctor MF, Rood SB. 2016. Gravel-bed river floodplains are the ecological nexus of glaciated mountain landscapes. *Science Advances*. 2(6):e1600026. doi:10.1126/sciadv.1600026.

- Heller T. 2001. Otago. In: Rosen MR, White PA, editors. *Groundwaters of New Zealand*. Wellington (NZ): New Zealand Hydrological Society. p. 465–480.
- Henderson R. 2019. Personal communication. Principal Scientist, National Institute of Water & Atmospheric Research, Christchurch, NZ.
- Hudson N, Baddock E. 2019. Review of high frequency water quality data, advice regarding collection, management and use of nitrate-nitrogen data. Hamilton (NZ): National Institute of Water & Atmospheric Research Ltd. 179 p. Prepared for Environment Southland, Otago Regional Council and Environment Canterbury.
- Hvorslev MJ. 1951. Time lag and soil permeability in ground-water observations. Vicksburg (MS): US Army Waterways Experiment Station. 50 p. Bulletin 36.
- Hyde Resources Ltd. 2019. Relinquishment Report, Mineral Prospecting Permit (PP) 60466. 30 p. Located at: Ministry of Business, Innovation and Employment (MBIE), Wellington, NZ. New Zealand Unpublished Mineral Report MR5622.
- HydroMetrics. HydroMetrics nitrate GW50 groundwater optical nitrate sensor, general specifications. 2022. Christchurch (NZ): HydroMetrics; [accessed 2022 Nov 15].
<https://www.hydrometrics.co.nz/Specifications/>
- International Atomic Energy Agency. 2006. Use of chlorofluorocarbons in hydrology: a guidebook. Vienna (AT): International Atomic Energy Agency. 277 p. (STI/PUB; 1238).
- Irricon Consultants. 1995. Preliminary well/borehole location survey, monitoring requirements and recommendations for further studies. Dunedin (NZ): Irricon Consultants. 14 p.
- Lachniet MS, Moy CM, Riesselman C, Stephen H, Lorrey AM. 2021. Climatic and topographic control of the stable isotope values of rivers on the South Island of New Zealand. *Paleoceanography and Paleoclimatology*. 36(5):e2021PA004220. doi:10.1029/2021PA004220.
- Lis G, Wassenaar LI, Hendry MJ. 2008. High-precision laser spectroscopy D/H and $^{18}\text{O}/^{16}\text{O}$ measurements of microliter natural water samples. *Analytical Chemistry*. 80(1):287–293. doi:10.1021/ac701716q.
- LRIS Portal. 2020. Lincoln (NZ): Landcare Research New Zealand. LCDB v5.0 – Land Cover Database version 5.0, mainland New Zealand; [accessed 2020 May 19].
<https://iris.scinfo.org.nz/layer/104400-lcdb-v50-land-cover-database-version-50-mainland-new-zealand/>
- Manaaki Whenua Landcare Research. 2022. Smap Online: the digital soil map for New Zealand. Lincoln (NZ) Manaaki Whenua Landcare Research; [accessed 2022 Oct 25].
<https://smap.landcareresearch.co.nz/>
- Martin A, Smith Lyttle B, Allibone A, Blakemore H, Cox S, Craw D, Doyle S, Kellett R, MacKenzie D, Mortimer N, et al. 2021. Geology of the Hyde-Macraes Shear Zone and Waihemo Fault Zone area, northeastern Otago. Lower Hutt (NZ): GNS Science. (GNS Science geological map 9).
- Martindale H, Knowling MJ, van der Raaij R, Lovett A, Morgenstern U, Mourot F. 2017. A hypothesis-testing approach to quantifying groundwater discharge using Radon-222 in the Shag River [abstract]. In: *New Zealand Hydrological Society Annual Conference*; 2017 Nov 28–Dec 1; Napier, New Zealand. Wellington (NZ): New Zealand Hydrological Society. p. p. 131–132.
- Martindale H, Lovett A. 2017. Groundwater-surface water interaction in the Shag River. Lower Hutt (NZ): GNS Science. 8 p. Consultancy Report 2017/45 LR. Prepared for Otago Regional Council.
- Martindale H, van der Raaij R. 2018. Investigation of groundwater-surface water interaction in the Te Arai River, Gisborne, using radon-222 and concurrent stream flow gauging. Lower Hutt (NZ): GNS Science. 27 p. (GNS Science report; 2018/13). doi:10.21420/G2SD24.
- McMillan SGc. 1999. Geology of Northeast Otago: Hampden (J42) and Palmerston (J43). Lower Hutt (NZ): Institute of Geological & Nuclear Sciences. 55 p. (Institute of Geological & Nuclear Sciences science report; 98/25).
- Meilhac C, Minni G, Cameron SG. 2010. Compilation of aquifer test data for sites in the National Groundwater Monitoring Programme. Lower Hutt (NZ): GNS Science. 22 p. + 1 CD. (GNS Science report; 2009/19).

- Ministry for the Environment. 2020. National Policy Statement for Freshwater Management 2020. Wellington (NZ): Ministry for the Environment. 70 p.
- Ministry for the Environment Data Service. 2017. Wellington (NZ): Ministry for the Environment. Irrigated land area, 2017 [map]; [updated 2018 Apr 18; accessed 2020 May 19]. <https://data.mfe.govt.nz/layer/90838-irrigated-land-area-2017/>
- Ministry of Health. 2018. Drinking-water Standards for New Zealand 2005 (Revised 2018). Wellington (NZ): Ministry of Health. 120 p.
- Mourot F. 2017. Anthropogenic effects on the water levels and dynamics of the lower Shag River and connected alluvial aquifer complex. In: *New Zealand Hydrological Society Annual Conference*; 2017 Nov 28-Dec 1; Napier, NZ. Wellington (NZ): New Zealand Hydrological Society. p. 162–163.
- Mourot F. 2018. Shag alluvial ribbon aquifer: factual investigations and monitoring report. Dunedin (NZ): Otago Regional Council. 51 p.
- Olsen D, Ozanne R. 2014. Shag River/Waihemo catchment: water quality and ecosystem. Dunedin (NZ): Otago Regional Council. 88 p.
- Otago Regional Council. 2000. North and Coastal Otago river catchments monitoring report. Dunedin (NZ): Otago Regional Council.
- Otago Regional Council. 2004. Regional Plan: water for Otago. Updated to 16 May 2020. Dunedin (NZ): Otago Regional Council.
- Otago Regional Council. 2009. Channel morphology and sedimentation in the Shag River, North Otago. Dunedin (NZ): Otago Regional Council. 42 p.
- Otago Regional Council. 2022. Water quality ecological assessment 2016 to 2021. Dunedin (NZ): Otago Regional Council. 17 p.
- Pellerin BA, Bergamaschi BA, Downing BD, Saraceno JF, Garrett JD, Olsen LD. 2013. Optical techniques for the determination of nitrate in environmental waters: guidelines for instrument selection, operation, deployment, maintenance, quality assurance, and data reporting. Reston (VA): U.S. Geological Survey. 48 p. Techniques and methods 1-D5.
- Stewart D. 2003. Shag River Catchment water resources. Prepared for Waitaki District Council. April 2003.
- Stewart M, Morgenstern U. 2001. Age and source of groundwater from isotope tracers. In: Rosen MR, White PA, editors. *Groundwaters of New Zealand*. Wellington (NZ): New Zealand Hydrological Society. p. 161–183.
- Sun H, Koch M. 2014. Under- versus overestimation of aquifer hydraulic conductivity from slug tests. In: Lehfeldt R, Kopmann R, editors. *ICHE 2014 – 11th International Conference on Hydroscience & Engineering*; 2014 Sep 28-Oct 2; Hamburg, Germany. [Karlsruhe] DE: p. Bundesanstalt für Wasserbau. p. 327–335.
- Tonina D, Buffington JM. 2011. Effects of stream discharge, alluvial depth and bar amplitude on hyporheic flow in pool-riffle channels. *Water Resources Research*. 47(8):W08508. doi: 10.1029/2010WR009140.
- TriOS optical sensors. Rastede (DE): TriOS. NICO; [accessed 2022 Nov 15]. <https://www.trios.de/en/nico.html>
- Turnbull IM, Fraser HL. 2005. Groundwater of the lower Shag Valley, North Otago: Phase 2 investigations. Lower Hutt (NZ): Institute of Geological & Nuclear Sciences. 38 p. Client Report 2005/48. Prepared for Waitaki District Council.
- van der Raaij R. 2019. Residence time determination for lower Shag Valley groundwater and surface water. Lower Hutt (NZ): GNS Science. 8 p. Consultancy Report 2019/43 LR. Prepared for Otago Regional Council.
- Williams J. 2014. Channel morphology of the Shag River, North Otago. Dunedin (NZ): Otago Regional Council.

APPENDICES

This page left intentionally blank.

APPENDIX 1 RAINFALL DATA

Table A1.1 Rainfall statistics for EM359/Stoneburn monitoring station from January 2000 to July 2022 (based on Otago Regional Council data).

Month	2000	2001	2002	2003	2004	2005	2006	2007	2008	2009	2010	2011	2012	2013	2014	2015	2016	2017	2018	2019	2020	2021	2022	Monthly Average (mm/month)
January	125	48	227	39	32	65	56	35	36	46	36	34	110	122	55	20	90	80	32	83	17	212	25	71
February	28	45	32	38	68	106	45	16	24	156	22	113	81	21	29	67	14	52	204	17	65	18	69	58
March	94	6	20	18	23	61	22	28	34	57	18	58	71	34	77	49	25	65	63	26	22	25	33	40
April	83	16	112	40	14	19	146	27	13	27	61	31	10	83	220	50	18	146	116	28	51	22	22	59
May	30	44	33	33	58	22	17	10	62	106	328	72	18	118	88	20	114	31	29	39	5	71	12	59
June	29	40	46	49	25	15	32	43	22	18	48	3	19	246	17	103	45	26	14	29	14	43	24	41
July	13	144	38	16	7	40	14	176	58	76	26	12	53	12	24	9	48	136	37	50	22	40	252	57
August	185	17	30	23	80	8	21	19	127	9	73	33	191	31	13	31	60	23	39	67	14	20	-	51
September	111	9	28	83	31	22	6	48	43	64	30	17	25	28	29	26	26	57	41	15	25	39	-	37
October	52	61	32	39	54	34	23	57	42	33	35	117	95	54	25	42	76	40	49	101	38	51	-	52
November	60	45	36	52	59	25	49	18	11	11	20	77	54	37	38	44	94	14	253	48	35	68	-	52
December	80	38	22	5	88	92	132	75	93	41	100	16	48	110	14	27	41	49	85	59	67	99	-	63
Annual mean (mm/yr)	890	513	656	435	539	509	563	552	565	644	797	583	775	896	629	488	651	719	962	562	375	708	-	Long term annual mean: 637

APPENDIX 2 EARLIER GEOLOGICAL MAP AND ASSOCIATED GEOLOGICAL CROSS-SECTIONS

A2.1 Earlier Geological Map

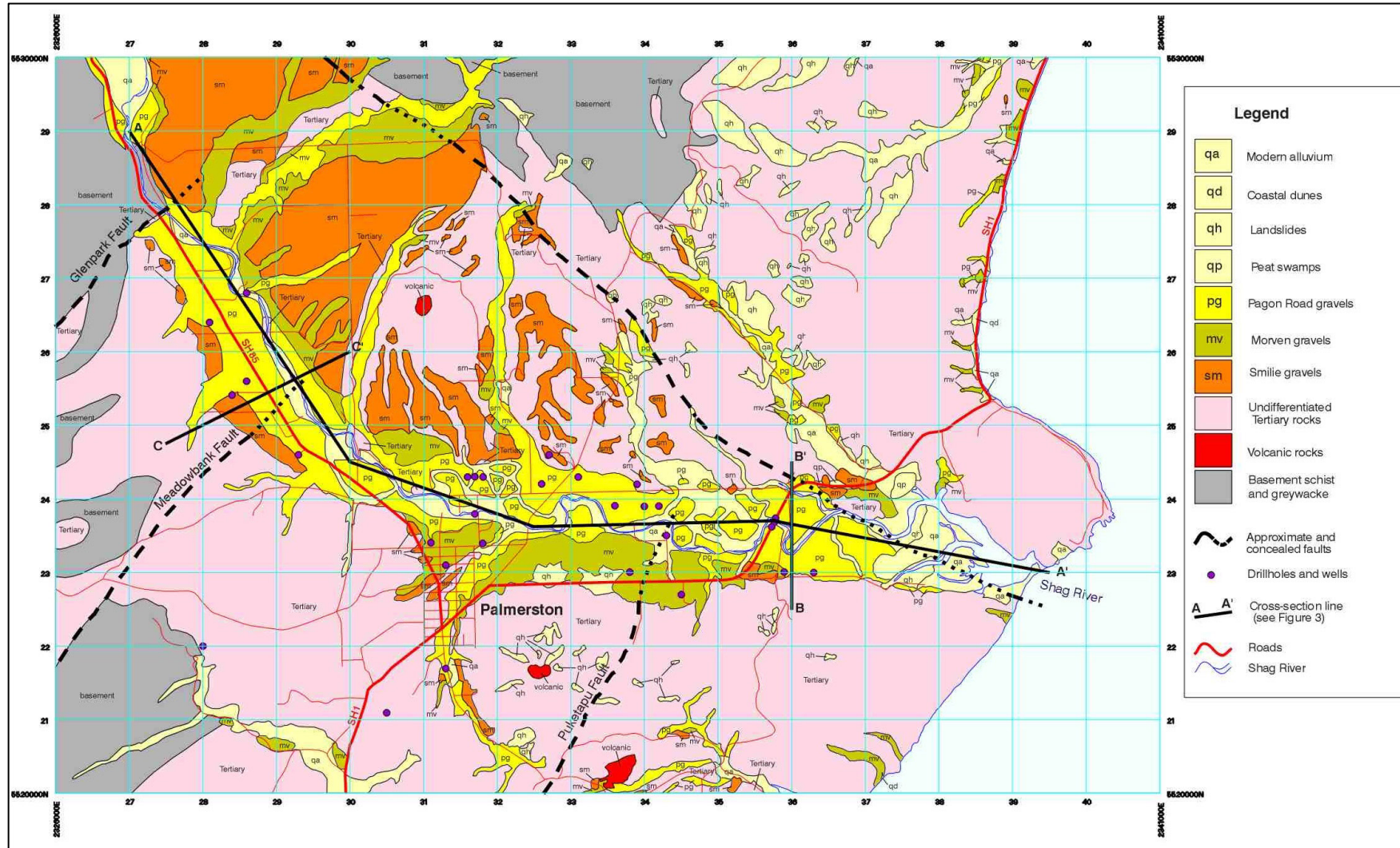


Figure A2.1 Detailed geology (particularly of Quaternary gravel deposits) of the Lower Waihemo/Shag River Valley (Cameron et al. 2003).

A2.2 Earlier Geological Cross-Sections

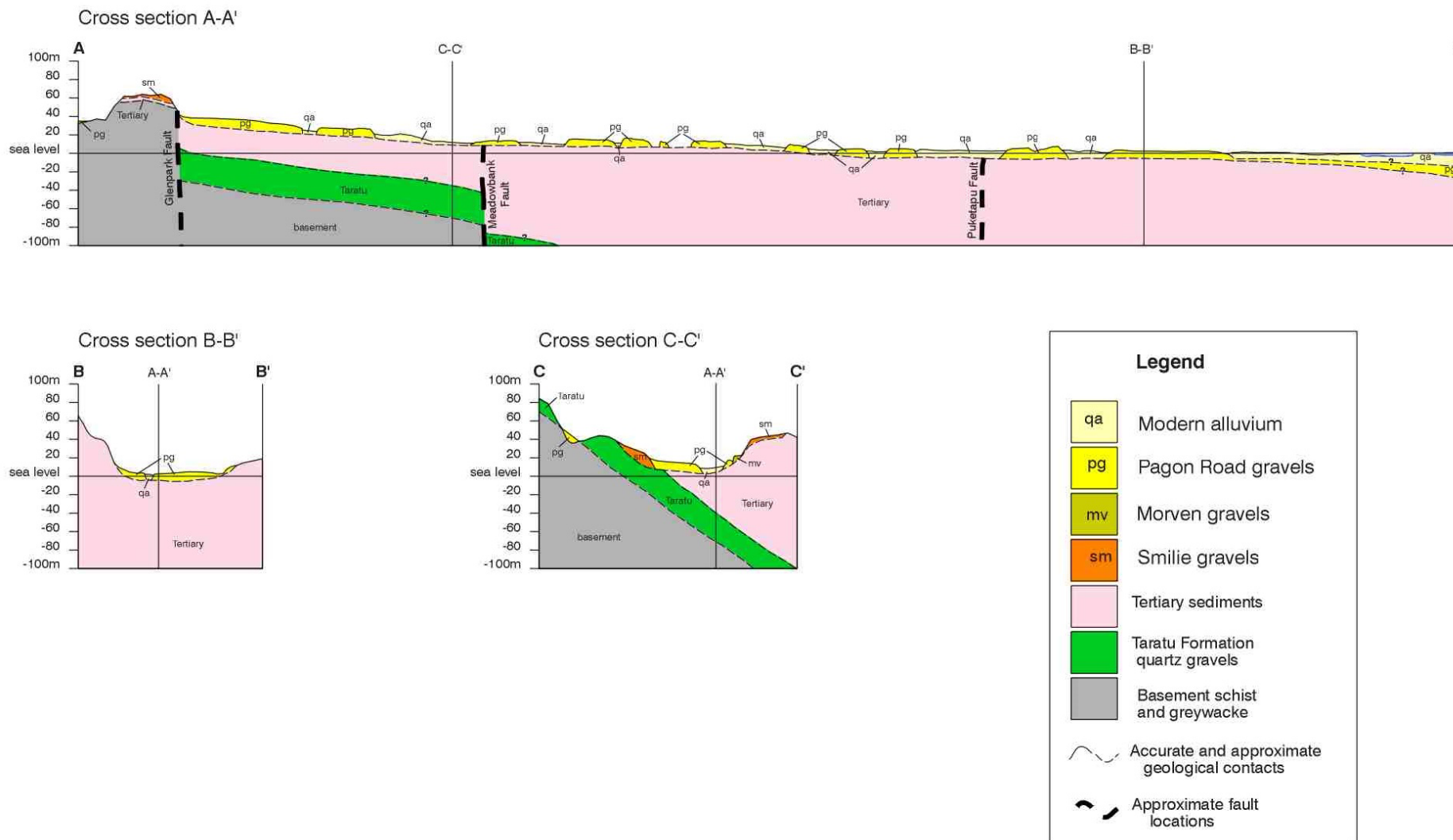


Figure A2.2 Geological cross-sections of the Lower Waihemo/Shag Aquifer Valley (Cameron et al. 2003).

APPENDIX 3 LITHOLOGICAL LOGS OF THE BORES DRILLED FOR THE PROGRAMME

Table A3.1 Lithological description of the new bores of the monitoring programme as logged by the driller and the geologist after Mouroit (2018).

Bore ID	Other ID	NZTM Easting	NZTM Northing	Driller's Log			Geologist's Log		
J43/0119	BH3	1420396	4962478	From Depth 0.0 1.5 4.3	To Depth 1.5 4.3 6.0	Lithology Pre drill Gravel Mudstone	From Depth 0.0 0.2 2.0 4.3	To Depth 0.2 2.0 4.3 6.0	Lithology Top soil Fine sandy GRAVEL, sub angular Yellow claybound GRAVEL, some cobbles dark grey MUDSTONE
J43/0120	BH4	1422339	4961519	From Depth 0.0 1.5 3.0 5.8	To Depth 1.5 3.0 5.8 6.0	Lithology Pre drill – Clayey Loam Yellow sandy clay Silty claybound gravels Grey mudstone	From Depth 0.0 0.2 3.0 5.6 5.8	To Depth 0.2 3.0 5.6 5.8 6.0	Lithology Top soil Yellowish sandy CLAY Silty and sandy GRAVEL, some cobbles Reddish / oxidised sandstone Dark grey MUDSTONE soft
J43/0121	BH5	1421850	4962405	From Depth 0.0 1.5 6.0	To Depth 1.5 6.0 6.2	Lithology Pre drill Gravels Mudstone	From Depth 0.0 0.2 3.0 5.0	To Depth 0.2 3.0 5.0 6.0	Lithology Top soil Brown-yellowish sandy GRAVEL, minor silt Sandy GRAVEL sub-angular, some cobbles Grey MUDSTONE
J43/0122	BH6	1423961	4961427	From Depth 0.0 1.5 2.8 3.6 9.7	To Depth 1.5 2.8 3.6 9.7 12.5	Lithology Pre drill Gravel / clay Clay Claybound gravel Mudstone some gravel	From Depth 0.0 0.2 2.8 3.6 9.7	To Depth 0.2 2.8 3.6 9.7 12.5	Lithology Top soil Grey and yellow gravelly CLAY Yellow CLAY Yellow clayey GRAVEL, sub-angular. MUDSTONE / oxidised rock?
J43/0123	BH7	1423610	4962461	From Depth 0.0 1.5 2.3 7.2 9.0	To Depth 1.5 2.3 7.2 9.0 10.0	Lithology Pre drill Clay Gravels Mudstone / gravels Mudstone	From Depth 0.0 0.2 2.3 4.4 6.6 10.0	To Depth 0.2 2.3 4.4 6.6 10.0 10.1	Lithology Top soil Yellowish clayey SAND / Sandy CLAY Brown-yellowish clayey GRAVEL sub-angular, some COBBLES Silty COBBLES Grey clayey GRAVEL, some mudstone debris Dark grey-green MUDSTONE
J43/0124	BH8	1426129	4962266	From Depth 0.0 1.5 5.5 10.0	To Depth 1.5 5.5 10.0 10.5	Lithology Pre drill Yellow clay few gravels Silts gravels Mudstone	From Depth 0.0 0.2 5.5 10.0	To Depth 0.2 5.5 10.0 10.5	Lithology Top soil Grey CLAY some gravels Grey silty GRAVELS sub-angular, some cobbles MUDSTONE

APPENDIX 4 SOIL MAPS AND INFORMATION

A4.1 Soil Maps with Soil Drainage

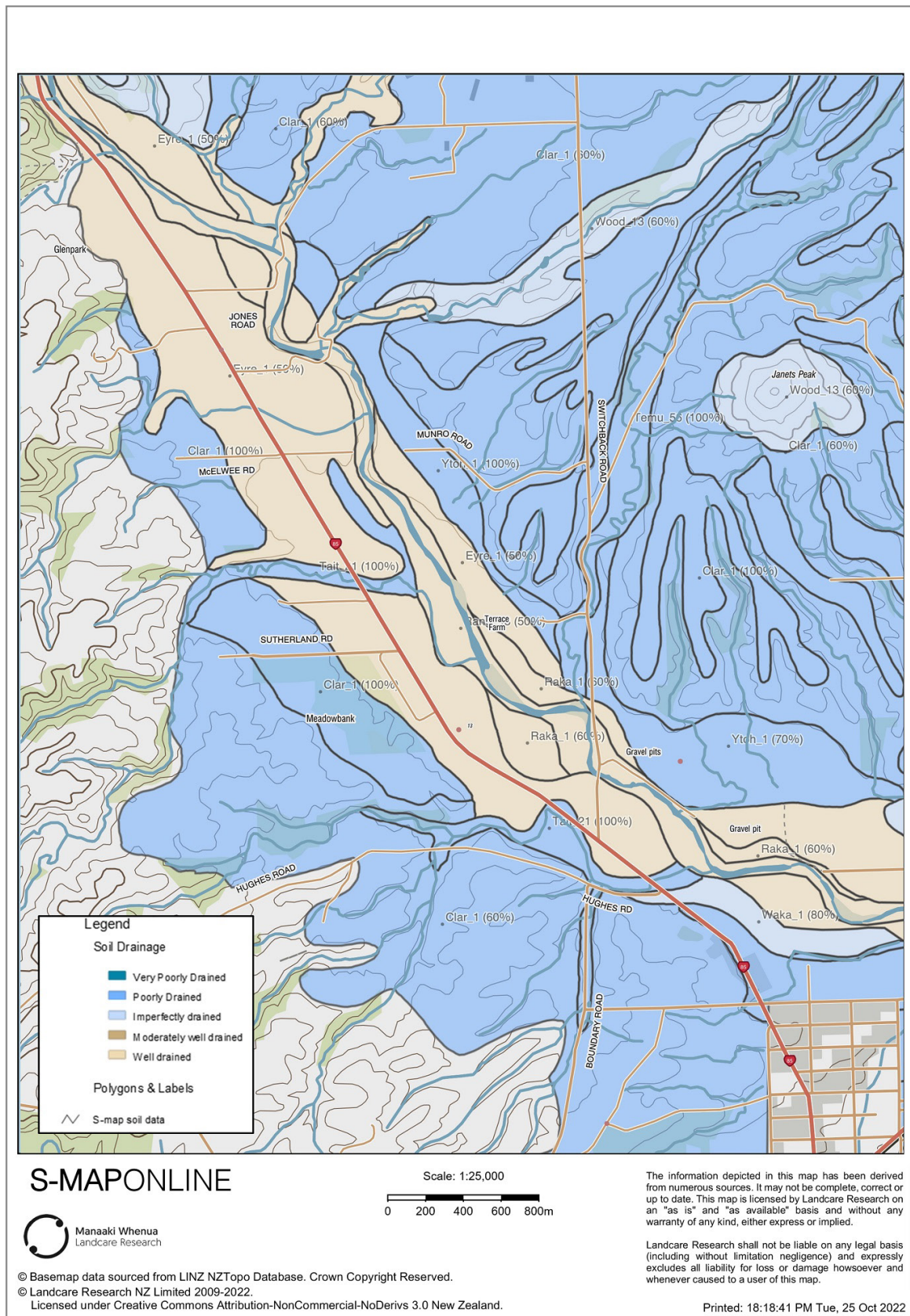


Figure A4.1 Soil types and drainage capability in the Lower Waihemo/Shag River Valley (northwest part) (Manaaki Whenua Landcare Research 2022).

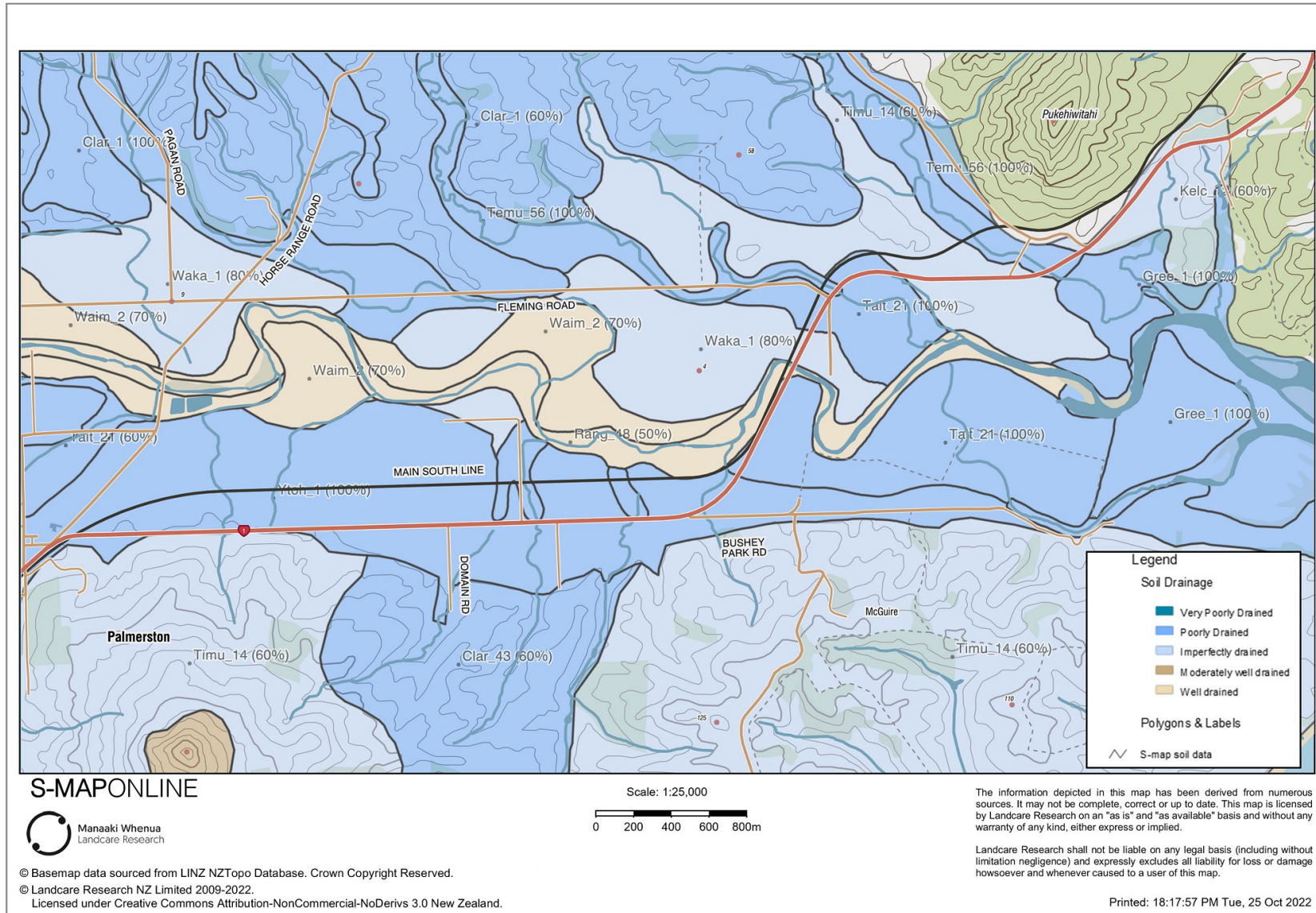


Figure A4.2 Soil types and drainage capability in the Lower Waihemo/Shag River Valley (eastern part) (Manaaki Whenua Landcare Research 2022).

A4.2 Soil Reports

Table A4.1 Description of the soils present in the Lower Waihemo/Shag River Valley, based on Smap after Manaaki Whenua Landcare Research (2022).

Map Code	Sibling Name	Family Name	Soil Classification	Soil Profile Material	Profile Texture	Stones/Rocks	Soil Material	Origin	Depth Class	Soil Drainage
Barr_30	Barrhill_30a.1	Barrhill (Barr)	Typic Immature Pallic Soils (PIT)	Moderately deep soil	Silt	Hard sandstone rock	Hard sandstone rock	Alluvium	Moderately deep (45–100 cm)	Well drained
Clar_1	Claremont_1a.1	Claremont (Clar)	Fragic Perch-gley Pallic Soils (PPX)	Stoneless soil	Silt	Not applicable	Hard sandstone rock	Loess	Moderately deep (40–80 cm)	Poorly drained
Gree_1	Greenpark_1a.1	Greenpark (Gree)	Saline Sandy Gley Soils (GSQ)	Stoneless soil	Sand	Not applicable	Hard sandstone rock	Alluvium	Deep (>1 m)	Poorly drained
Rang_48	Rangitata_48a.1	Rangitata (Rang)	Typic Fluvial Recent Soils (RFT)	Rounded stony soil	Sand	-	Hard sandstone rock	Alluvium	Very shallow (10–20 cm)	Well drained
Tait_21	Taitapu_21a.1	Taitapu (Tait)	Typic Recent Gley Soils (GRT)	Stoneless soil	Silt	Not applicable	Hard sandstone rock	Alluvium	Deep (>1 m)	Poorly drained
Timu_14	Timaru_14a.2	Timaru (Timu)	Mottled Fragic Pallic Soils (PXM)	Stoneless soil	Silt	Not applicable	Hard sandstone and schist rock	Loess	Moderately deep (35–65 cm)	Imperfectly drained
Waim_2	Waimakariri_2a.1	Waimakariri (Waim)	Weathered Fluvial Recent Soils (RFW)	Moderately deep soil	Silt	Hard sandstone rock	Hard sandstone rock	Alluvium	Moderately deep (45–90 cm)	Well drained
Waka_1	Wakanui_1a.1	Wakanui (Waka)	Mottled Immature Pallic Soils (PIM)	-	Silt	Not applicable	Hard sandstone rock	Alluvium	Deep (>1 m)	Imperfectly drained
Eyre_1	Eyre_1a.1	Eyre (Eyre)	Weathered Orthic Recent Soils (ROW)	Rounded stony soil	Silt	Hard sandstone rock	Hard sandstone rock	Alluvium	Shallow (20–45 cm)	Well drained
Raka_1	Rakaia_1a.1	Rakaia (Raka)	Weathered Fluvial Recent Soils (RFW)	Rounded stony soil	Loam	Hard sandstone rock	Hard sandstone rock	Alluvium	Shallow (20–45 cm)	Well drained
Ytoh_1	Waitohi_1a.1	Waitohi (Ytoh)	Argillic Perch-gley Pallic Soils (PPJ)	Stoneless soil	Silt over clay	Not applicable	Hard sandstone rock	Loess	Moderately deep (60–80 cm)	Poorly drained

Table A4.2 Glossary of soil description vocabulary after Manaaki Whenua Landcare Research (2022).

Soil Family	Families of mineral soils are identified by four sets of criteria describing soil materials occurring within 100 cm of the soil surface. The criteria are: soil-profile-material class, rock class, texture class and the permeability class of the slowest horizon. Soil families are given a geographic name and are also identified with a 4- or 5-character abbreviated name. The family name is suffixed with an italicised f to distinguish the family from the old soil series name. For example, Templeton family is written as Templetonf and is abbreviated as Temp.
Sibling	A sibling is a member of a soil family. The sibling partitions soil families on the basis of unique combinations of drainage class, topsoil stoniness, soil depth, texture contrasts, and a sequence of up to six functional horizons. Functional horizons are defined in terms of topsoil/subsoil, stoniness class, texture class, ped size and consistence. Functional horizons also distinguish soil materials derived from acidic and basic tephra.
Soil Classification	The New Zealand soil classification, which describes the characteristics, qualities and limitations of different soils. More information: https://soils.landcareresearch.co.nz/topics/soil-classification/nzsc/
Soil Profile Material	Soils are assigned to one of 10 'soil-profile-material' classes depending on the presence or absence, within specified depths, of distinctive types of mineral substrates with 100 cm depth (e.g. gravels, bedrock).
Soil Texture	Soil texture is used to describe the particle distribution of those particles in a mass of soil that are less than 2 mm in diameter. Particles coarser than 2 mm are described as gravel and are not regarded as a textural component. Soil texture is usually described as a class determined from a standard texture triangle based on the relative proportions of sand, silt and clay.
Rock Class of Stones/Rocks	Describes the rock class of underlying rock (if rock occurs within 100 cm) or of stones occurring within the soil profile within a depth of 0–100 cm. Twenty-two rock classes have been identified to record rock type.
Parent Material	The geological origin of the sediments or rocks from which the soil has formed.
Depth Class	Otherwise known as 'diggability', this is the soil depth to the layer that makes digging difficult. This could be a very stony layer, a soft or hard rock surface, shattered rock or other firm material. Depth class is classified as very shallow (<20 cm), shallow (20–40 cm), moderate (40–90 cm) and deep (>90 cm).
Profile Available Water (PAW)	<p>The amount of water potentially available to plant growth that can be stored in the soil to 100 cm depth. PAW takes into account variations in soil horizons and is expressed in units of millimetres of water, i.e. in the same way as rainfall. A PAW of 100 mm implies that 10% of the soil volume is water available to plants. Low PAW is <60 mm, moderate is between 60 and 150 mm, and high is ≥150 mm.</p> <p>Plants can only extract water where roots can grow. Thus where a root barrier occurs within 100 cm, the PAW reported will be the PAW to the root barrier. It is important to recognise that PAW is a potential value and not all the water is equally available. For example, as the soil dries out the water becomes more difficult to extract. As a general 'rule of thumb', plant growth will begin to slow down when 50% of PAW has been extracted. There are some crops that have shallow rooting depth, e.g. potatoes usually only root to a depth of 60 cm. In this case the PAW to 60 cm depth should be used.</p> <p>Top 60 cm available water as above but to a depth of 60 cm.</p> <p>Top 30 cm available water as above but to a depth of 30 cm, available to the widest range of crops, including shallow-rooting grasses and crops.</p> <p>Note that the Soil Moisture – Profile Available Water map shows the average PAW in the polygon (i.e. area-weighted by the sibling proportions).</p>

A4.3 Nitrogen Leaching Susceptibility

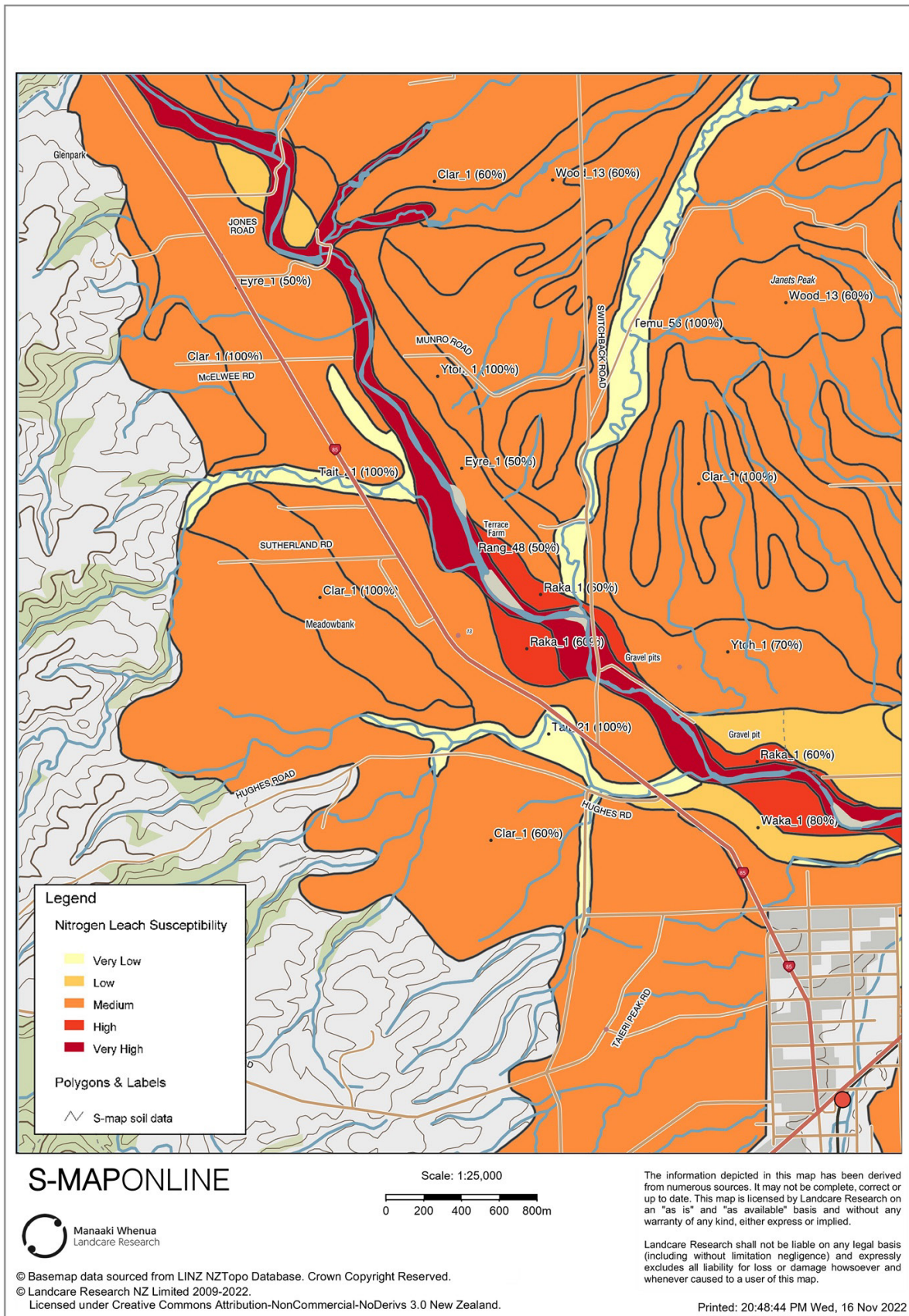


Figure A4.3 Soil nitrogen leaching susceptibility in the Lower Waihemo/Shag River Valley (northwest part) (Manaaki Whenua Landcare Research 2022).

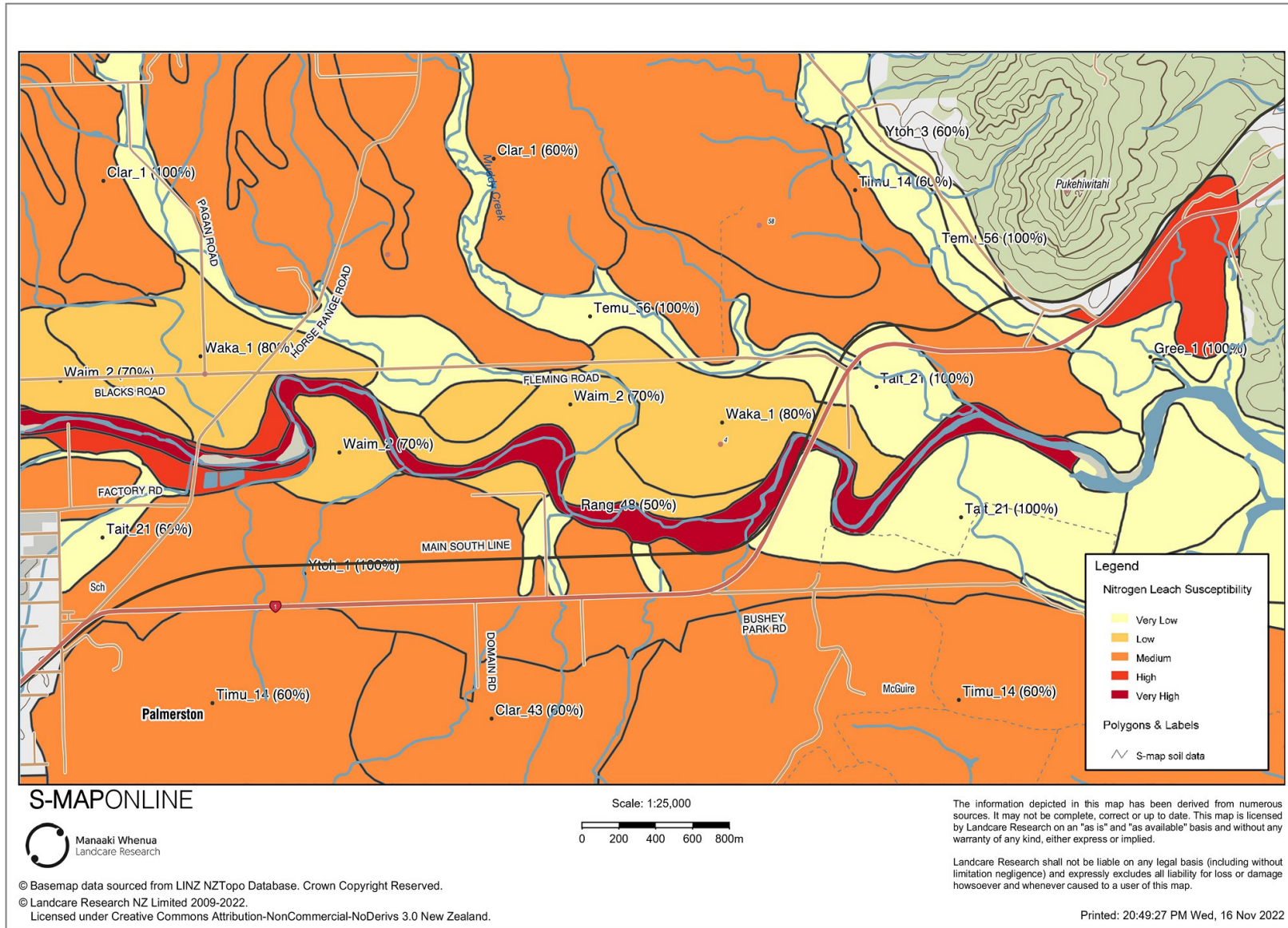


Figure A4.4 Soil nitrogen leaching susceptibility in the Lower Waiheho/Shag River Valley (eastern part) (Manaaki Whenua Landcare Research 2022).

A5.2 Age Dating Results

Table A5.2 Tritium, CFCs, and Halon-1301 results. Note that these were originally reported in van der Raaij (2019).

Location ID	Sample Date	Tr (TU)	± Tr	DO (mg/L)	Conductivity (µS/cm)	pH	Temp (°C)
J43/0119-Dec	14/12/2017	1.912	0.037	9.33	421	5.99	11.22
J43/0119-May	22/05/2018	2.082	0.033	7.05	429	6.14	12.88
J43/0121-Dec	14/12/2017	2.117	0.043	7.06	219	6.07	10.87
J43/0121-May	22/05/2018	2.149	0.035	5.85	232	6.32	12.93
J43/0122-Dec	14/12/2017	1.100	0.027	4.81	341	5.70	11.44
J43/0122-May	22/05/2018	1.058	0.023	4.03	386	5.81	11.96
EM495-Dec	14/12/2017	1.936	0.041	8.87	224	-	15.56
EM495-May	22/05/2018	2.128	0.036	11.97	193	-	6.66

Location ID	SF ₆ (pptv)	± SF ₆	CFC-11 (pptv)	± CFC-11	CFC-12 (pptv)	± CFC-12	CFC-113 (pptv)	± CFC-113	Halon-1301 (pptv)	± Halon
J43/0119-Dec	9.6	3.3	215	44	505	94	67.3	16.4	2.7	0.5
J43/0119-May	8.6	0.4	194	16	497	37	66.8	7.3	2.6	0.2
J43/0121-Dec	8.1	1.3	200	24	461	50	54.8	8.6	2.4	0.2
J43/0121-May	8.5	0.3	199	15	495	33	75.7	7.3	2.6	0.2
J43/0122-Dec	6.7	1.4	142	21	380	53	50.7	9.6	2.0	0.3
J43/0122-May	7.6	0.3	179	14	472	32	68.4	6.9	2.5	0.2

Location ID	SF ₆ (fmol/kg)	± SF ₆	CFC 11 (pmol/kg)	± CFC-11	CFC 12 (pmol/kg)	± CFC-12	CFC 113 (pmol/kg)	± CFC-113	Halon (fmol/kg)	± Halon
J43/0119-Dec	3.65	0.08	4.35	0.06	2.66	0.06	0.419	0.036	9.64	0.24
J43/0119-May	3.22	0.09	3.83	0.04	2.56	0.06	0.410	0.030	9.17	0.22
J43/0121-Dec	3.64	0.08	4.89	0.07	2.88	0.07	0.420	0.036	9.98	0.25
J43/0121-May	3.25	0.09	3.92	0.04	2.55	0.06	0.460	0.030	9.09	0.22
J43/0122-Dec	3.01	0.07	3.41	0.05	2.34	0.08	0.381	0.036	8.11	0.22
J43/0122-May	2.99	0.09	3.57	0.05	2.46	0.06	0.420	0.030	8.64	0.22

pptv: parts per trillion by volume.

fmol: femtomoles.

APPENDIX 6 HIGH-FREQUENCY NITRATE MONITORING SENSORS

A6.1 TriOS NICO Sensor

NICO

NICO

155XXXXXX



The image shows a sleek, cylindrical stainless steel sensor. It has a black label with 'TriOS Optical Sensors' and 'NICO' printed on it. A cable is attached to the right end.

TriOS's new low-cost nitrate meter

Based on the device platform concept of TriOS sensors like OPUS, LISA and VIPER, TriOS introduces NICO: a low-cost UV photometer for the determination of nitrate. The four detection channels enable a precise optical determination of nitrate by absorption, taking into account turbidity and organic substances that pose a problem for many products currently on the market.

An internal temperature correction additionally increases stability of the measured values.

Benefits

- Proven UV-absorption method
- Without sampling and preparation of test samples
- Real-time sensor
- Without reagents
- Optical window with nano coating

Applications

- Sewage treatment plants
- Environmental monitoring
- Drinking water monitoring

Equipped with our G2 interface with web browser configuration and internal data logger NICO includes features that are much more advanced than those of comparable devices available on the market.

The unified platform of all TriOS photometers also facilitates a standardized spare parts and consumables system, which allows the use of a wide range of accessories for our devices. Furthermore the cutting-edge G2 interface enables quick integration into third-party systems.



The image shows a black rectangular G2 interface unit with a Wi-Fi symbol and three indicator lights (Power, Sensor-Link, WiFi status). Below it are three silver sensor heads of different sizes.

D02-062en201810 brochure NICO

TriOS Mess- und Datentechnik GmbH · Bürgermeister-Brötje-Str. 25 · D-26180 Rastede · Germany
 fon: +49 (0) 4402 69670 - 0 · fax: +49 (0) 4402 69670 - 20 · info@trios.de · www.trios.de

1

Figure A6.1 General description of the TriOS NICO sensor (TriOS 2022).

NICO

Technical Specifications

Measurement-technology	light source	Xenon flash lamp	
	detector	4 photo diodes + filter	
Measurement principle		Attenuation	
Optical path		0.3 mm, 1 mm, 2 mm, 5 mm, 10 mm, 50 mm	
Parameters		NO ₃ -N, NO ₂ -N, NO _x -N, NO _x (calibrated with NO ₃ standard solution)	
Measurement range	1 mm path	0.5...60 mg/L NO ₃ -N	
	10 mm path	0.05...6 mg/L NO ₃ -N	
Measurement accuracy		± (5 % + 0.1 mg/L NO ₃ -N) with 10 mm path ± (5 % + 1 mg/L NO ₃ -N) with 1 mm path	
Turbidity compensation		Yes	
Data Logger		~ 2 GB	
Reaction time T100		20 s	
Measurement interval		≥ 10 s	
Housing material		Stainless steel (1.4571/1.4404) or titanium (3.7035)	
Dimensions (L x Ø)		~ 470 mm x 48 mm (10 mm path)	~ 18.5" x 1.9" (with 10 mm path)
Weight	stainless steel	~ 3 kg	~ 6.6 lbs
	titanium	~ 2 kg	~ 4.4 lbs
Interface	digital	Ethernet (TCP/IP)	
		RS-485 (Modbus RTU)	
Power consumption		≤ 7 W	
Power supply		12...24 VDC (± 10 %)	
Required supervision		Typically ≤ 0.5 h/month	
Calibration/maintenance interval		24 months	
System compatibility		Modbus RTU	
Warranty	1 year (EU: 2 years)		US: 2 years
INSTALLATION			
Max. pressure	with Subconn	30 bar	~ 435 psig
	with fixed cable	3 bar	~ 43.5 psig
	in flow unit	1 bar, 2...4 L/min	~ 14.5 psig at 0.5 to 1.0 gpm
Protection type		IP68	NEMA 6P
Sample temperature		+2...+40 °C	~ +36 °F to +104 °F
Ambient temperature		+2...+40 °C	~ +36 °F to +104 °F
Storage temperature		-20...+80 °C	~ -4 °F to +176 °F
Inflow velocity		0.1...10 m/s	~ 0.33 to 33 fps



D02-062en201810 brochure NICO

TriOS Mess- und Datentechnik GmbH · Bürgermeister-Brötje-Str. 25 · D-26180 Rastede · Germany
 fon: +49 (0) 4402 69670 - 0 · fax: +49 (0) 4402 69670 - 20 · info@trios.de · www.trios.de

2

Figure A6.2 Technical specifications of the TriOS NICO sensor (TriOS 2022).

A6.2 HydroMetrics Nitrate GW50 Sensor



HydroMetrics™

**HydroMetrics – Nitrate GW50
Groundwater Optical Nitrate Sensor**

Introduction

Many countries around the world are in the process of adopting nitrate caps via nitrogen discharge allowances to manage nitrate losses into freshwater bodies and groundwater drinking supplies from agricultural production. One area that remains unclear is how nitrate losses will be reliably measured to monitor and enforce these limits. Current approaches are principally based on modelling, rather than direct measurement of nitrate losses, as options such as regular physical sampling or real-time sensors are too expensive to be scalable. To address this, Lincoln Agritech has developed a low-cost sensor capable of measuring the concentration of nitrates in groundwater via monitoring wells.

General Specifications

- Groundwater deployment to measure nitrate nitrogen concentrations.
- Deployment in low ionic strength groundwater means organic carbon or chloride interferences are minimal.
- Designed to allow installation in 50 mm wells. These are often able to be installed by low cost direct push technologies, reducing the overall installation cost.
- Remote data-logging capability for real-time data.
- A fit for purpose Nitrate Sensor at a low price point that enables feasible deployment across multiple sites at the catchment or farm scale.
- Low power consumption (solar power installation possible).
- The sensor utilises optical sensor technology to extend the service interval when compared to other lower cost technologies such as Ion Selective Electrodes, which often suffer from significant calibration drift. This makes the HydroMetrics optical sensor more suitable for long term unattended deployment.
- Periodic cleaning rather than calibration required, reducing ongoing maintenance.
- Continuous monitoring as opposed to laboratory analysis is rapidly growing within the agricultural community due to increased data frequency.



Figure A6.3 General description of the HydroMetrics Nitrate GW50 sensor (HydroMetrics 2022).

Technical specification

Measurement technology (light source)	Xenon flash
Measurement principle	UV Absorbance
Measurement cell	10 mm tube
Parameter	NO ₃ -N
Measurement range	0 - 60 mg/L (without measurement cell alteration)
Measurement accuracy	+/- 5% +0.1 mg N/L
Turbidity compensation	Yes
Data logger	- 8 GB internal storage
Measurement interval	≥ 1 min
Housing material	316 stainless steel
Dimensions (ø x L)	42.2 mm x 455 mm
Weight	1.55 kgs
Interface	SDI-12 / RS-232
Power consumption	< 100 mW
Power supply	11.5 - 15.5 V
Guarantee	1 year
Max pressure	2.0 bar as standard

Specifications are subject to change without notification.

For more information, contact:
 Blair Miller - Group Manager,
 Environmental Research Lincoln Agritech Ltd
 Phone: +64 3 325 3724
 Email: blair.miller@lincolnagritech.co.nz
 Web: www.lincolnagritech.co.nz



Figure A6.4 Technical specifications of the HydroMetrics Nitrate GW50 sensor (HydroMetrics 2022).

APPENDIX 7 SLUG TESTS

A7.1 Summary of the Slug Test Parameters

Table A7.1 Summary of the slug test parameters at each bore, adapted from Mourot (2018).

Bore ID	Piezo Depth from Borelog (m BGL)	Top of the Screen (m BGL)	Bottom of the Screen (m BGL)	Screen Diameter (mm)	Piezo Depth Measured (m BGL)	Slug Test Type	Date	Time	Slug Length used or Volume of Water Poured	SWL Before Test (m Below TOC)	SWL After Test (m Below TOC)	Comment
J43/0119	4.3	2.5	4.0	100	4.8	Slug falling head	5/06/2018	Between 14:39 and 14:42	0.6 m	4.01	-	Several trials with the slug as no significant change in the water table height.
						Slug rising head			-	-		
						Water falling head		14:44	20 L	-	-	
J43/0120	5.8	3.6	5.8	50	5.9	Water falling head	5/06/2018	13:34	10 L	5.20	5.10 at 14:25 / 5.11 at 15:46	Not possible to use the slug as the bore diameter is 50 mm. Very slow recovery of the SWL.
J43/0121	5.0	1.5	4.5	100	5.9	Slug falling head	5/06/2018	13:05	0.6 m	4.27	-	A high-frequency monitoring sensor was installed in the bore and had to be removed.
						Slug rising head		13:07		-	-	
						Water falling head		13:14	20 L	-	-	
J43/0122	10.0	6.5	9.5	100	10.4	Slug falling head	5/06/2018	15:14	1.2 m	5.11	-	Confined conditions inferred.
						Slug rising head		15:18		-	-	
						Water falling head		15:22	20 L	-	5.08 at 15:27	
J43/0123	9.0	5.0	8.0	100	9.6	Slug falling head	5/06/2018	12:18	1.2 m	2.26	-	Slug down to 2.5–3 m, lowered too gently.
						Slug rising head		12:22		-	-	
						Water falling head		12:44	20 L	-	2.25	
J43/0124	9.0	5.5	8.5	100	9.5	Slug falling head	5/06/2018	11:09	1.2 m	1.74	-	First trial with the slug. The depth to which the slug went down (6 m) was too deep and it was submerged too gently.
						Slug rising head		11:19		-	-	
						Water falling head		11:46	20 L	-	-	

Note: BGL: below ground level, SWL: static water table, TOC: top of casing.

A7.2 Slug Test Analyses

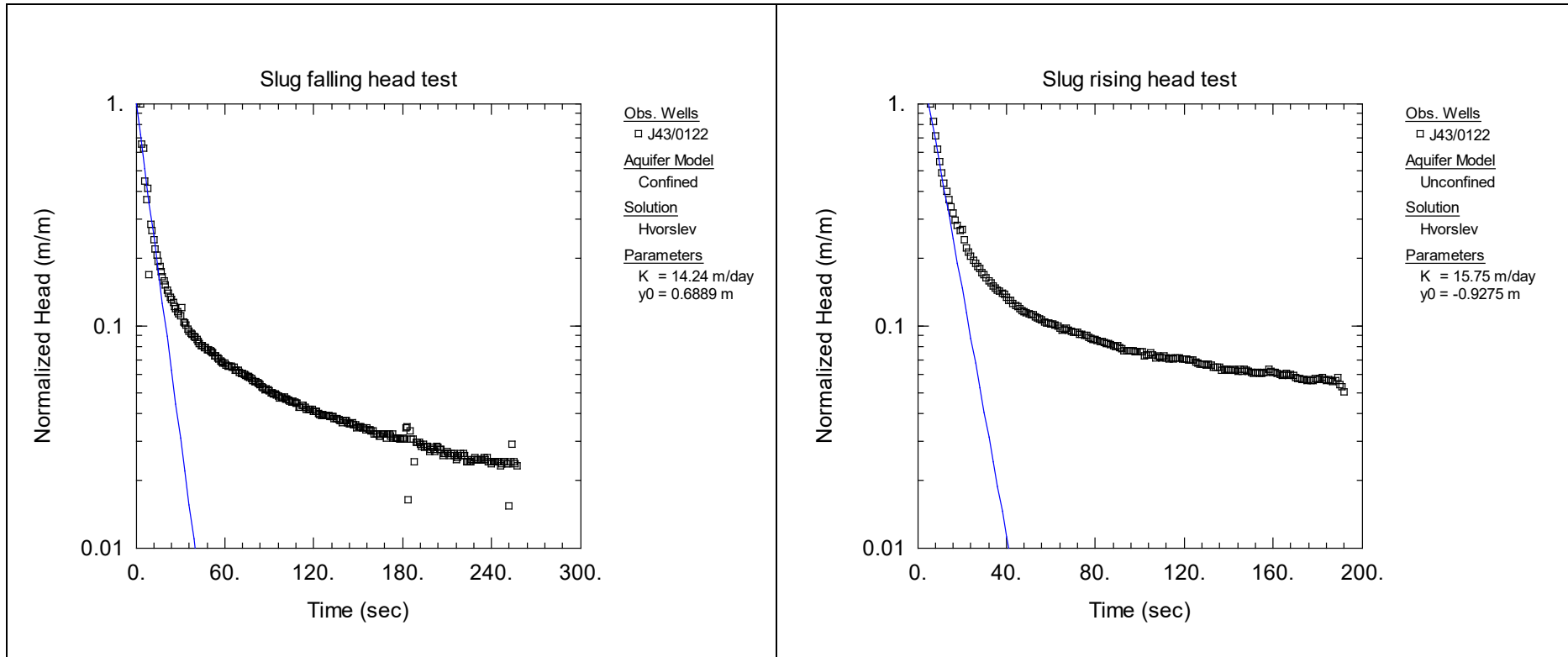


Figure A7.1 AQTESOLV Pro curve fitting analysis for bore J43/0122.

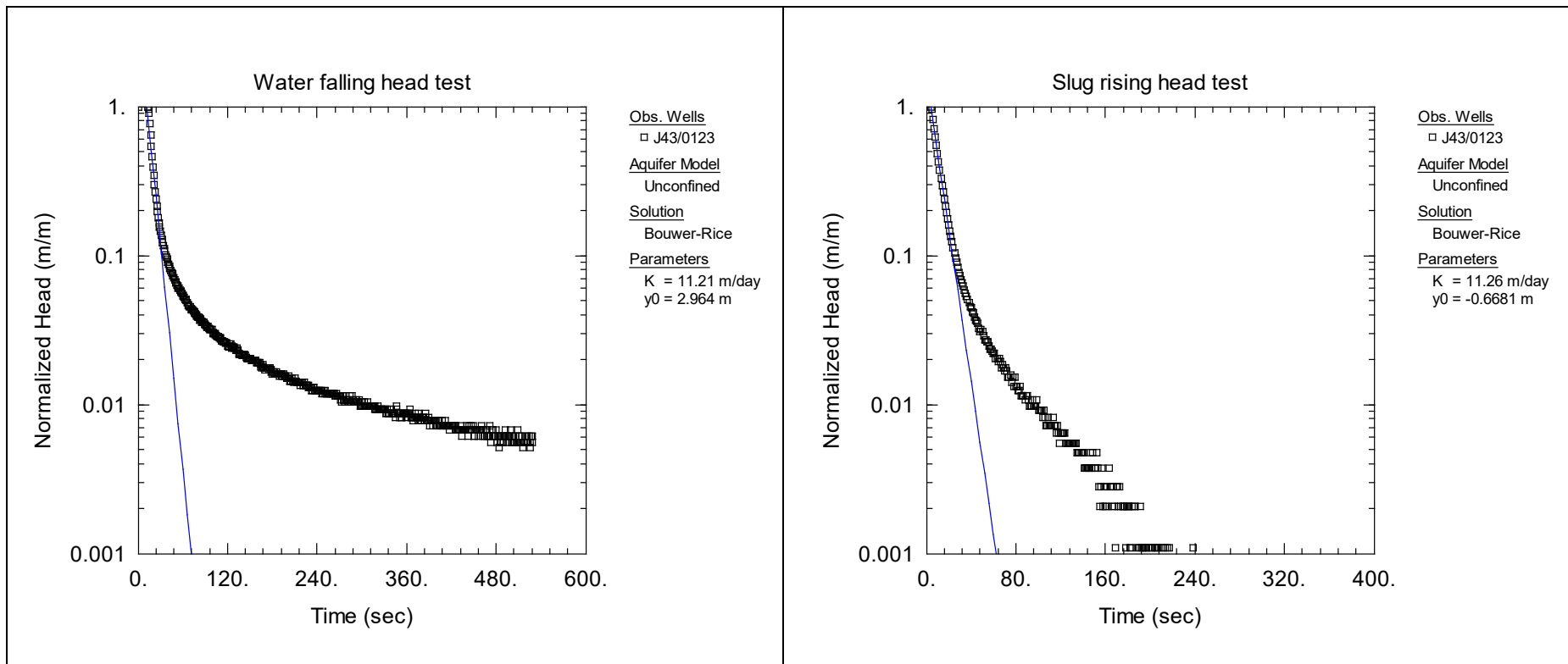


Figure A7.2 AQTESOLV Pro curve fitting analysis for bore J43/0123.

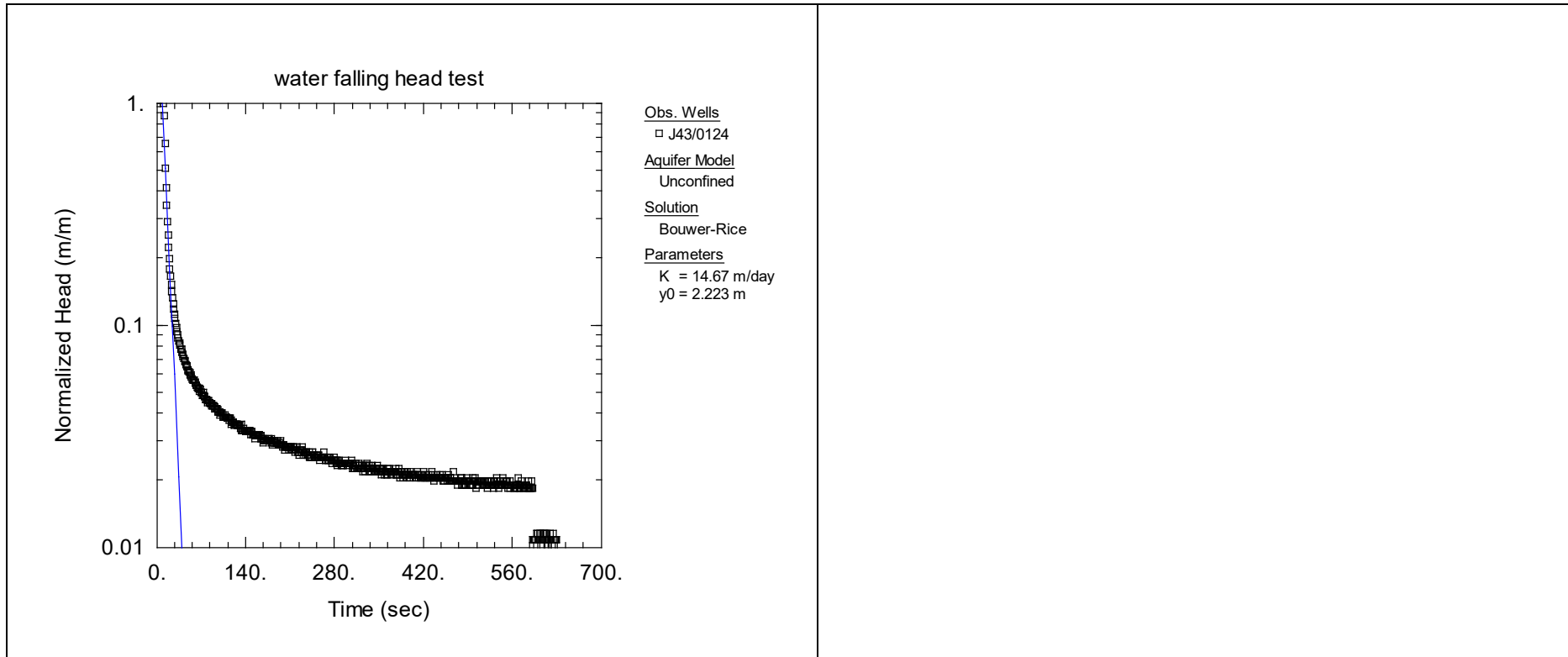


Figure A7.3 AQTESOLV Pro curve fitting analysis for bore J43/0124.

APPENDIX 8 PIEZOMETRIC MAP FOR JANUARY 2018

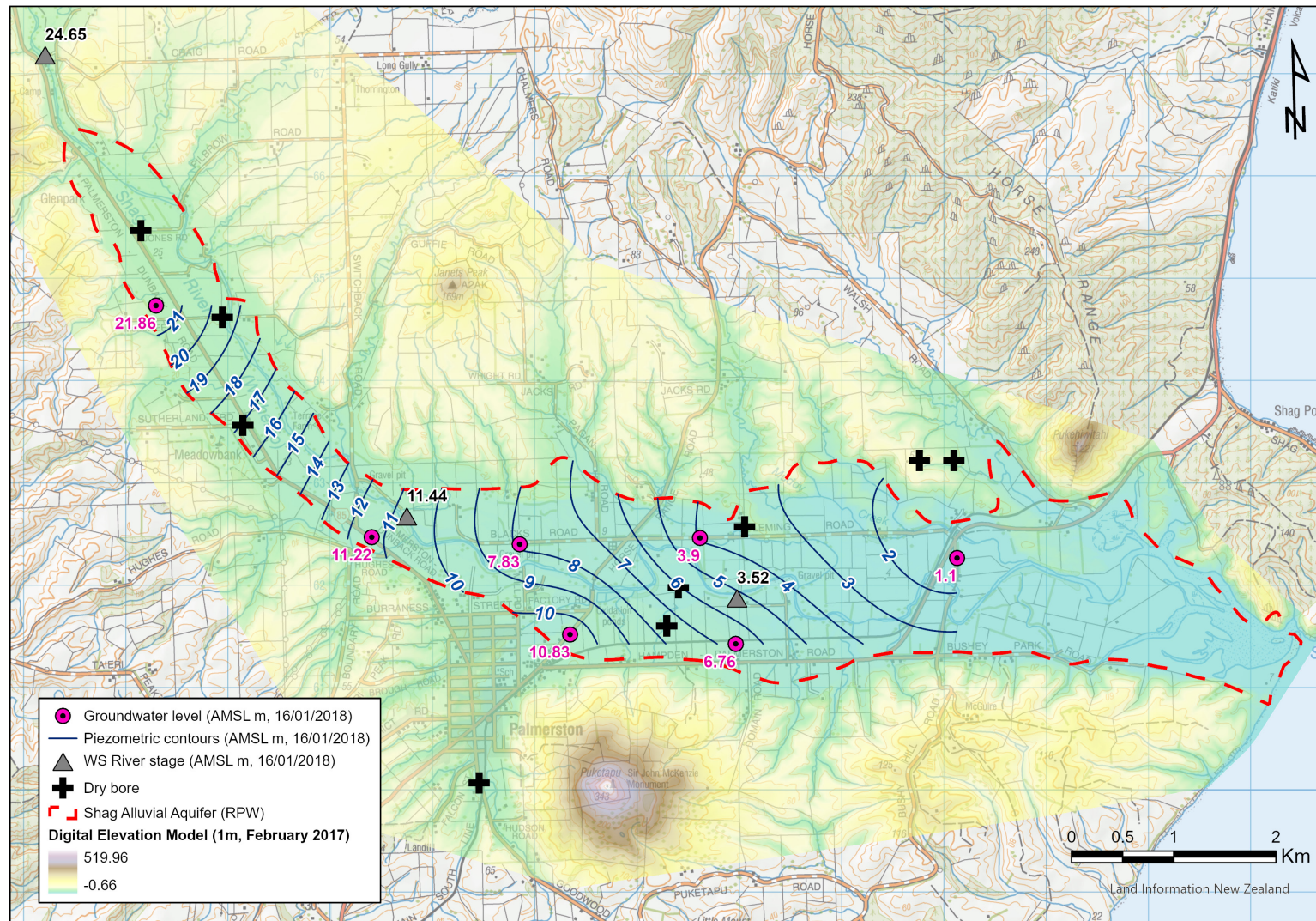


Figure A8.1 Piezometric contours for the Shag Alluvial Aquifer based on groundwater level measurements on 16/01/2018 (relatively low Waihemo/Shag River stage and groundwater level conditions). River stage data (and inferred connection between surface water and groundwater) were not used to draw these contours, and corrections to consider dry bores have not been applied.

APPENDIX 9 WAIHEMO/SHAG RIVER FLOW AND NITRATE LOADS

A9.1 Waihemo/Shag River Flow (High-Frequency Monitoring)

Table A9.1 Mean monthly and mean annual flows (in m³/s) for the Waihemo/Shag River high-frequency flow monitoring sites EM495/Craig Road, EM542/Switchback Road and FD208/Shakey Bridge (from September 2017 to May 2020).

Year	2017			2018			2019		2020	
Month	EM495 Craig Road	EM542 Switchback Road	FD208 Shakey Bridge	EM495 Craig Road	EM542 Switchback Road	FD208 Shakey Bridge	EM495 Craig Road	FD208 Shakey Bridge	EM495 Craig Road	FD208 Shakey Bridge
January	0.61	-	-	0.15	0.11	0.10	1.69	0.99	0.36	0.03
February	0.38	-	-	6.94	6.71	9.64	0.66	0.16	0.59	0.15
March	0.57	-	-	3.07	2.40	3.34	0.38	0.07	0.23	0.01
April	5.20	-	-	4.30	3.92	5.44	0.30	0.09	0.53	0.18
May	1.28	-	-	3.89	4.30	4.78	0.43	0.21	0.37	0.04
June	1.08	-	-	1.59	1.73	1.83	0.80	0.30	0.44	-
July	16.08	-	36.87	1.38	1.21	1.72	1.62	0.99	1.06	-
August	2.90	-	4.81	1.70	-	1.78	2.37	1.35	0.40	-
September	3.24	6.30	4.31	1.03	-	1.20	0.97	0.22	0.73	-
October	1.46	1.94	1.85	0.85	-	1.02	3.21	1.58	0.42	-
November	0.60	0.73	0.67	24.97	-	25.72	1.68	0.54	0.39	-
December	0.21	0.19	0.15	3.74	-	2.89	0.67	0.13	0.25	-
Annual mean (m ³ /s)	2.80	NA	NA	4.47	NA	4.96	1.23	0.55	0.48	NA

A9.2 Waihemo/Shag River Flow (Gauging Measurements)

Table A9.2 Results of monthly gauging measurements (in m³/s) for the Waihemo/Shag River (February 2017 to May 2020 period). Site locations are provided in to Figure 4.15.

Measurement Time	Jones Road (between Reach 1 and Reach 2)	Switchback Road (between Reach 2 and Reach 3)	Mill Road (between Reach 3 and Reach 4)	Shakey Bridge (between Reach 5 and Reach 6)
27/02/2017 14:18	-	0.30	-	-
20/03/2017 12:08	-	0.58	-	-
20/03/2017 13:49	-	0.58	-	-
10/10/2017 13:23	1.46	1.45	1.31	1.45
20/11/2017 11:50	0.51	0.53	0.45	0.55
21/12/2017 12:25	0.19	0.17	0.12	0.21
26/01/2018 12:32	0.14	0.11	0.05	0.11
26/03/2018 13:22	3.88	4.04	4.14	4.13
27/04/2018 13:11	0.88	0.89	0.83	0.92
31/05/2018 14:29	1.77	1.84	1.71	1.78
29/06/2018 11:10	-	1.34	-	-
4/07/2018 13:28	1.31	1.28	1.24	1.34
7/08/2018 14:27	2.72	2.57	2.61	2.71
5/10/2018 13:06	-	-	-	1.09
7/11/2018 08:55	-	-	-	0.77
8/02/2019 11:01	-	-	-	0.66
10/04/2019 10:31	-	-	-	0.29
7/06/2019 12:28	-	-	-	0.91
5/07/2019 13:46	-	-	-	0.45
22/08/2019 13:48	-	-	-	2.39
7/10/2019 12:42	-	-	-	2.33
25/11/2019 13:23	-	-	-	1.52
9/01/2020 13:56	-	-	-	0.46
6/03/2020 11:11	-	-	-	0.15
26/05/2020 11:39	-	-	-	0.31

This page left intentionally blank.

A9.3 Waihemo/Shag River Nitrate Load Estimates

Table A9.3 Annual mean daily nitrate loads estimated from high-frequency (HF) and grab-sample (GS) monitoring data for the Waihemo/Shag River at three locations: EM495/Craig Road, EM542/Switchback Road and FD208/Shakey Bridge (from September 2017 to August 2018).

Year	Month	EM495 – Craig Road							EM542 – Switchback Road							FD208 – Shakey Bridge						
		NO ₃ -N Mean Concentration GS (mg/L)	Number of GS	NO ₃ -N Mean Concentration HF Monitoring (mg/L)	Number of Days with HF Monitoring	Flow (m ³ /s)	Load (kg/d)		NO ₃ -N Mean Concentration GS (mg/L)	Number of GS	NO ₃ -N Mean Concentration HF Monitoring (mg/L)	Number of Days with HF Monitoring	Flow (m ³ /s)	Load (kg/d)		NO ₃ -N Mean Concentration GS (mg/L)	Number of GS	NO ₃ -N Mean Concentration HF Monitoring (mg/L)	Number of Days with HF Monitoring	Flow (m ³ /s)	Load (kg/d)	
							GS	HF Monitoring						GS	HF Monitoring						GS	HF Monitoring
2017	September	0.25	4	0.46	30	3.24	69.2	128.2	0.37	3	0.49	30	6.30	201.4	264.5	0.45	3	0.59	30	4.31	166.5	221.5
	October	0.11	4	0.33	31	1.46	14.3	41.2	0.20	3	0.28	31	1.94	33.1	47.7	0.29	3	0.44	31	1.85	45.7	69.8
	November	0.15	4	0.33	30	0.60	8.0	17.3	0.20	4	0.25	30	0.73	12.8	15.9	0.35	4	0.44	30	0.67	20.5	25.8
	December	0.11	4	0.31	31	0.21	2.0	5.7	0.19	3	0.24	31	0.19	3.2	4.0	0.38	3	0.48	31	0.15	5.0	6.3
2018	January	0.13	4	0.31	31	0.15	1.7	4.1	0.16	3	0.20	31	0.11	1.4	1.9	0.29	3	0.34	31	0.10	2.6	3.0
	February	0.32	2	0.56	28	6.94	192.8	334.1	0.09	1	0.49	28	6.71	49.9	283.8	0.20	1	0.56	26	9.64	166.6	464.4
	March	0.17	3	0.46	31	3.07	45.6	121.5	0.29	2	0.37	31	2.40	60.2	76.9	0.34	2	0.43	31	3.34	98.2	125.0
	April	0.09	2	0.37	30	4.30	34.6	138.9	0.12	2	0.23	29	3.92	39.5	79.4	0.18	2	0.33	30	5.44	85.6	155.1
	May	0.48	4	0.73	31	3.89	162.3	244.8	0.56	2	0.67	31	4.30	208.0	247.8	0.63	2	0.74	31	4.78	258.4	305.1
	June	0.23	2	0.46	30	1.59	31.6	62.6	0.30	1	0.39	30	1.73	44.9	58.0	0.36	1	0.46	30	1.83	57.1	72.3
	July	0.19	2	0.42	31	1.38	22.9	50.3	0.26	1	0.36	11	1.21	27.2	37.6	0.38	1	0.49	31	1.72	56.4	73.3
	August	0.26	2	0.48	31	1.70	38.1	69.9	0.33	1	-	-	-	-	-	0.40	1	0.50	31	1.78	61.4	77.4
	Annual mean	0.21	-	0.43	-	2.38	51.9	101.5	0.26	-	0.36	-	2.68	62.0	101.6	0.35	-	0.48	-	2.97	85.3	133.2
	Total #	-	37	-	365	-	-	-	-	26	-	313	-	-	-	-	26	-	363	-	-	-

This page left intentionally blank.

APPENDIX 10 ESTIMATION OF GROUNDWATER FLUXES TO THE WAIHEMO/SHAG RIVER

Martindale et al. (2017) attempted to quantify groundwater fluxes to the gaining river reaches, and where the radon and flow gauge results were inconsistent with one another.

These authors used a mass-balance calculation and assumed that conditions were constant between neighbouring radon measurements (i.e. the calculated discharge at each measurement point represents a spatially aggregated discharge between that point and the downstream point). Furthermore, the calculated discharge at each measurement point was added to the total flow for the next calculation of the adjacent downstream radon measurement.

$$Q \frac{dc_r}{dx} = I(c_{gw} - c_r) + wEc_r + F_h + F_p - kdwc_r - \lambda dwc_r \quad \text{Equation 1}$$

Where I is the groundwater inflow along a reach ($\text{m}^3 \text{m}^{-1} \text{day}^{-1}$), Q is river discharge ($\text{m}^3 \text{day}^{-1}$), x is the distance of the reach measured (m), w is stream width (m), E is the evaporation rate (m day^{-1}), F_h is the flux of radon from the hyporheic zone ($\text{Bq m}^{-1} \text{day}^{-1}$), F_p is the flux of radon from the parafluvial zone ($\text{Bq m}^{-1} \text{day}^{-1}$), k is the gas transfer coefficient (day^{-1}), d is river depth (m), λ is the radon decay constant (0.181day^{-1}), c_{gw} is the concentration of radon in groundwater (Bq m^{-3}) and c_r is the radon concentration in the river water (Bq L^{-3}).

Uncertainty associated with the input variables in Equation (1) (i.e. c_{gw} , c_r , Q , w , E , F_h , k and d) was approximated by a Monte Carlo statistical analysis. Discharge flux was calculated assuming zero radon input from parafluvial flow (F_p). Thus, if the calculated discharge (Equation 1) significantly exceeded the discharge measured by concurrent gauging, it was assumed that the discrepancy indicated discharge from parafluvial flow. However, it should be noted that these mass-balance results can vary widely based on the assumed groundwater radon concentration, which has been shown to be highly variable in this area.

The gauged discharge rates were compared to those calculated using the mass-balance Equation (1) assuming two different groundwater radon input concentrations (c_{gw}) of 16 and 180 Bq L^{-1} for Reaches 2, 3 and 5 (Figure A10.1). In general, the calculated discharge was higher, assuming a radon input of 16 Bq L^{-1} , compared to calculations assuming an input of 180 Bq L^{-1} . For example, for Reaches 2 and 5, the gauged discharge (blue dots in Figure A10.1) overlapped, within error, the calculated discharge range (green polygon) assuming $c_{gw} = 180 \text{Bq L}^{-1}$, whereas for gaining Reach 3, the gauged discharge result best agreed with the calculated discharge range assuming a significantly higher $c_{gw} = 180 \text{Bq L}^{-1}$ value (Figure A10.1). This suggests that there were at least two different groundwater sources interacting with the river, and that the contribution of radon from parafluvial flow did not appear to be statistically significant.

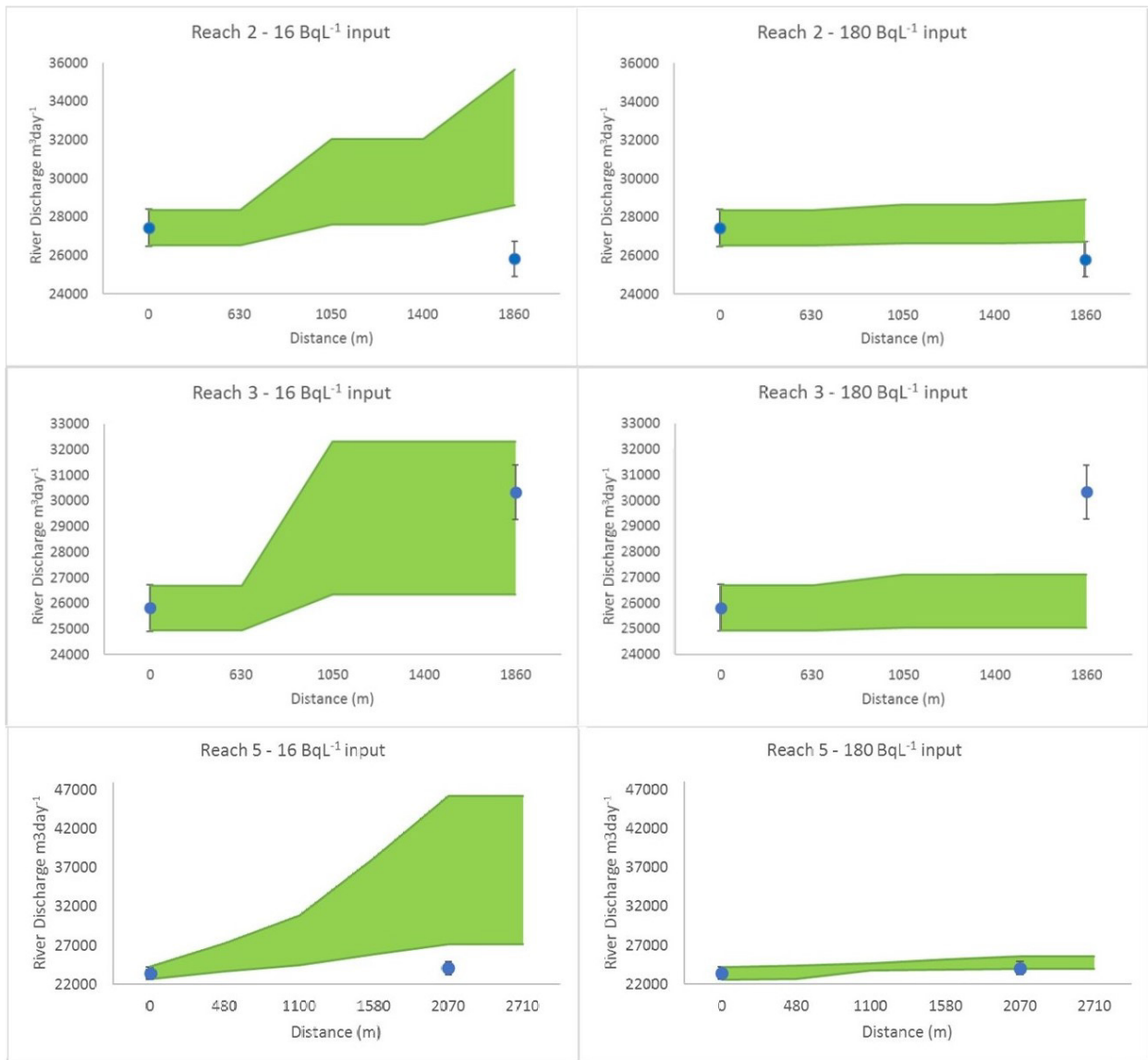


Figure A10.1 Range of calculated discharge rates for reaches 2, 3 and 5 (see locations in Figure 4.15) of the Waihemo/Shag River using different radon groundwater input concentrations. The measured gauge flows are shown by blue symbols (Martindale et al. 2017).



www.gns.cri.nz

Principal Location

1 Fairway Drive, Avalon
Lower Hutt 5010
PO Box 30368
Lower Hutt 5040
New Zealand
T +64-4-570 1444
F +64-4-570 4600

Other Locations

Dunedin Research Centre
764 Cumberland Street
Private Bag 1930
Dunedin 9054
New Zealand
T +64-3-477 4050
F +64-3-477 5232

Wairakei Research Centre
114 Karetoto Road
Private Bag 2000
Taupo 3352
New Zealand
T +64-7-374 8211
F +64-7-374 8199

National Isotope Centre
30 Gracefield Road
PO Box 30368
Lower Hutt 5040
New Zealand
T +64-4-570 1444
F +64-4-570 4657